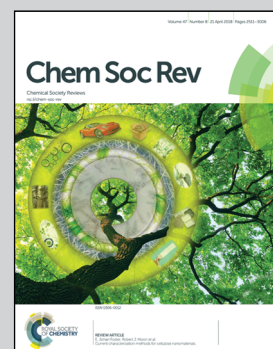


Featuring work from the research group of Professor M. I. Burguete, Professor S. V. Luis, Dr B. Altava and Dr E. García-Verdugo at the Department of Inorganic and Organic Chemistry of the University Jaume I in Castellón, Spain. The group has been working for many years on polymeric supports for the immobilization of a variety of catalysts and the understanding of the effect of the support on the resulting systems.

Chiral catalysts immobilized on achiral polymers: effect of the polymer support on the performance of the catalyst

Attachment of a chiral catalyst on an achiral polymeric support provides advantages for the enantioselective process like improvements in activity, stability and selectivity, including enantioselectivity in some instances.

### As featured in:



See Eduardo García-Verdugo, Santiago V. Luis et al., *Chem. Soc. Rev.*, 2018, **47**, 2722.



Cite this: *Chem. Soc. Rev.*, 2018, 47, 2722

Received 23rd October 2017

DOI: 10.1039/c7cs00734e

rsc.li/chem-soc-rev

## Chiral catalysts immobilized on achiral polymers: effect of the polymer support on the performance of the catalyst

Belén Altava, M. Isabel Burguete, Eduardo García-Verdugo \* and Santiago V. Luis \*

Positive effects of the polymeric support on the performance of supported chiral catalysts, in terms of activity, stability and selectivity–enantioselectivity, have been reported when the support is properly selected and optimized opening the way to the design of more efficient catalytic systems.

### Introduction and scope

Chirality plays a major role in chemistry. The physicochemical and biological properties of enantiomeric compounds can significantly differ, for instance due to stereospecific interactions with enzymes and receptors in biological systems. Enantiomers of chiral drugs can present differences in pharmacological activity and accordingly in toxicity. In this regard, new therapeutic formulations, driven by both regulatory and therapeutic motivations, are moving towards the use of enantiopure ingredients.<sup>1</sup> Indeed, the chiral drug industry constitutes approximately

Department of Inorganic and Organic Chemistry, University Jaume I, Avda Sos Baynat s/n, E-12071, Castellón, Spain. E-mail: cepeda@uji.es, luiss@uji.es



**Belén Altava**

asymmetric catalysis, ionic liquids, green chemistry and supramolecular chemistry. For the last 12 years she has been involved in the Spanish Interuniversity Master and PhD Programs in Sustainable Chemistry.

one-third of all drug sales worldwide. It is expected that nearly 95% of the pharmaceutical drugs would be chiral by 2020.<sup>2</sup> Enantiopure chiral compounds are also gaining importance in agrochemicals, such as fungicides, herbicides, and insecticides.<sup>3</sup> Improvements in performance and the elimination or reduction of harmful effects can be achieved by switching from racemic pesticides to single enantiomers.<sup>4–6</sup> Among the different methodologies for the preparation of enantiopure chiral compounds, asymmetric catalysis can be envisioned as an ideal methodology where a small amount of a well-designed chiral catalyst is able to transform achiral substrates into enriched chiral compounds stereoselectively in a large quantity.<sup>7,8</sup> Since the early days of this field thousands of chiral ligands and their transition metal complexes have been developed and many of



**M. Isabel Burguete**

*Maria Isabel Burguete graduated in Chemistry at the University of Zaragoza in Spain and after a stay at the University of Pittsburgh (USA) under the supervision of Dr J. Rebek, she completed her PhD at the University of Valencia in 1989 under the direction of Dr F. Gaviña working on regulated crown ethers and convergent diacids. In 1989 she took an academic appointment at the University Jaume I in Castellón (Spain), where she is currently Professor of Organic Chemistry. Her main field of research is developing new tools, in particular homogeneous and supported catalysis approaches, in Green and Sustainable Chemistry.*



them have been proved to be highly effective in the asymmetric formation of C–H, C–C, C–O, and C–N bonds.<sup>9</sup> The award, in 2001, of the Nobel Prize in Chemistry to W. S. Knowles,<sup>10</sup> R. Noyori,<sup>11</sup> and K. B. Sharpless<sup>12</sup> recognised the impact of this field on modern chemistry. Furthermore, in the last few years, organocatalytic asymmetric methods have blossomed as an alternative way to produce enriched chiral molecules.<sup>13–15</sup>

Since the early developments in homogeneous asymmetric catalysts, their immobilisation onto inorganic or organic supports has been targeted.<sup>16,17</sup> The supported versions of reagents and catalysts present, ideally, several distinct advantages in terms of their practical use, relative to their homogeneous analogues.<sup>18,19</sup> In particular, we should mention the facilitation of the work up, with the possibility of easy separation and recovery of the supported systems from the reaction mixture and the concomitant facilitation of recycling. These advantages are even more pronounced when enantioselective reagents and catalysts are considered. For those cases, the possibility of recovering and reusing the chiral component, which is generally the most expensive component of the system, can be a critical factor for assessing their practical utility.

A large number of efforts have been devoted in recent years to the heterogenisation of systems that have been proved useful in solution in particular as enantioselective reagents and catalysts.<sup>20–23</sup> However, in spite of the well-stabilised advantages of a supported catalyst combining the best of both homogeneous and heterogeneous worlds, after 40 years of research and development enough examples of large scale processes using chiral supported catalysts are still lacking.

Usually, the immobilisation is carried out on commercially available polymeric supports, which are not optimised for immobilisation, thus leading sometimes to deceiving catalytic performances. It is often reported that results obtained with the supported systems, even successfully enabling the separation and recovery of the catalysts, are quite different from those

expected from solution studies, and can suffer from lower activities and selectivities. Moreover, it is generally concluded, not necessarily a correct idea, that “*the best homogeneous catalyst will remain the best upon immobilization*”, assuming that the polymeric matrix can have either no effect, in the best case, or a negative one, leading to less efficient catalysts upon immobilisation.

Hence, when analysing data from the literature, many authors conform to the idea that enantioselective supported reagents and catalysts are usually less efficient than the homogeneous ones in terms of the three critical catalytic parameters: activity, stability and selectivity, in particular enantioselectivity.<sup>24</sup>

Fortunately, this is not always true. Many results clearly reveal how the presence of the matrix can be used advantageously to increase the efficiency of the supported species over that of the related homogeneous ones.

The present critical review intends to highlight significant recent examples of how the matrix can really contribute to improve the global efficiency of chiral immobilized catalysts. The period from 2000 to 2017 has been mainly covered, although some selected older references have also been included when their relevance to a given aspect made it appropriate. This work does not intend to cover exhaustively the literature in this field for the above mentioned period but to present examples able to illustrate the main concepts discussed here. The challenge is not anymore the immobilisation of catalysts to facilitate their recovery and reuse, but the development of methodologies and new advanced materials to enhance their catalytic properties as to surpass those of the soluble counterparts. These effects will be analysed taking into account the above mentioned three main factors: activity, stability and selectivity. For the sake of clarity and to provide well identified elements of comparison, this review will be focused on the use of organic polymeric matrices as supports. The use of silica and other inorganic materials as supports for the asymmetric catalysts is out of the scope of this



**Eduardo García-Verdugo**

*Eduardo García-Verdugo obtained his chemistry degree from the University of Valencia (1995) and his PhD from the University Jaume I (2001). After working as a researcher at Nottingham University (M. Poliakoff, until 2004), he returned to Spain as a Ramon y Cajal fellow at the University Jaume I until 2009, and then obtained a permanent position at the CSIC-ICP (Madrid, 2009–2010). In 2010, he moved to a permanent academic*

*position at the University Jaume I, working on the integration of different enabling techniques (catalysis, polymers, continuous flow processes, microreactors, bio-catalysis, neoteric solvents) to develop efficient and greener organic transformations.*



**Santiago V. Luis**

*Santiago V. Luis studied Chemistry at the University of Zaragoza and completed his PhD at the University of Valencia in 1983 working on mechanistic studies. After a postdoctoral work at the University of Pittsburgh under the supervision of Dr J. Rebek, in Supramolecular chemistry, he obtained an academic appointment at the University Jaume I in Castellón (Spain) where he is currently Professor of Organic Chemistry and Head of the research group in Supramolecular and Sustainable Chemistry. His research areas involve Supramolecular and Biomimetic chemistry and new tools in Sustainable and Green Chemistry, with emphasis on catalysis and flow chemistry.*

work and will only be mentioned as illustration in a few cases. Some reviews dealing with the effect of the inorganic support on the efficiency of immobilised asymmetric catalysts can be also found in the literature.<sup>25–28</sup> Some examples of non-chiral systems or from supported reagents (stoichiometric instead of catalytic systems) will also be presented, when appropriate, to highlight the effects of the support.

A very particular case regarding the influence of the polymer matrix on the efficiency of the catalyst is given by the immobilisation of the catalyst onto chiral polymer supports.<sup>29,30</sup> Although examples of such systems are still limited, attempts at using the chirality of the polymer matrix to exert control over catalytic efficiency, in particular over enantioselectivity, are gaining great success. Immobilised catalysts containing either chiral catalytic pendant units<sup>31</sup> or achiral ones have been developed.<sup>32,33</sup> In the latter class, the asymmetric induction solely relies on the chirality of the polymer matrix, in particular through the adoption of helical structures. Although these new types of catalysts supported on chiral polymer matrices are undergoing very rapid development in recent years, they are not discussed in depth in this review article as they lie out of its main scope.

## The polymer matrix as a design vector

In the initial steps of the work with polymers as supports, it is sometimes assumed that the polymer, if appropriately selected, would play no other role than that of an inert matrix supporting the active sites and facilitating their simple isolation and reuse. This is a naive and wishful thinking and in most of the cases distinct polymer effects can be detected.<sup>34–37</sup> This is even true when the nature of the support is carefully chosen as to avoid the presence of any other interfering functional group or when the active site is separated from the matrix through a long spacer. Clearly, the support determines, to a good extent, not only the diffusion of the reagents and products to and from the active sites but also the actual conditions and microenvironment of the reaction taking place. Therefore, the selection of the nature of the polymeric support and how the catalyst is immobilised are key factors for developing efficient polymeric supported asymmetric catalysts.

At least four elements should be considered when designing an immobilized catalyst: (i) the nature of the attachment of the catalytic sites to the support, (ii) the nature and length of the spacer between the catalytic sites and the polymeric network, (iii) the density of catalytic sites and their location along the polymeric network and (iv) the physicochemical nature of the polymeric backbone. Thus, the methodology employed for the preparation of an immobilised catalyst defines, to a great extent, its resulting properties and potential applications. In this regard, the challenge is to develop methodologies where both ligand and polymeric matrix are specifically designed to obtain a given supported catalyst. Accordingly, through the optimisation of the ligand and support, the same matrix effects leading to negative effects after immobilization of a good homogeneous catalyst might be able to improve those

obtained with a less optimal one. Some results based on systematic studies clearly reflect how the presence of a well-designed support can be advantageous to increase the efficiency, especially in terms of activity and selectivity, of the supported species relative to that of the homogeneous ones.

There are a wide range of classical and new methodologies to develop chiral polymer-supported catalytic systems and this section briefly summarises these approaches. Different strategies have been evaluated for immobilisation: (i) covalent bonding, (ii) ion-pair formation, (iii) encapsulation or (iv) entrapment.<sup>38–40</sup> Without any doubt, covalent binding is by far the most frequently used strategy, significantly limiting the potential leaching of catalytically active components. Two main possibilities exist for carrying out this approach. The first one relies on the chemical modification of preformed polymeric supports. Alternatively, the polymerization of functional monomers with the desired functionality, by themselves or in the presence of additional monomers, has also been exploited.

Among the different types of polymeric supports, a clear differentiation can be established regarding their solubility in the reaction medium. Both soluble and insoluble polymeric materials have been investigated as supports. Linear soluble polymers have been early envisioned as suitable media for catalyst immobilisation.<sup>41,42</sup> They can significantly limit the diffusional problems found in crosslinked systems. However, their recovery and recycling is not so straightforward, requiring tuneable solubility properties.<sup>43–45</sup> With the advances made in macromolecular chemistry in recent years, it is now possible to design and synthesize complex soluble polymers with new architectures and well-defined catalyst location and loading along the polymeric chain. Besides, the control of the polymer structure allows not only the immobilisation of the catalyst but also mimicking of the form and function of Nature's nanostructures using, for instance, amphiphilic block copolymers that spontaneously self-assemble in selective solvents into specific assemblies.<sup>46</sup>

Dendrimers have emerged as alternative soluble supports for the immobilisation of different types of catalytic units filling the gap between homogeneous and heterogeneous systems.<sup>47</sup> They are highly branched macromolecules with the larger ones having precisely defined globular structures. It is possible to control the incorporation of the catalytic sites within the dendrimer either at the core, at the periphery, or at intermediate positions.<sup>48</sup> The different locations can be used to define and tune their catalytic performance. Dendrimer recovery can be achieved by precipitation from solution or, if large enough, using membrane filters.<sup>49</sup>

Polystyrene and styrene/divinylbenzene (PS-DVB) copolymers (Merrifield type resins) are by far the most common insoluble polymeric supports exploited for the preparation of immobilised catalysts.<sup>50,51</sup> This type of supports, especially the ones with a low crosslinking degree (1–2% DVB gel-type) initially developed for solid-phase peptide synthesis,<sup>52</sup> have been widely used as functionalized polymers because of their stability and compatibility with a wide range of reaction conditions, their good swelling properties or their reasonably high loading capacity



( $>1 \text{ mmol g}^{-1}$ ), providing access to a large number of post-functionalization processes.<sup>53</sup> The swelling or solvation, the effective pore size, the surface area and the chemical and mechanical stability of the polymer are important factors that control the diffusion of reagents and substrates into the active sites. The degree of crosslinking of the resin, the functional fragments introduced and the conditions employed during the preparation of the polymers allow fine-tuning of these properties. Therefore, along with the originally used microporous or gel-type resins, a variety of macroporous/macroporous resins have also been developed to improve the performance of these polymers as catalyst supports. They can be produced, for example, by phase separation, emulsion polymerization, or by templating methods.<sup>54,55</sup> In the same way, in addition to the classical PS–DVB polymeric networks of Merrifield resins, other organic polymers like polyvinyls, polyacrylates, cellulose or PS–DVB copolymerised with other polar monomers or modified with hydrophilic flexible units such as polyglycol chains acting as crosslinking units or linkers have been developed and tested as alternative polymeric supports.<sup>56–60</sup>

In the last decade, a whole new range of different porous networks, including crystalline and amorphous structures, have blossomed as suitable alternatives to traditional organic polymers.<sup>61</sup> In some instances, they can combine high surface areas, good physicochemical stability and an increasing degree of functional modularity.

Among these materials based on an organic skeleton, the design and synthesis of chiral Metal–Organic Frameworks (MOF) or self-supported systems offer a new strategy for the generation of robust immobilized asymmetric catalysts combining supramolecular chemistry, coordination chemistry and catalysis concepts. These systems are obtained in a straightforward way through the coordination of a polytopic ligand and metal species leading to the self-assembly of the metal–ligand components to generate an extended organometallic/coordination network.

Porous Organic Polymers (POPs) with high permanent porosity, high accessible specific surface areas and very robust chemical properties have been developed by using extensive crosslinked covalent bonds between organic building blocks. Conceptually, the component organic fragments in POPs are connected in a similar way as in MOFs but using strong covalent bonds with the linkers acting as connectors, instead of the relatively weak coordinative bonds to metal ions and clusters present in MOFs.<sup>62–64</sup> They can be obtained by a variety of synthetic routes offering new types of functionalised polymeric networks. Their topology and porosity can be tailored by varying the connectivity, size, and geometry of the building blocks by a bottom-up approach leading ideally to a perfect control of the size and shape of the catalytic environment formed inside the cavities of the material or on the surface of the solid, enhancing the control of the reaction.<sup>61,65</sup> Within this category of supports (POPs) it is possible to consider Hyper-Cross-linked Polymers (HCPs), which are obtained by post-crosslinking of polystyrene-type precursors in their swollen state (Davankov's hypercrosslinked polystyrene polymers) or from the condensation of small building blocks (Webster's poly(arylcarbinol) networks).<sup>66</sup>

They present a very rigid non-collapsible polymeric matrix with small pore sizes and high surface areas, and micropore volumes.<sup>67</sup> Alternatively, different synthetic strategies have been developed to bring together numerous organic building blocks directly or with the aid of suitable linkers onto predesigned skeletons of porous networks. Depending on the nature of the synthetic motifs and methodologies, these systems can be defined as Covalent Organic Frameworks (COFs),<sup>68,69</sup> or Polymer Organic Frameworks (POFs),<sup>70,71</sup> which can be Conjugated Microporous Polymers (CMPS),<sup>72,73</sup> Polymers with Intrinsic Microporosity (PIMs),<sup>74</sup> or Porous Polymeric Aromatic Frameworks.<sup>75</sup>

## Evaluating the matrix effect

Different factors should be considered to rationalize the effect of the polymeric matrix on the efficiency of immobilised catalysts leading to enhanced turnover numbers and frequencies, stability, and selectivity. The first one is related to the modifications needed, on the catalytic structure, to provide a way for the efficient immobilization onto the polymeric matrix. It is well known that for stoichiometric or catalytic enantioselective transformations, even minor structural modifications in the chiral system can have important effects on the results obtained.<sup>76,77</sup>

The second factor is related to the effect of the polymeric matrix itself. In order to detect and understand experimental results directly connected with the nature of the matrix, a very systematic approach is required. This involves the preparation of the appropriate homogeneous counterpart having exactly the same structural features as the supported one, including the presence of the additional groups required for anchoring, and carrying out the corresponding reaction strictly under the same experimental conditions with both the homogeneous and the heterogeneous system. For instance, Larionov *et al.* have recently reported the immobilization of a chiral-at-metal iridium Lewis acid catalyst (**1**) on polystyrene macro beads using different linkers (**2**, **3**) for the attachment (Fig. 1).<sup>78</sup> When the resulting immobilised Ir-chiral complexes were tested as catalysts for the Friedel–Crafts alkylation of indole (**6**) with the  $\alpha,\beta$ -unsaturated 2-acyl imidazole **7**, the supported catalysts (**2–3**) provided, in comparison to the homogeneous original catalyst (**1**), higher enantioselectivities (97% ee vs. 93% ee) while featuring lower catalytic activities. However, when the results were evaluated in comparison with their structural homogeneous homologues (**4**, **5**), the activity and enantioselectivity were comparable and the results could be correlated with the structural modification required for the immobilisation. Many times, this is not taken into account and claims about the preparation of supported reagents or catalysts performing differently than the homogeneous ones need to be considered with caution and do not provide any hint towards the understanding of the effects of the matrix and for the design of new supported systems in which the polymeric backbone contributes to improve their efficiency.

A good understanding of the mechanistic role of the catalyst, *i.e.* the presence of monometallic *vs.* multi-metallic species in

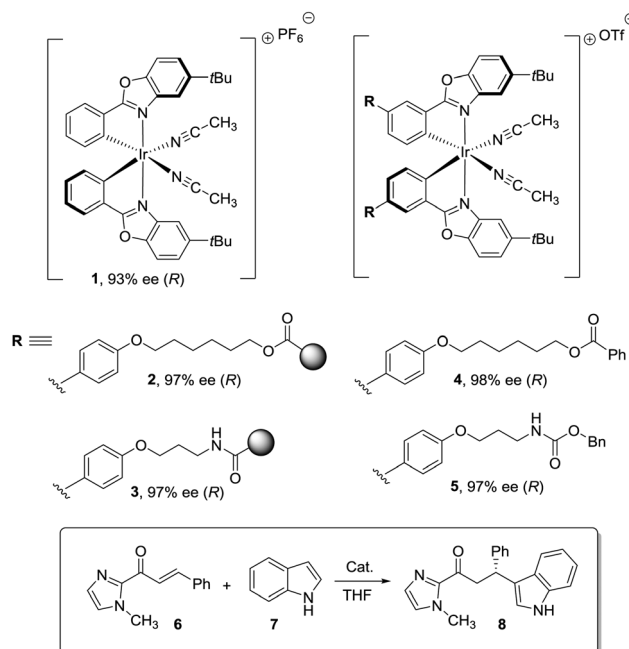


Fig. 1 Effect of structural modification and immobilization on the performance of chiral-at-metal iridium catalysts.

the transition state and how this affects the reaction efficiency, should be also taken into account to design the adequate immobilisation protocol either favouring the site isolation or the possible interaction between catalytic sites. Besides, to properly assess recyclability, stability and the mechanisms of deactivation, kinetic data should be provided in each cycle (*i.e.* initial rates or TOF at low conversion degrees).†

For the correct evaluation of the efficiency of a supported enantioselective catalyst, three different aspects need to be addressed: (i) activity, *i.e.* the effect of immobilization on the rate of the reaction under study; (ii) stability, *i.e.* the analysis of how much actually the heterogenisation process contributes to stabilize the reagent/catalyst and to increase the possibilities of reusing and recycling the reagents and/or catalysts, by performing systematic studies of the stability and deactivation of catalysts; and (iii) selectivity, and in particular, in the present context, enantioselectivity. Energy differences between the transition states leading to the formation of either one or the other enantiomer, with the help of a chiral reagent or catalyst, are usually small and, accordingly, they can be very much affected by the microenvironment.

## Activity

The catalyst immobilisation is usually carried out on commercially available polymeric supports, which are not optimised for immobilisation (Fig. 2). As a result, often the reactions taking place with the participation of polymer-supported species are reported to be slower than those using the homogeneous

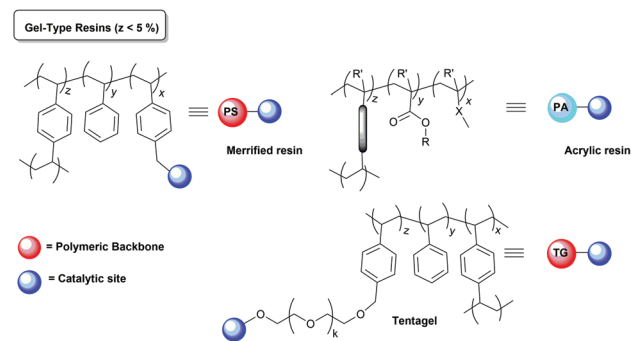


Fig. 2 Examples of polymeric supports commonly used for immobilization of chiral catalysts.

analogues and require much longer reaction times. In many cases, the morphology of the polymer network is one of the main factors determining the accessibility of the active catalytic sites and, accordingly, the activity of the corresponding supported systems.<sup>79</sup>

### Gel-type polymeric supports

Most examples of insoluble polymeric reagents and catalysts are related to the use of gel-type PS–DVB resins commercially available in the form of beads. Those gel-type resins do not have any permanent porosity and need to be swollen in an appropriate solvent in order to make accessible the functional sites inside the bead.<sup>80</sup> On the other hand, some crosslinking degree is necessary to obtain insoluble materials with the appropriate morphologies. In the case of polystyrene resins (PS), which are the most standard materials in this field, 1–4% of divinylbenzene (DVB, a commercial mixture of different isomers) is generally used as the crosslinking agent. Swelling is always less effective at the crosslinked regions of the polymer and accordingly functional sites located at those positions become less accessible.<sup>81</sup>

Accordingly, an increase in crosslinking for this type of polymers is usually accompanied by a lower swelling and by a decrease in the accessibility of the functional sites.<sup>82</sup> This is always reflected in slower reaction rates. Thus, when working with this kind of materials, it is important to keep in mind that the activity of a given supported species will be very much dependent on the solvent used and the crosslinking degree of the polymer.<sup>83–85</sup> This has been studied in detail in the case of different families of functional, catalytic resins.<sup>86–88</sup>

**The use of spacers.** Different approaches have been evaluated in order to overcome the above difficulties.<sup>89</sup> Since the pioneering work of Soai and coworkers, spacers have been used to attach the ligand to the polymer by a point remote from the active site (tail-tie),<sup>90,91</sup> hoping that the catalyst will be able to mimic a solution-like behaviour reducing any possible “polymeric (negative) effect”.

In this regard, the introduction of long aliphatic or ether spacers favouring compatibility with a wide range of solvents<sup>58–60,92,93</sup> or the substitution of DVB by more flexible crosslinkers has been widely explored.<sup>84</sup> Thus, Montanari and coworkers found that the use of long aliphatic spacers (up to 10 methylene units)

† TOF from literature data or calculated from data reported as: (mol of substrate/mol catalyst) × (yield (%)/100) × (1/time (h)).



and low crosslinking degrees (1%) increased the corresponding activities 2–4 times in polymer-supported phase transfer catalysts. This classical effect was based on the higher flexibility of the functional chain and the increase in the lipophilicity of the polymer facilitating its swelling.<sup>93–96</sup>

Dyer *et al.* also illustrated nicely those concepts in the case of Ti-diol complexes supported using spacer-modified gel-type resins (Fig. 3).<sup>97</sup> In this work, functional resins **9** were used as catalysts for the Diels–Alder reaction between cyclopentadiene (**10**) and methyl acrylate (**11**). The catalyst **9c** with the larger spacer ( $-(\text{CH}_2)_9-$ ) was the most active one, suggesting that the use of a long spacer improves the accessibility to the Lewis acid sites. Rather surprisingly, introducing a modified spacer unit (**13**,  $X = -(\text{CH}_2)_5-\text{C}_6\text{H}_4-\text{CH}_2$ ) led to markedly slower catalysts. This was associated with the poor swelling behaviour of those polymers. No improvement in activity relative to the homogeneous system was reported in this case, although the homogeneous counterpart selected presented some structural differences with the polymer-bound system. Similar trends were found in the case of 2% crosslinked polymer-bound lithium dialkylamides **14**.<sup>98</sup>

The introduction of spacer chains between the polymeric backbone and the lithium dialkylamide fragment enhanced the yields observed for the crossed aldol reaction of various carbonyl compounds with aldehydes. An increase in the size of the spacer seems to have a favourable effect up to  $n = 5$ . For  $n > 5$ , no further improvement was observed. Given the complex nature of many lithium derivatives, it is reasonable to assume that the small increases in activity found in some instances, relative to LDA, for polymer-bound dialkylamides **14**, can be associated with the same phenomenon.<sup>98</sup> Nevertheless, data given need to be used with some caution as no kinetic data were provided, with just yields of isolated compounds given as proof of activity.

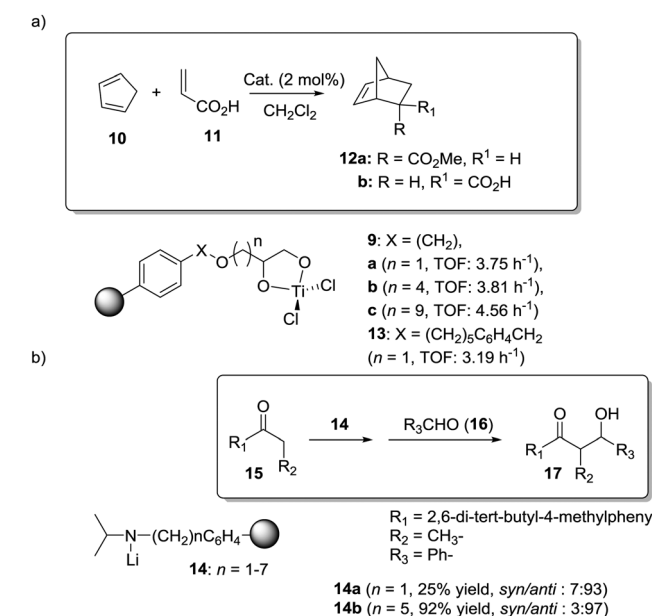


Fig. 3 Examples of supported catalysts where the length and nature of the linker enable modification of the activity.

Toy and coworkers have also demonstrated a direct relationship between catalytic efficiency, crosslinker nature, catalyst loading and swelling in the aza-Baylis–Hillman reactions catalysed by JandaJel-PPh<sub>3</sub>.<sup>99,100</sup> Similar effects were observed in the work of Pedrosa, Andres and coworkers with a series of chiral ureas and thioureas immobilized on PS–DVB resins by either grafting and copolymerisation methodologies and studied for the aza–Henry reaction between *N*-Boc-benzaldimine (**18**) and nitromethane (**19**) under solvent free conditions (Fig. 4).<sup>101,102</sup> Their results suggested that the linker connecting the catalytic moieties with the polymer framework led to marginal effects on enantioselectivity while the effects on activity were more relevant.

Thus, for the systems prepared by grafting using sulfonamide groups for the attachment, up to a 12 times enhancement in activity was observed with the length of the spacer (3.17 h<sup>-1</sup> for **21b** with six methylene units *vs.* 0.257 h<sup>-1</sup> for **21a** with two methylene units). In good agreement with previous reports in

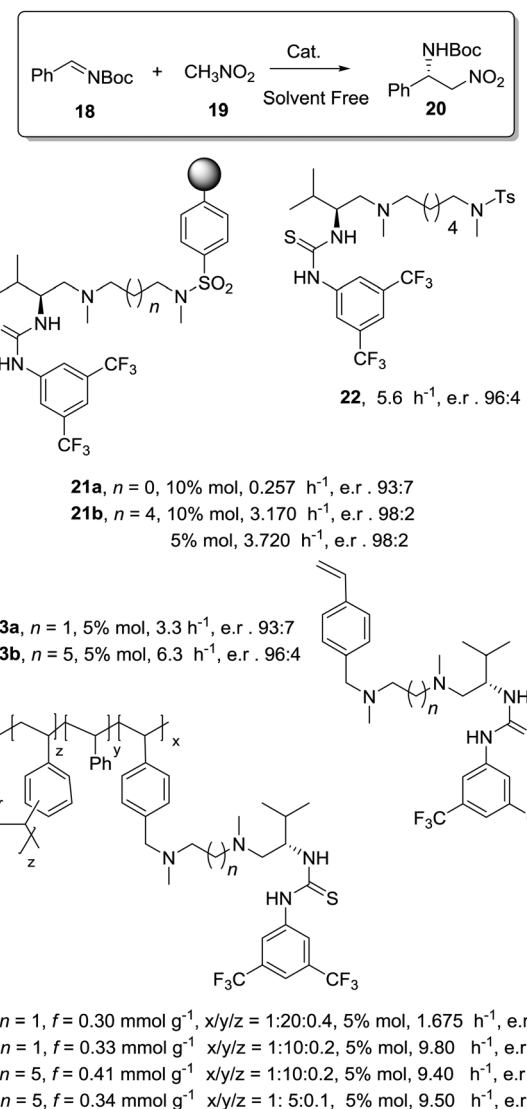


Fig. 4 Activity of some supported thioureas for the aza–Henry reaction between *N*-Boc-benzaldimine (**18**) and nitromethane.

this field presented above, the longer spacers locating the active sites away from the polymeric backbone provide more “solution-like” and active systems by improving the accessibility to the functional sites inside the bead. However, the extent of this effect is not enough to surpass the activity found for the homogeneous counterpart ( $5.6\text{ h}^{-1}$  for **22**). A different situation was found for the catalysts obtained by a bottom-up synthesis of chiral bifunctional thioureas by copolymerization of styrene, 4-vinyl benzylamine derivatives and divinylbenzene as the crosslinker. Some of these systems (**24a–b**) showed an enhancement of the catalytic activity of 2.9–1.5 times in comparison with the homogeneous counterpart (**23a–b**). Noteworthily, in this case the role of the spacer had a minimal effect. These results highlight the importance of the methodology used in the preparation of the catalysts (grafting *vs.* polymerisation). When immobilisation takes place by polymerisation in the presence of the corresponding chiral monomers a more uniform and accessible distribution of the chiral catalytic sites within the polymeric network can be achieved. Hence, a bottom-up methodology usually provides better accessibility of the catalytic sites, minimizing the role played by the spacer. It must be noted that using a different attachment group in the linker ( $-\text{CH}_2-$  instead of  $-\text{SO}_2-$ ) led to some changes in the activity, highlighting once again the importance of selecting the appropriate homogeneous counterpart in order to evaluate the performance of the immobilised catalysts.

The exact origin of the positive effects of the matrix on the rates is not so well defined in other cases. In general, they can be ascribed to the local microenvironment of the active site and this includes effects such as the hydrophobic/hydrophilic balance, the conformational flexibility of the functional sites or the interaction with functional groups or fragments present in the polymeric network. In many senses, the heterogenisation process can affect the rates (and likely the whole reactivity) very much in the same way a change in the solvent does.<sup>103</sup> In this context, Pericàs and coworkers have recently reported the immobilization of a modified version of the triflate ammonium salt of the chiral vicinal diamine **25** and its use as catalyst for the Robinson annulation reaction.<sup>104</sup> The substitution of one of the ethyl groups on the tertiary amine by a hydroxyethyl group allowed both the preparation of the polymer supported system (**27**) *via* the nucleophilic substitution of the chlorine atoms of a commercially available microporous Merrifield resin and the synthesis of the homogeneous counterpart **26** by reaction with benzyl bromide (Fig. 5). Important effects on activity were observed for the reaction between the commercially available diketone (**28**) and methyl vinyl ketone (**29**) in 2-MeTHF. Under identical experimental conditions, the immobilised catalyst (**27**,  $\text{TOF } 8.8\text{ h}^{-1}$ , 91% ee) was 2.8 times more active than its homogeneous counterpart (**26**,  $\text{TOF } 3.1\text{ h}^{-1}$ , 90% ee). Larger enhancements, up to 18.7 times, were found in comparison with unmodified homogeneous catalyst **25** ( $\text{TOF } 0.47\text{ h}^{-1}$ , 89% ee). The polymer efficiently provided a suitable microenvironment to favour the local concentration of the substrates within the polymeric network, and in this case, the reaction inside the polymeric network takes place much more efficiently than

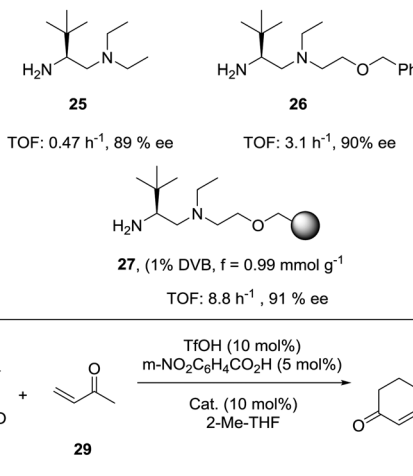


Fig. 5 Enhancement in activity for a PS-supported chiral vicinal diamine.

in solution.<sup>80</sup> While this effect could be somewhat masked by mass transfer limitations at room temperature, it became fully operational at 55–60 °C with a tenfold enhancement of the activity on going from room temperature to 55 °C.

An important point to take into account for understanding the activity of insoluble polymer-supported systems is that, as rates can be much affected by diffusion, the temperature can have a very important effect on activity. A marked decrease in activity is often found on lowering the temperature, and this, sometimes, puts some limits on the use of low temperatures that are usually employed for enantioselective transformations under homogeneous conditions.<sup>105–107</sup>

As mentioned before, spacers have been used to attach the ligand to the polymer by a point remote from the active site (tail-tie), reducing any possible “polymeric (negative) effect” associated with the bulky polymeric matrix. However, in some cases, the spacer and/or linker themselves can play a non-innocent role in catalytic activity. These effects can be related to the modification of the hydrophobic/hydrophilic balance and/or to the presence of an additional functional group. Alexandratos and co-workers have systematically studied how the microenvironment surrounding the active sites in polymer-supported systems can be used to enhance the reactivity of the intermediates and the rate of product formation, using the Mitsunobu reaction as the benchmark reaction.<sup>108</sup>

The potential of the 1,2,3-triazole moiety as the attachment point in the linker has been extensively exploited. Its use has facilitated the immobilization of catalytic units with a wide range of structural diversity using a clean 1,3-dipolar cycloaddition reaction (Fig. 6). This triazole linker allows not only the grafting of catalytic moieties but also the incorporation of spacers drawing them away from the polystyrene chain, in an attempt to improve the mass transfer and to accelerate the reaction. By using several variations of this click-chemistry strategy, different derivatives of 4-hydroxyproline have been grafted onto several commercially available resins (Merrifield, ArgoPore and PS-PEG NovaBioSyn) (Fig. 6).<sup>109–111</sup> The results observed with the resulting supported proline organocatalysts for the aldol

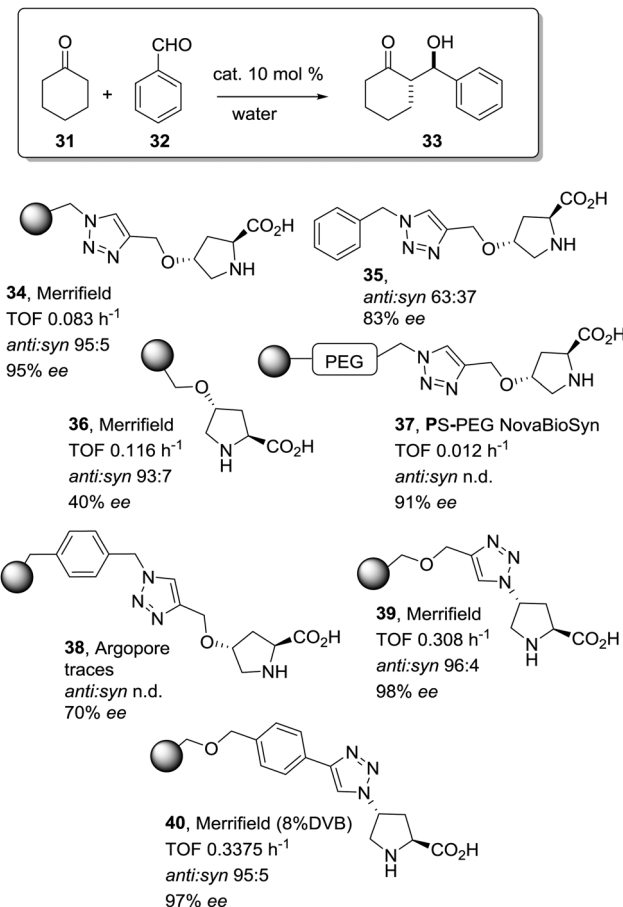


Fig. 6 Immobilization of 4-hydroxyproline fragments on different polymeric supports using a click strategy with the formation of linkers containing the 1,2,3-triazole moiety.

reaction between cyclohexanone and benzaldehyde in water at room temperature suggest the non-innocent nature of this linker/spacer.

Noteworthily, the polymer **34** exhibited a much better catalytic performance than its monomeric counterpart in terms of selectivity. However, this resin still presents low reaction rates in water (TOF  $0.083 \text{ h}^{-1}$ ). The use of an analogous macroporous resin in substitution of a gel-type support did not improve the situation and only traces of the product were found for this catalyst (**38**). However, a controlled manipulation of the linker and spacer between the catalytic unit and the polymeric backbone allowing tuning the improvement of the catalytic performance. The lack of the 1,2,3-triazole moiety in the linker (**36**) led to similar activity but much poorer enantioselectivity. The use of a resin bearing more flexible and hydrophilic ethylene glycol units (**37**) rendered a significant activity drop. Polymer **39**, where the 1,2,3-triazole moiety is directly grafted to the proline ring, exhibited an optimal catalytic performance, with a notable rate acceleration over those of the other studied resins (up to 3.7 by comparing **34** and **39**).

Noticeably, and in sharp contrast with other resins, polymer **39** showed a perfect swelling behaviour in water. The observed activity enhancement can be related to the interaction of water

molecules connecting the amino acid and the 1,2,3-triazole moieties building an aqueous microenvironment around the catalytic sites resembling the effect of essential water on some natural enzymes used in organic media. The introduction of an additional spacer unit (4-ethynylbenzyl ether, **40**) increased the separation between the hydrophilic, catalytically active moiety and the hydrophobic polymer backbone. This catalyst, based on a PS polymer with 8% of DVB, showed a higher activity and diastereoselectivity than the homogeneous counterpart for all the solvents tested (homogeneous vs. heterogeneous:  $\text{H}_2\text{O}$ :  $0.3125 \text{ h}^{-1}$  *anti*:*syn* 93:7, 97% ee vs.  $0.3375 \text{ h}^{-1}$ , *anti*:*syn* 95:5, 97% ee;  $\text{DMF}$ : $\text{H}_2\text{O}$  (1:1)  $0.321 \text{ h}^{-1}$ , *anti*:*syn* 79:21, 97% ee vs.  $0.383 \text{ h}^{-1}$ , *anti*:*syn* 95:5, 97% ee;  $\text{CH}_2\text{Cl}_2$   $0.187 \text{ h}^{-1}$ , *anti*:*syn* 80:2, 77% ee vs.  $0.354 \text{ h}^{-1}$ , *anti*:*syn* 95:5, 85% ee).

The same group has also observed similar results in Michael reactions regarding the role of the *p*-phenylene spacer for a chiral pyrrolidine PS-support tethered by the 1,2,3-triazole moiety.<sup>112</sup>

**The effect of neighbouring groups.** Alexandratos and coworkers have also demonstrated that the presence and content of neighbouring groups can be an important variable in tuning the performance of an immobilised catalyst.<sup>113</sup> Hence, the catalytic activities of polymer-supported sulfonic acid catalysts for the Prins reaction were shown to be strongly influenced by the microenvironment surrounding the acid ligands. The high acid density within the polymer is probably very important in determining the catalytic activity and this is accentuated or attenuated by the neighbouring groups. The cooperative effect with the organocatalytic sites of the hydroxyl groups present in the matrix has been demonstrated by Kwong *et al.*<sup>114</sup> Morita–Baylis–Hillman reactions, catalysed by polymer supported triphenylphosphine or DMAP, were significantly accelerated by the presence of hydroxyl groups in the polymeric backbone. Again, the introduction of additional groups at the polymer main chain can tune the hydrophilic–hydrophobic balance around the catalytic sites and control their activity.

In this regard, Itsuno has exploited this phenomenon to design highly active supported catalysts for the transfer hydrogenation in neat water and in organic solvents.<sup>115</sup> The supported catalysts were based on the chiral ruthenium(II)–*N*-toluenesulfonyl-1,2-diphenylethylene-diamine (TsDPEN) complex developed by Ikariya and Noyori,<sup>116</sup> and prepared as microreticular resins by copolymerisation (Fig. 7). These authors have systematically evaluated the influence of the polymer composition in terms of catalyst loading, degree of crosslinking and the content and nature of pendant groups on the efficiency of the Rh, Ru and Ir catalysts derived from this supported chiral ligand for the asymmetric transfer hydrogenation of different substrates.<sup>117–120</sup> The balance between hydrophilicity and hydrophobicity induced by the presence of additional polar groups on the polymer backbone was the most important factor controlling the efficiency of the catalyst in the transfer hydrogenation of ketones and imines. The presence of additional polar groups not only allows the reaction in water to be carried out, but also allows adjustment of the activity of the catalyst through the selection of the appropriate hydrophilic, hydrophobic, or amphiphilic moieties. The most dramatic activity effect was found for the

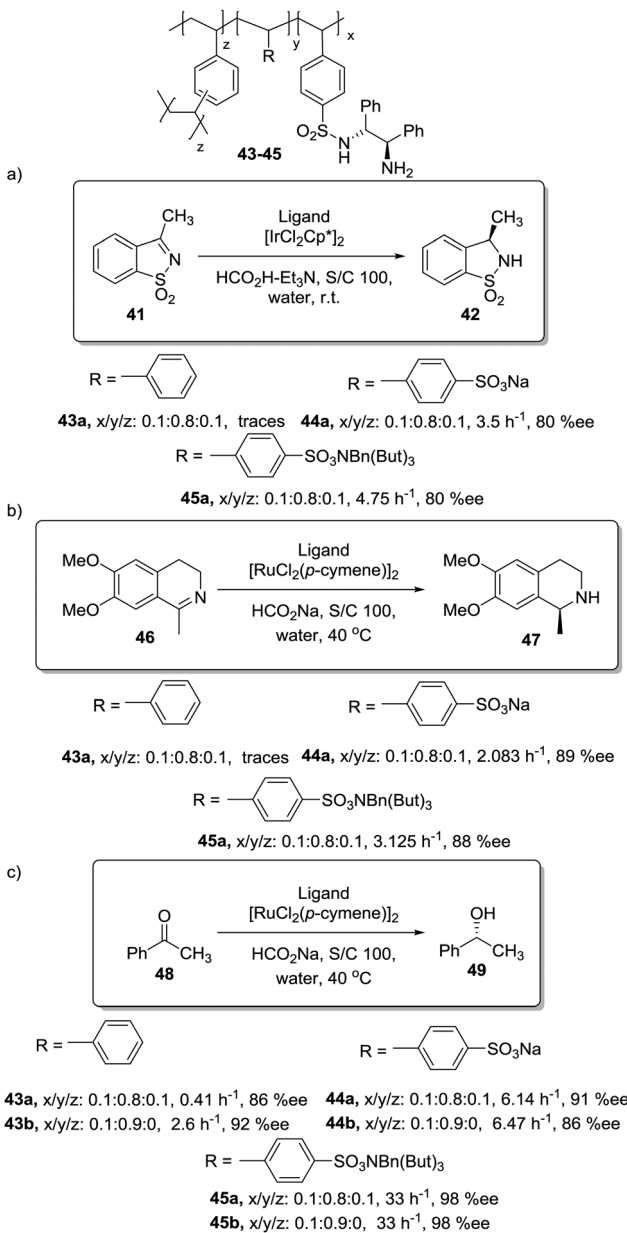


Fig. 7 Polymer supported TsDPEN ligand for the Ir or Ru catalysed transfer hydrogenation of sulfonimines (a), imines (b) and ketones (c).

hydrogenation of cyclic sulfonimine **41** in neat water (Fig. 7a). The soluble catalyst TsDPEN showed no catalytic activity due to its hydrophobic character. The polystyrene-immobilized chiral catalyst (**43a**), which consists of a gel-type hydrophobic polymer chain, was also not suitable for the reaction. However, the introduction of polar functional groups in the polymeric network turned the inactive supported catalyst into an active one in water (see **44a** and **45a**, Fig. 7a).<sup>117</sup>

The pendent polar functional groups in the multifunctional polymeric framework can induce proper polymer swelling and solvation. Indeed, styrene based polymer **43a** swelled in traditional good solvents for crosslinked polystyrene such as DMF, THF and toluene, but completely shrunk in water due to its hydrophobic character. In contrast, polymers bearing

sulfonate groups (*i.e.* **44a** and **45a**) were found to swell in polar solvents such as dimethylsulfoxide and water. This effect was also confirmed when the asymmetric transfer hydrogenation of cyclic imine **46** was studied (Fig. 7b).<sup>118</sup> Catalysts **44a** and **45a** bearing either sodium or benzyltributylammonium sulfonate groups were active in water ( $2.08\text{ h}^{-1}$ , 89% ee and  $3.125\text{ h}^{-1}$ , 89% ee, respectively), but became inactive in methylene chloride, leading to only traces of the product, while the hydrophobic catalyst **43a** (not active in water) displayed a good activity and enantioselectivity ( $3.83\text{ h}^{-1}$ , 92% ee) in this organic solvent.

The lack of catalytic activity of the hydrophobic resin **43a** for the asymmetric transfer hydrogenation of acetophenone (**48**) was clearly related to the limited accessibility of the catalytic sites in water (Fig. 7c). In fact, the soluble polymeric counterpart of this polymer (**43b**), where diffusion issues encountered in the crosslinked polymer **43a** due to the lack of swelling are minimised, was active for this asymmetric transfer hydrogenation in water. Interestingly, the same catalytic activity was found for the two soluble polymers **44b** and **45b** having polar pendent groups in the polymeric network and their crosslinked counterparts (**44a** and **45a**). These results highlight that diffusional limitations in gel-type resins can be minimised by the presence in the polymeric network of functional sites able to tune the swelling of the polymer in the presence of a given solvent.

**The pseudodilution effect.** A gel-type polymeric matrix can also have a positive effect regarding activity through a pseudodilution effect. The selection of a resin with appropriate loading reduces the possible site to site interactions that could have a detrimental effect on catalytic efficiency. This pseudodilution effect has been demonstrated by the results of several authors showing that the activity of different polymer-bound reagents and catalysts is increased by low levels of functionalization.<sup>83,100,121</sup>

This is the case, for instance, of supported pseudopeptides **55** and **56** prepared by grafting onto gel-type resins,<sup>122–125</sup> whose copper complexes were studied for the catalytic cyclopropanation of styrene (Fig. 8).<sup>126</sup> When the copper complexes of the homogeneous analogues **53** and **54** were evaluated for this reaction, the presence of an induction period was observed. No conversion of **50** to **52** was detected for a period

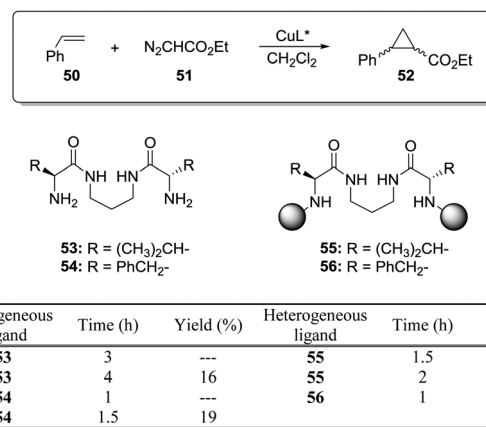


Fig. 8 Homogeneous and supported pseudopeptidic ligands assayed for the enantioselective cyclopropanation of styrene with ethyl diazoacetate.



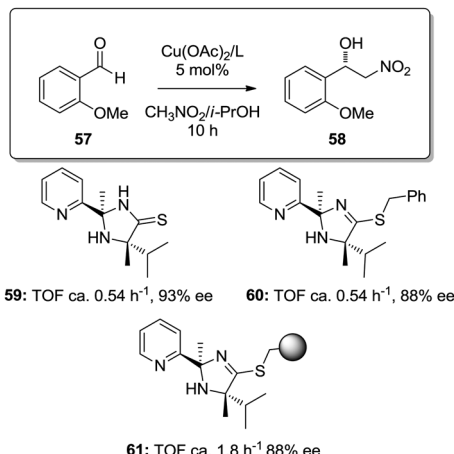


Fig. 9 Homogeneous and supported 2-(pyridine-2-yl)imidazolidine-4-thione ligands assayed for the enantioselective Henry reaction.

of 1 to 3 hours. Such an induction time was, however, absent for the supported polymeric catalysts derived from **53** and **54** that, accordingly, showed a higher activity at shorter reaction times. The pseudodilution effect seems to be responsible for this behaviour.<sup>81</sup> All data suggest that in  $\text{CH}_2\text{Cl}_2$  soluble copper complexes of **53** and **54** tend to form aggregates that present a very low activity. Non-catalysed decomposition of ethyl diazoacetate results in the formation of polar species that finally favour disruption of the aggregates. Aggregation is inhibited or, at least, very much diminished for the supported species and, accordingly, the inhibition period is not observed.

Similar effects were also found for the supported copper-2-(pyridine-2-yl)imidazolidine-4-thione complex in the asymmetric Henry reactions (Fig. 9).<sup>127</sup> The homogeneous catalysts based on the copper complexes with **59** and **60** were *ca.* 3 times less active than the copper complex obtained with the immobilized ligand obtained through grafting onto a commercially available JandaJel™ polymeric resin (**61**). The site-isolation on the polymer matrix reduces the possible dimer/oligomer adducts found in the homogeneous case,<sup>128</sup> enhancing the catalytic activity.

Some increases in activity, relative to the homogeneous phase, have been also reported by Irurre *et al.* using polymer-supported Ti-TADDOLates.<sup>129,130</sup> The high potential of TADDOL ligands ( $\alpha,\alpha,\alpha',\alpha'$ -tetraaryl-1,3-dioxolane-4,5-dimethanol) as chiral auxiliaries in catalysis and separation processes<sup>131</sup> has led different groups to study their immobilization on a variety of supports.<sup>132–139</sup> In the case of supported Ti-TADDOLates **62** (Fig. 10) prepared by grafting and studied for the Diels–Alder cycloaddition of cyclopentadiene and 3-crotonoyl-1,3-oxazolidin-2-one using a 10 : 1 catalyst dienophile ratio,<sup>129,130</sup> no clear rationale was given to explain the observed increase in activity, but the presence of changes in the mechanism can be envisaged, in particular taking into account the potential participation in this reaction of several complexes with different molecularities.<sup>140</sup>

An even more dramatic effect was observed in the case of some  $\beta$ -amino alcohol derivatives (Fig. 11).<sup>141</sup> Heterogeneous derivatives of (1*R*,2*S*)-ephedrine (**64**) and (1*R*)-3-pyrrolidinol (**65**) were easily prepared by direct reaction of the corresponding

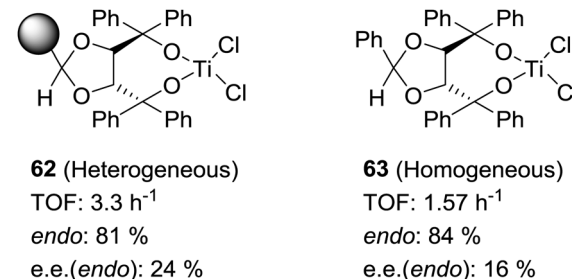


Fig. 10 General structures of supported Ti-TADDOLates and of supported  $\beta$ -aminoalcohols and their *N*-benzylated homogeneous analogues.

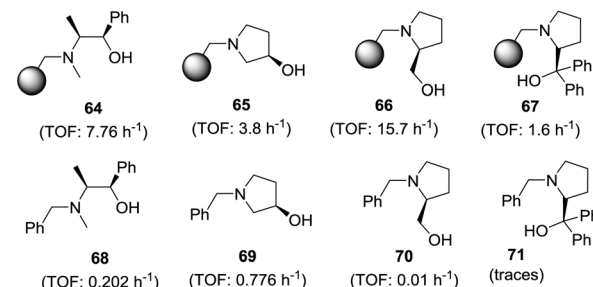


Fig. 11 General structure of supported chiral Lewis acids and the results for their application as catalysts for the Diels–Alder reaction of methacrolein with cyclopentadiene.

$\beta$ -amino alcohol with a Merrifield resin, while prolinols **66** and **67** were better prepared by initial reaction of the proline methyl ester with a chloromethylated resin followed by treatment with an excess of lithium aluminium hydride (**66**) or  $\text{PhMgBr}$  (**66**).<sup>142–144</sup> The corresponding *N*-benzylated derivatives (**68–71**) were prepared as the homogeneous analogues. The related chiral Lewis acids were obtained by the reaction of **64–71** with  $\text{EtAlCl}_2$  (see general structure, Fig. 11) and evaluated as catalysts for the Diels–Alder reaction of methacrolein with cyclopentadiene (Fig. 11).

The results presented in Fig. 11 clearly reveal that reaction times required to achieve the same chemical yields are much shorter always for the polymer-supported systems. Thus, for instance, in the case of (1*R*)-3-pyrrolidinol (**65**), the supported system allows obtaining a 95% conversion after 60 min (TOF:  $3.8 \text{ h}^{-1}$ ), whilst the catalyst derived from the *N*-benzylated analogue **69** requires a fivefold increase in time (300 min) to achieve a similar conversion (TOF:  $0.776 \text{ h}^{-1}$ ). In the case of the ephedrine derivatives **64** and **68**, the homogeneous system catalyses the reaction 38 times slower than the heterogeneous one. For the prolinol derivatives, it can be seen that, essentially, only the supported species are active (**66** and **67**). As could be expected, the more hindered derivatives (catalysts derived from **67** and **71**) are less active both in solution and in the supported

species. Again, the formation of aggregates in solution, which should be greatly inhibited on the heterogeneous systems, seems to be responsible for this behaviour.

A similar effect has been observed in the case of  $\alpha$ -amino amides derived from natural amino acids. They can be considered as structural equivalents of amino alcohols providing an acidic *N*-fragment instead of the hydroxyl group. Accordingly, their Ni(II) complexes were shown to be efficient chiral catalysts for the addition of Et<sub>2</sub>Zn to aldehydes.<sup>145</sup> However, in the absence of Ni(II) these ligands were unable to catalyse this reaction in opposition to the general behaviour observed for amino alcohols. Interestingly, when these amino amides were prepared attached to polystyrene matrices, the supported systems were found to be very active also in the absence of Ni(II), leading to the formation of 1-phenyl ethanol from benzaldehyde and Et<sub>2</sub>Zn in almost quantitative yields and >90% ee.<sup>146</sup>

### Dendrimers as supports

The use of dendrimers as supports is a suitable alternative to mitigate some of the diffusional problems ascribed to the gel-type resins, while maintaining some of the advantages found for the gel-type polymeric supports related to site isolation and suitable hydrophilic–hydrophobic balance.<sup>147–149</sup>

Their soluble nature and the possibility to locate the catalytic species in well-defined positions within the dendrimer can be used to tune the catalytic activity of a given catalyst (Fig. 12).<sup>150–152</sup> Different examples in non-asymmetric transformations have demonstrated significant enhancements in yields and activity in comparison with their homogeneous counterparts.<sup>153,154</sup> Such effects can be observed for the original monomeric component and/or for larger dendrimer generations and show a strong dependence on both the generation used and the localisation of the active sites. Indeed, the localization of the catalytic sites in the core of the dendrimer may lead to “positive dendrimer effects” originating either from the influence of the branches on the core, modifying the polarity of the environment, or from site isolation effects.

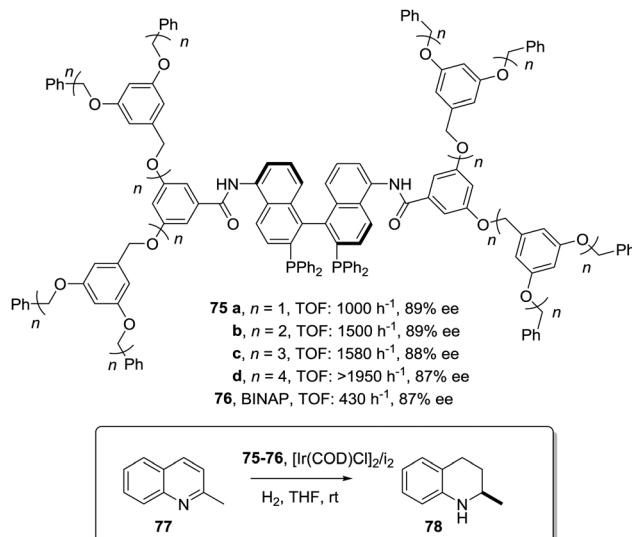


Fig. 13 Modified BINAP ligands at the core of dendrimeric structures and their application to the Ir-catalysed asymmetric hydrogenation of quinolines.

This can be illustrated in the case of 5,5'-modified BINAP ligands immobilized on the core of Frechet type dendrimers (Fig. 13). This supported catalyst provided impressive results for the Ir-catalyzed asymmetric hydrogenation of quinolones (77),<sup>155</sup> with an important enhancement in the catalytic activity from a TOF of  $1 \times 10^{-3}$  h<sup>-1</sup> for the first generation to  $19 \times 10^{-3}$  h<sup>-1</sup> for the fourth one without compromising the enantioselectivity. Noteworthily, the supported catalyst (75) was more active than the related homogeneous BINAP Ir complex (TOF 430 h<sup>-1</sup>). Indeed, the best catalytic dendrimer, under optimized conditions, behaved as a highly active catalyst with a maximum initial TOF of 3450 h<sup>-1</sup> and with a TON of 43 000, highlighting the non-innocent effect played by the support. This effect is attributed to the efficient site isolation reducing the formation of dimers observed for the unsupported complex.

Similar positive effects were also found for the asymmetric hydrogenation of 2-(4-isobutylphenyl)acrylic acid (79) catalysed by the same dendritic BINAP systems (75) complexed this time with Ru (Fig. 14).<sup>150,156</sup> Again the higher generation dendrimers showed an enhanced activity (up to a 3 times increase) than the unsupported homogeneous counterpart. Such a rate enhancement was not observed for the mono-substituted dendrimer and the activity was by far higher in toluene : methanol

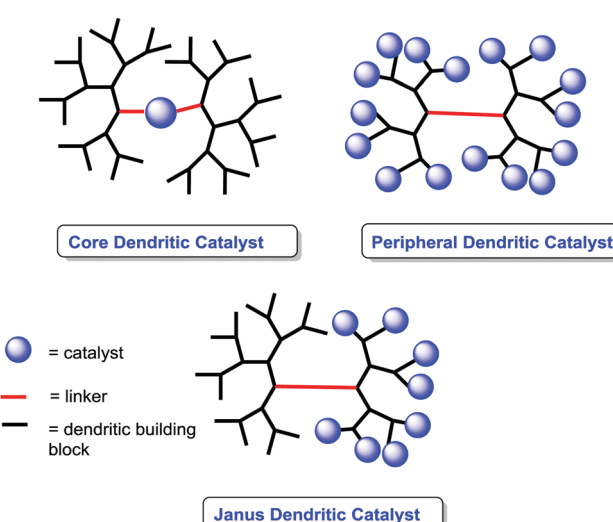


Fig. 12 General representation for dendritic catalysts.

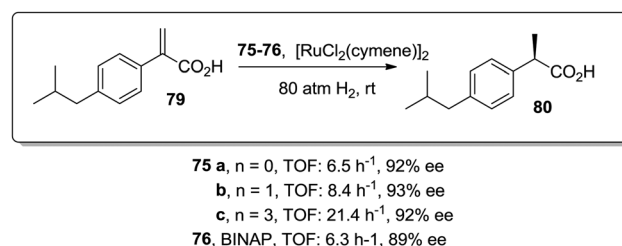


Fig. 14 Ru-Catalysed asymmetric hydrogenation in the presence of the modified BINAP ligand at the core of dendrimeric structures.



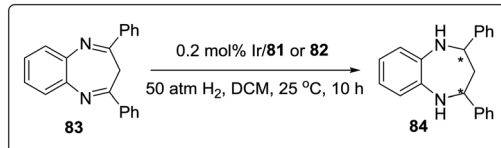
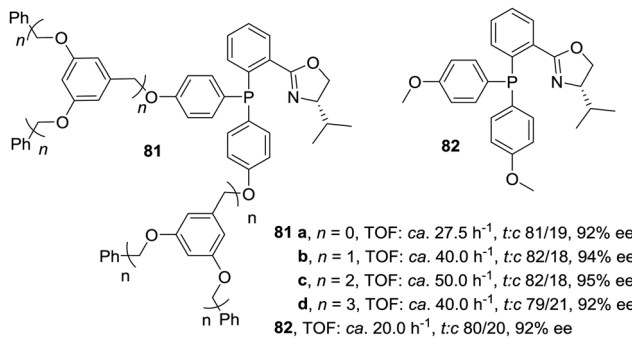


Fig. 15 Modified phosphinooxazoline ligands immobilized onto Fréchet type dendrimers for the asymmetric Ir-catalysed hydrogenation of diaryl-1,5-benzodiazepines.

(1:1, v/v).<sup>157,158</sup> These facts suggest that the dendrimers contribute to generate a suitable polar micro-environment to induce a pseudoconcentration effect of the substrates on the proximity of the catalytic sites. The same effect on activity was found when the Ru-BINAP homogeneous complex was encapsulated inside an analogous third generation Fréchet dendrimer lacking the catalytic center.

The activity observed for chiral Ir-phosphinooxazoline (PHOX) complexes immobilized onto Fréchet type dendrimers also surpassed the activity found for the homogeneous systems in the hydrogenation of diaryl-1,5-benzodiazepines (83). (Fig. 15).<sup>159</sup> Usually, the activity of the Ir-PHOX complexes is highly affected by the formation of polynuclear complexes,<sup>160</sup> but in the dendrimer supported systems (81) the sterically demanding dendrimer branches facilitate suitable site isolation reducing such adverse effect. In this way, the second-generation dendritic catalyst (81c) was *ca.* 4 times more active than the non-dendrimeric counterpart (82). However, the third-generation dendritic catalyst (81d) was only 2 times more active. This suggests that a compromise between site isolation and mass transfer is required to design a suitable catalytic dendrimer.

A similar reasoning has been used to explain the changes in activity found for dendritic systems containing 4-(dialkylamino)pyridines supported onto gel-type polymers as catalysts for acylation reactions.<sup>161</sup> From the experimental results, it was concluded that the nano-environment created by the dendrimer within the polymeric network played a dominant role in determining the activity of those supported catalysts.

A second type of “dendrimer effect” can be found when the catalytic units are located in the dendrimer periphery. In those cases, cooperativity between catalytic units is expected due to the high local concentration of these sites within well-defined nanoscopic peripheral space, which, in some cases, may result in a positive effect enhancing the catalytic properties. This can be illustrated, for instance, by the application of BINAP

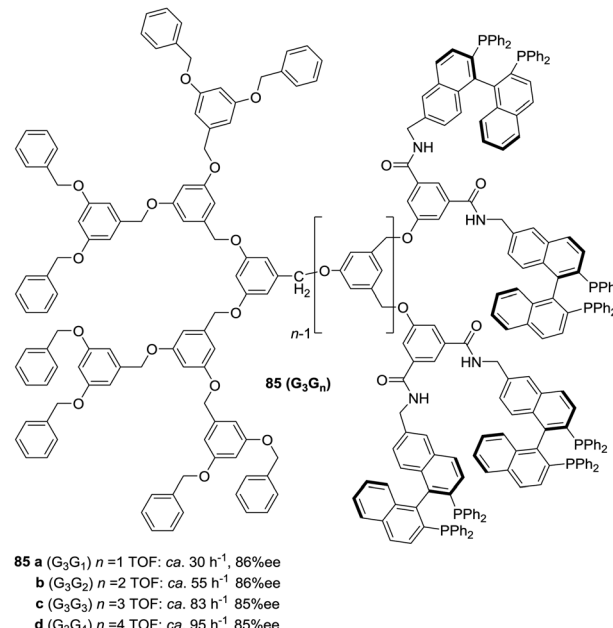


Fig. 16 Janus-type dendrimer structure containing BINAP peripheral subunits on one of the faces.

Janus-type dendrimers 85 formed by a Fréchet-type polyether dendrimeric unit fused to a second one having up to 16 peripheral BINAP moieties.<sup>162</sup> These BINAP subunits were able to form the corresponding ruthenium complexes for the asymmetric hydrogenation of 2-aryl-acrylic acid 79. The generation of the dendrimer influenced the reactivity of these catalysts with increasing reaction rates (more than 3.5 times increase) for the higher generations (Fig. 16).

An even more dramatic increase was found by Jacobsen for Co-salen complexes immobilized onto NH<sub>2</sub>-terminated PAMAM dendrimers (86) in the hydrolytic kinetic resolution of terminal epoxides (88; Fig. 17).<sup>163</sup> Mechanistic studies had suggested an increase in the catalytic activity by a cooperative interaction between catalyst units.<sup>164</sup> The presence of Co-salen units in the periphery of the dendrimer led to important cooperative interactions between [Co-(salen)] units due to their higher local concentration, affording an up to 24 times increase of the relative rate per [Co(salen)] unit in comparison with the homogeneous system 87. Hence, it is clear that dendritic supports offer very interesting opportunities to tune the activity of different types of catalytic systems, although an important drawback is the need for complex synthetic and purification processes in their preparation.

### Macroporous polymers as supports

A different possibility to minimise diffusional limitations is the use of macroporous polymers with permanent porosity. In this case, the functional sites are distributed both at the surface and

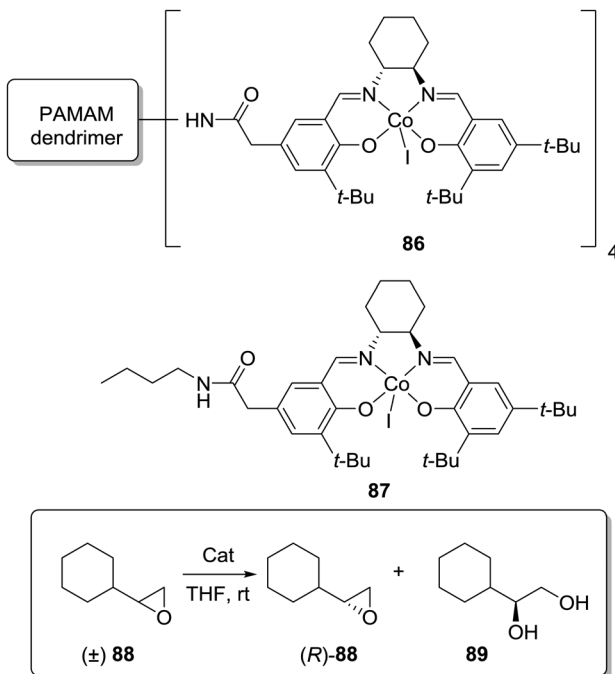


Fig. 17 General structure of a Co-salen complex immobilized onto  $\text{NH}_2$ -terminated PAMAM dendrimers used for the hydrolytic kinetic resolution of terminal epoxides.

at the interior of the dense polymer particles. Accessibility of sites located on the surfaces is greatly enhanced and does not depend very much on the solvent. In contrast, the functional groups located on the interior of the particles may not be easily accessible. The balance between surface and non-surface sites determines the activity of the resulting species and very often, this can be regulated through an appropriate selection of the polymerisation conditions.

This can be illustrated by the work of Abu-Elfotoh *et al.* with a macroporous polymer-supported chiral ruthenium(II)/phenyloxazoline (Ru-PHEOX) complex (90; Fig. 18), prepared by copolymerization of the corresponding monomeric complex with styrene and 1,4-divinyl benzene (DVB) in water:  $\text{CH}_2\text{Cl}_2$  (7:2).<sup>165</sup> The resulting catalyst displayed, in the cyclopropanation of styrene (50) with EDA (51), a higher activity than the homogeneous catalyst 93 (TOF of  $3.034 \text{ h}^{-1}$ , *cis:trans*: 88:12, 94% ee vs. TOF of  $2.694 \text{ h}^{-1}$  *cis:trans*: 90:10, 98% ee). Interestingly, the polymer 92, obtained under the same conditions as 90, but by initial polymerisation of the phenyloxazoline ligand followed by complexation with the metal, suffered from a significant drop in catalytic efficiency in terms of both activity and enantioselectivity (TOF of  $1.102 \text{ h}^{-1}$ , *cis:trans*: 83:17, 74% ee). Furthermore, the polymeric catalyst 90 was also more active than the one based on a macroreticular polymer (91, *ca.* 50% DVB) (TOF of  $1.265 \text{ h}^{-1}$ , *cis:trans*: 82:18, 84% ee). The difference in activity can be explained based on the macroporous structure of the different materials. The direct polymerisation of the Ru-complex, in the presence of water:  $\text{CH}_2\text{Cl}_2$ , afforded a

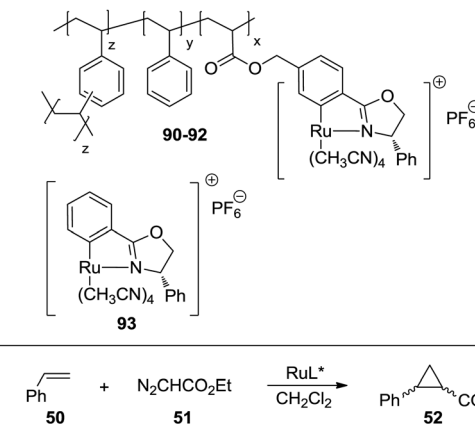


Fig. 18 Structure of Ru-PHEOX polymers studied as catalysts for the cyclopropanation of styrene.

uniform distribution of the catalytic sites in the polymeric matrix, which also presented a larger internal surface area than the macroreticular-type catalyst 91.

Petri *et al.* have studied how the asymmetric dihydroxylation of alkenes, catalysed by cinchona alkaloid derivatives (96–98; Fig. 19), is strongly affected by the appropriate design of the polymeric matrix.<sup>166</sup> The rate of dihydroxylation of styrene

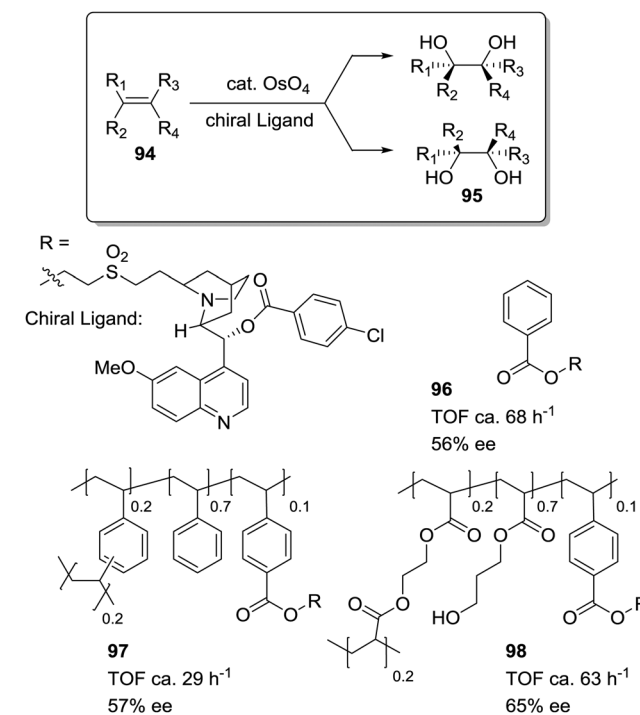


Fig. 19 Cinchona alkaloids supported on polymeric matrices of different polarity for the dihydroxylation of alkenes.



depends on the hydrophobic/hydrophilic properties of the polymeric backbone. The activity increases for supports with a more hydrophilic backbone (**98**) (introduction of HEMA and EGDMA as comonomers), showing similar results to those obtained under homogeneous conditions (**96**). Only one hour is required to afford an 80% conversion with **96** and **98**. With a PS-DVB matrix (**97**), however, four hours are required to get a similar conversion.

Ti-TADDOLates also provide a useful example. In fact, when the kinetics for the Et<sub>2</sub>Zn addition to PhCHO using supported Ti-TADDOLate catalysts such as **102** (Fig. 20) was initially considered, the measured rates were significantly slower than for the homogeneous analogue, and this was ascribed to the reduced accessibility to the catalytic sites.<sup>167</sup> One of the strategies considered to overcome this limitation, improving the accessibility of the active sites, was the incorporation of the chiral ligand at the core of a polymerizable dendrimer (**99**).<sup>168,169</sup> Only for the polymer prepared from **99** and styrene, the rate of the heterogeneous reaction increased relative to that in the homogeneous phase using directly **99**.

The rate depended on the loading, with slower rates observed for higher loadings. This is reasonable, as this functional monomer acts as the crosslinker and, accordingly, higher loadings increase crosslinking and would make it difficult to access the reactive sites. Several reasons are given to explain this behaviour. They include considering that the attachment of the dendritic arms of **99** to the polymeric backbone could hinder them from wrapping around the TADDOL core, allowing, in this way, a better diffusion of reactants to and from the catalytic center.

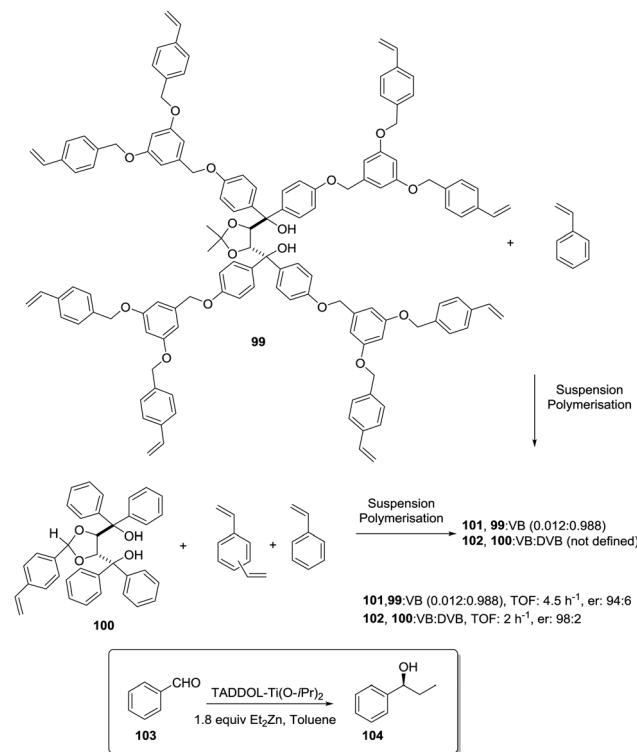


Fig. 20 Preparation of polymer-supported TADDOLs via copolymerization of the corresponding vinylic TADDOL derivatives.

On the other hand, the “oxygen-rich” dendritic branches could provide a more polar environment around the active sites within the apolar polystyrene matrix. This could, for instance, favour the accumulation of polar substrates (PhCHO, Et<sub>2</sub>Zn) in the proximity of the catalytic centres, increasing the local concentrations and, hence, leading to higher rates.

As mentioned, a possible alternative to obtain supports with good diffusional properties is the use of polymeric macroporous monoliths, which can be moulded in different shapes according to the required uses.<sup>170</sup> In a polymeric monolith,<sup>171</sup> the resin can be described as a continuous material integrated with highly crosslinked particles and presenting a complex network of permanent pores. Usually, those materials are prepared by polymerisation of a mixture containing a functional monomer along with styrene (VB) and divinylbenzene (DVB) (or the corresponding crosslinking agent, *i.e.* **106** or **107** in Fig. 21) in the presence of an appropriate porogen.

Polymer-supported bis(oxazolines) (BOX) can be prepared following this strategy as monolithic polymers. The accessibility of the functional sites can be assessed through the analysis of the copper uptake after treatment with Cu(OTf)<sub>2</sub> (Fig. 21).<sup>172–175</sup> Several resins were prepared using monomeric mixtures containing variable amounts of the functional monomer **105**, styrene and DVB. As can be seen from the data depicted in Fig. 21, the accessibility of the bis(oxazoline) groups on the polymer seems to be related to the loading and the crosslinking degree. The number of non-accessible sites increases, in general, with both parameters. The increase with loading is reasonable, as the functional monomer acts as a crosslinker and, accordingly, higher loadings increase crosslinking and would make it difficult to access the reactive sites. Nevertheless, this is

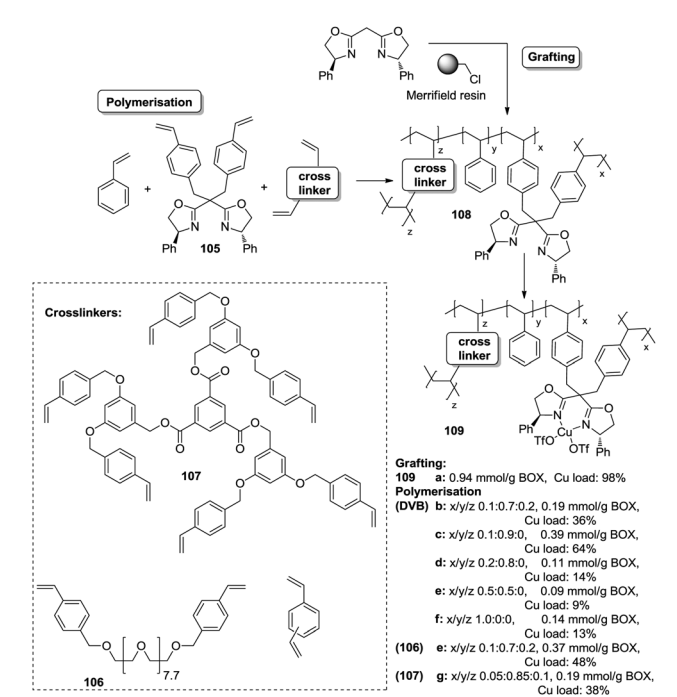


Fig. 21 Preparation of monolithic polymers by polymerization of vinylic BOX derivatives.

not a simple relationship, and thus the copper uptake of the homopolymer **109f** (100% of functional monomer, 100% of crosslinking) is comparable with that obtained for a polymer containing only 20 molar% of the functional monomer and 80% of styrene (**109d**). As also shown by the use of JandaJel and related resins,<sup>58,176,177</sup> the use of more flexible crosslinking agents, such as the vinylic derivative **106** (Fig. 20) containing a PEG chain, favours the accessibility of the bis(oxazoline) moieties. Thus, for one of the monomeric compositions used for polymer **109e** (10 : 70 : 20), but using **106** instead of DVB, 48% of the reactive sites were loaded with Cu.<sup>172,178</sup> Some increase in the Cu uptake was also observed for the polymer **109g** where first generation dendrimers containing at least six vinylic groups (**107**) were used as the crosslinkers (up to 38% of functional groups loaded with copper).<sup>179</sup>

Finally, the exact balance between accessible and non-accessible sites is clearly dependent on the polymerisation conditions and here the porogen can play a central role. Thus, for the homopolymers prepared from **105**, the use of toluene/dodecanol as the porogenic mixture produces a polymer in which about 13% of the functional groups are accessible, whilst only 1% of the groups are accessible when toluene, which has been described to form small pores,<sup>85,180,181</sup> is the only component of the porogenic mixture.

As the BOX monomer conserving the  $C_2$ -symmetry acts itself as a crosslinking agent and can reduce the accessibility of some of the active sites, a “ $C_2$ -disruptive” design for the BOX monomeric derivative may provide a suitable alternative to reduce to a minimum the structural perturbation induced by polymerization, enhancing accessibility. Mandoli *et al.* have exploited this concept to immobilize the BOX ligand by either copolymerisation or grafting (Fig. 22).<sup>182,183</sup> Furthermore, and to minimise the backbone effect, an alkyl flexible linker was also used to tether the ligand to the support.

The copolymerisation of the corresponding functionalised monomer (**111**) with toluene as the porogenic agent rendered a support with *ca.* half of the functional sites accessible (**115**). This represents a significant accessibility improvement over the above mentioned  $C_2$ -BOX systems. In the case of the functionalised polymer prepared by grafting, all the ligands appeared to be accessible.<sup>183</sup>

However, the use of long linkers does not always represent an optimal approach. This can be illustrated by the differences in functional site accessibility observed for the case of polymer supported pyridinebis(oxazoline) ligands **116–117** (PYBOX) prepared by copolymerisation as crosslinked monoliths or by grafting onto commercially available Merrifield resins (Fig. 23).<sup>184,185</sup> It should be noted that Ru–PYBOX complexes, depending on the concentration, can lead to dimer formation. Thus, especially for resins with low crosslinking degrees, an increase in the spacer length could enhance accessibility at the expense of site–site isolation, favouring the formation of dimeric species, which will be also favoured by a pseudo-concentration effect on the polymeric network. The accessibility was estimated taking into account the Ru uptake relative to the ligand loading. For the resins obtained by polymerisation (**119d–g**), the Ru uptake

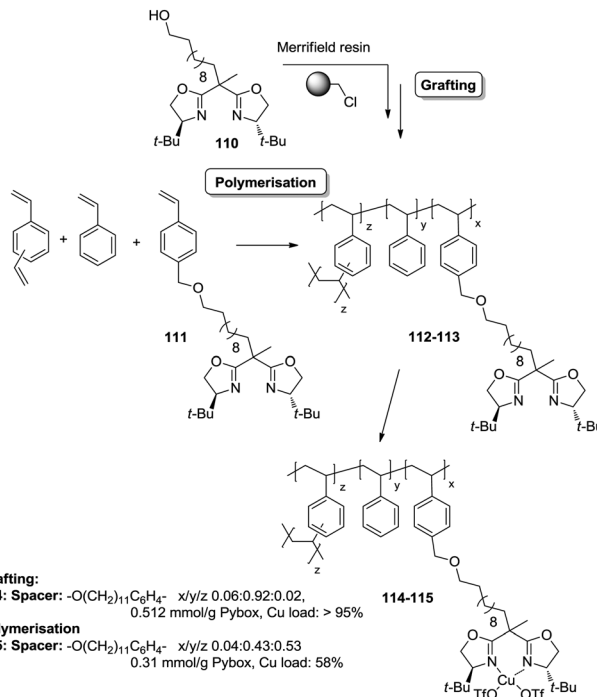


Fig. 22 Preparation of polymer-supported BOX derivatives through a  $C_2$ -disruptive strategy for improving the accessibility of the active sites.

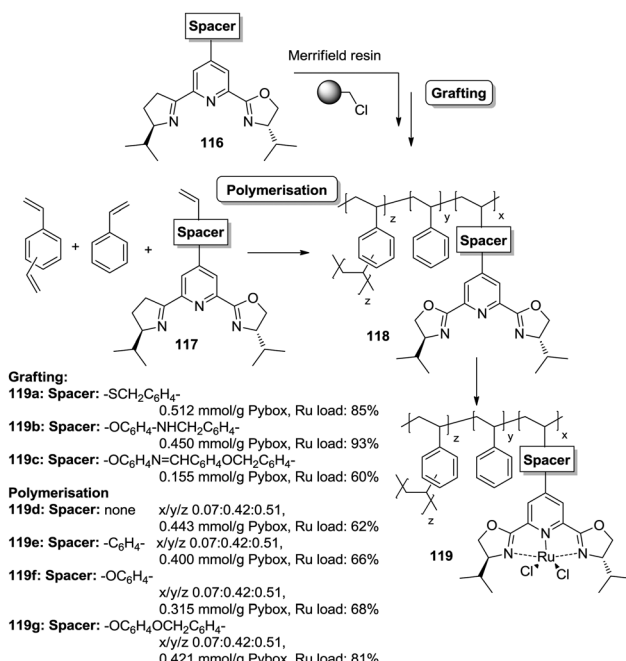


Fig. 23 Preparation of polymer-supported PYBOX derivatives through different strategies and with different linkers.

steadily increased from 62% to 82% with the length of the spacer. The larger spacers reduce the steric hindrance provided by the polymeric backbone improving PYBOX accessibility. For these highly crosslinked resins (51% DVB, **119d–g**), the crosslinking helps to reduce site–site interactions. In the case of



supported PYBOX ligands obtained by grafting, a positive effect of length of the spacer, facilitating good accessibility to the ligand, was observed for resins **119a** and **119b**, with Ru-uptakes of 85% and 93%, respectively. However, when the length of the spacer was further increased (**119c**), the Ru-uptake was only 60%, most likely due to the formation of dimeric species.

These examples illustrate the effects of the methodology used in the immobilisation of a given catalyst on the accessibility of the catalytic sites, especially for systems based on the polymerisation of the corresponding chiral ligand and/or complex. Different aspects like type and amount of porogen, type and degree of crosslinking, use of spacers, *etc.*, should always be carefully considered for optimization of the accessibility to the catalytic sites.

An illustrative example of how supported species on highly crosslinked polymeric frameworks can be more active, with better reaction rates, than the corresponding homogeneous analogues is provided by some of the polymer-supported bis(oxazolines) mentioned above. For the immobilized BOX ligand prepared using a dendrimeric crosslinking agent, the total TON was 70.8 moles cyclopropanes per mol BOX, while for the homogeneous analogue the TON observed under the same conditions was 3.2. The effect is more significant taking into account that less than 40% of the box moieties are able to form the corresponding Cu-BOX complex. According to this, the TON was calculated to be 184 moles cyclopropanes per mol Cu-BOX.<sup>178,179</sup> Some improvements were also observed for the PYBOX derivatives. In this case, the catalysts obtained by grafting displayed a similar activity as the homogeneous unmodified catalyst, but up to a twofold increase in catalytic activity was observed for some of the systems prepared by polymerisation.<sup>184</sup>

Immobilization on an appropriate support can be used to suppress site–site interactions, affording a great effect on activity. Although eventually this can be achieved in microreticular polymers, particularly for low catalyst loadings, this effect can be facilitated by the use of macroporous, highly crosslinked polymers. An interesting example is provided by ruthenium porphyrin catalysts immobilized in a highly crosslinked matrix, where catalyst deactivation by intermolecular reactions was strongly decreased.<sup>186</sup> The incorporation of a Ru(CO)(porphyrin) complex in such a matrix was carried out by suspension polymerization of the corresponding vinyl-substituted *meso*-tetraarylporphyrin complex with ethylene glycol dimethacrylate (EGDMA) in the presence of the appropriate porogenic mixture. The activity of this polymeric catalyst in epoxidation reactions was slightly higher than that of the homogeneous vinyl-substituted *meso*-tetraarylporphyrin complex (initial TOF value of  $40\text{ h}^{-1}$  vs.  $27\text{ h}^{-1}$  for the homogeneous system). The differences in activity were significantly much higher for the catalytic oxidation of aromatic alkanes or secondary alcohols to the corresponding ketones. In some instances, initial TOF values for the supported system were up to one order of magnitude higher than those of the homogeneous counterpart. A further increase in activity by a factor of up to 16 was achieved by preparing the corresponding imprinted polymer using diphenylaminomethane or 1-aminoadamantane as the template.<sup>187</sup> This suggested that

the presence of the appropriate pseudosubstrate coordinated to the vinylic Ru(CO)(porphyrin) complex can generate an imprint (substrate pocket) in close proximity to the active site. In agreement with this hypothesis, the rate enhancement observed was strongly dependent on the template. An alternative strategy for improving the activity of those supported Ru(CO)(porphyrin) complexes was the use of perfluoromethylcyclohexane as a cosolvent.<sup>188</sup> The presence of the fluorous solvent facilitated a favourable partitioning of substrates and oxidant into the polymeric matrix,<sup>189,190</sup> leading to an increased local concentration of substrates and reagent in the vicinity of the catalytic site.

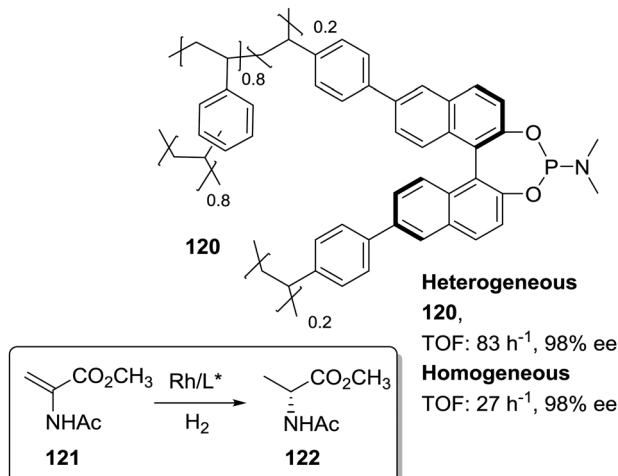
### Porous organic polymers as supports

In the search of more efficient predesigned polymeric frameworks for the immobilisation of chiral ligands, a bottom-up approach, in which different building blocks are assembled into hierarchical porous polymeric materials with well-defined and tuneable physicochemical properties, is gaining momentum.<sup>61–75</sup> These materials exhibit unique properties such as large BET surface areas and pore volumes, enhanced accessibility of catalytically active sites, and decreased diffusional limitations. Therefore, they can lead to highly active heterogeneous catalysts able to surpass the activity found for the homogeneous counterparts. This is illustrated, for example, by the 2D metallocporphyrin polymeric frameworks obtained by cross-coupling polycondensation that displayed impressive TON ( $6.7 \times 10^7$ ) and TOF ( $9300\text{ min}^{-1}$ ) values for the epoxidation of olefins with superior performance than the non-immobilised catalyst.<sup>191,192</sup>

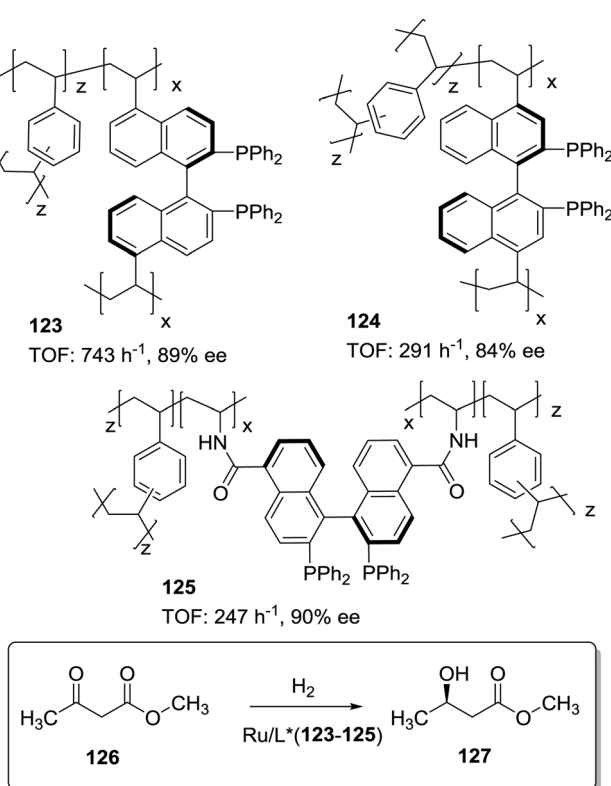
Among the different approaches for the preparation of POPs and related systems, copolymerization *via* free-radical polymerization of mono or poly-vinyl-functionalised chiral ligands with additional crosslinked monomers, especially DVB, under solvothermal conditions has led to the synthesis of highly crosslinked and functional polymers.<sup>193,194</sup> Based on this methodology the heterogeneous phosphoramidite ligand **120** was prepared by copolymerization of the corresponding di-vinyl-MonoPhos ligand with DVB (1 : 4 by weight; Fig. 24).<sup>195</sup> The corresponding Rh complex was at least three times more active than the homogeneous control. The highly crosslinked framework can inhibit the self-quenching found in solution *via* multimolecular deactivation. Besides, the excess of chiral ligand in the polymeric network seems to favour the stability of the catalytic complex against deactivation through decomposition into metallic Rh nanoparticles.

The position and type of polymerisable moieties introduced on a given chiral ligand are the factors that should be carefully considered. The rigid polymeric organic porous framework is built up through condensation of these functional groups by themselves or in the presence of an additional building block. Thus, the position, number and type of linker can play a decisive role in defining the catalytic activity. For instance, Wang *et al.* have demonstrated that (*S*)-5,5'-divinyl-BINAP-DVB (**123**) prepared by solvothermal copolymerisation of a modified BINAP with DVB (9 : 81 by weight) produced a mesoporous material with a large surface area ( $1058\text{--}1070\text{ m}^2\text{ g}^{-1}$ ), which was 2.5 times more active for the Ru-catalysed hydrogenation of





methyl acetoacetate than the analogous copolymer obtained by copolymerisation of (*S*)-4,4'-divinyl-BINAP and DVB (124; Fig. 25) for a substrate/catalyst ratio of 1000.<sup>196</sup> The derivatisation at the 4,4' positions, closer to the catalytic sites, is likely to reduce the flexibility of the resulting polymer around the BINAP fragments making the sites less accessible to the substrates. A similar material was prepared with a BINAP bearing at 5,5'-positions acrylate groups instead of the vinylic residues.<sup>197</sup>

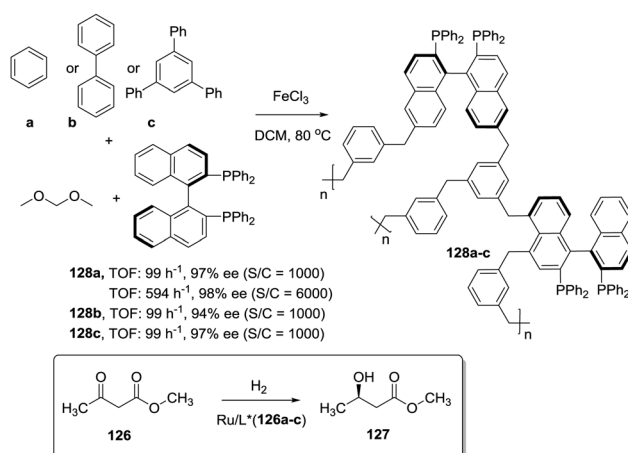


The material obtained by polymerisation with DVB (125, 20% DVB by weight) in spite of its lower surface area ( $524 \text{ m}^2 \text{ g}^{-1}$ ) was able to quantitatively convert methyl acetoacetate with good enantioselectivity (90% ee) and at very high substrate/catalyst ratios (up to 5000), being within the more active systems reported for this reaction.

In the knitting strategy developed by Tan and coworkers, the very reactive formaldehyde dimethyl acetal (FDA) is employed to crosslink, through rigid methylene bridges, a variety of simple aromatic building blocks like benzene or biphenyl in a  $\text{FeCl}_3$  catalysed Friedel-Crafts reaction. The resulting polymeric networks have predominant microporosity and a high surface area.<sup>198</sup> In this way BINAP has been immobilised in a variety of hypercrosslinked polymeric aromatic networks without requiring the previous preparation of modified BINAP structures (128, Fig. 26).<sup>199</sup> These materials are insoluble and porous, with large surface areas of  $1100\text{--}1200 \text{ m}^2 \text{ g}^{-1}$ . The optimised catalyst demonstrated a satisfactory activity for the hydrogenation of 126 at very high substrate/catalyst molar ratios (S/C = 6000) for 10 hours with similar enantioselectivity and activity as those prepared by polymerisation.

BINAP has been also immobilised in chiral conjugated microporous polymers (CMPs). Apart from the advantages of common POPs, such as large surface areas and high stability, the porous structure and surface area of CMPs can be finely controlled at a molecular level through the rigid node-strut topology of the monomer structure. CMPs functionalized with catalytic units can be regarded as heterogeneous catalysts.<sup>72,73</sup>

The preparation of BINAPO-CMPs was carried out through the Sonogashira-Hagihara reaction of (*R*)-4,4'-dibromo BINAPO (129) with alkynes of different lengths (Fig. 27).<sup>200</sup> The BET surface areas ranged from  $391 \text{ m}^2 \text{ g}^{-1}$  to  $509 \text{ m}^2 \text{ g}^{-1}$  depending on the alkyne used. The corresponding Ru-complexes were active for the asymmetric hydrogenation of  $\beta$ -keto esters. More interestingly, a significant activity enhancement was found when their Ir-complexes were used for the asymmetric hydrogenation of quinolines.<sup>201</sup> The catalyst 130 prepared by polycondensation



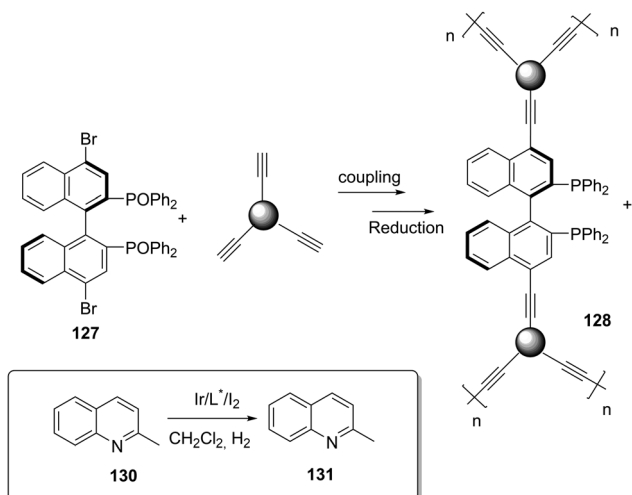


Fig. 27 Preparation of BINAPO–CMPs used for the Ir-catalysed hydrogenation of quinaldine.

of **129** with 1,3,5,7-tetrakis(4-ethynylphenyl) adamantine was four times more active than the homogeneous catalyst providing the same enantioselectivity. This effect was associated with the spatial site isolation of the BINAP catalytic sites that were evenly distributed within the rigid CMP framework preventing the formation of dimers.

As in the case of dendrimers discussed above, site isolation is not the only way by which the crosslinked matrix can contribute to increase the activity of supported systems. In fact, the opposite mechanism can also be found. Different catalytic systems involve the participation of more than one catalytic unit. In those cases immobilization with high loading degrees favours the presence of high local concentrations (pseudoconcentration effect) and this can contribute to facilitate the formation of the active species.<sup>202</sup>

A nice demonstration of the former principle was provided in the case of polymer-supported chiral Co-salen complexes.<sup>203</sup> Both silica (**133**) and polystyrene-bound (**134**) complexes were used for the hydrolytic kinetic resolution of terminal epoxides (Fig. 28). A clear correlation between the loading of the heterogeneous surface and the rate was observed in the case of silica-supported catalysts, with the presence of a minimum level of loading for the reaction to proceed. The polymeric backbone used for the preparation of **134** contained a very low degree of crosslinking (2%) and this seemed to provide enough flexibility as to favour inter-complex interactions.

The structure of the POPs can be also adjusted considering the mechanistic requirements of the catalyst to be immobilized, by properly selecting the nature of the building blocks to favour

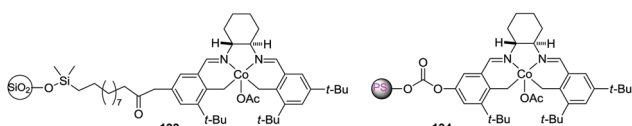


Fig. 28 Silica and PS supported chiral Co-salen complexes displaying positive pseudoconcentration effects in the kinetic resolution of terminal epoxides.

site–site interactions. Thus, Zhong *et al.* have designed flexible porous organic frameworks integrating high loading of Co-salen as the active sites, achieving higher activities than the homogeneous counterpart in the hydration of propylene epoxide (TOF: 3300 vs. 2670 h<sup>-1</sup>, calculated at a conversion <30%).<sup>204</sup> The polymeric porous structure was prepared by poly-condensation of cyclohexanediamine with 1,3,5-tris(3'-*tert*-butyl-4'-hydroxy-5'-formylphenyl) benzene (TBHFPB) and the 3D-flexible salen network was considered to enhance the cooperation of nearby Co-salen units. Thus, the polycondensation of different building blocks together with the chiral ligand and/or complex by a bottom-up approach offers a wide range of new exciting possibilities.

Sun *et al.* reported the immobilization of a Noyori–Ikariya asymmetric catalyst onto a superhydrophobic mesoporous polymer prepared by copolymerization of *N*-*p*-styrenesulfonyl-1,2-diphenylethylenediamine with DVB under solvothermal conditions (Fig. 29). This Ru catalyst (**137**) presented a higher activity than the homogeneous analogue for the asymmetric transfer hydrogenation of acetophenone.<sup>205</sup> A bottom-up approach allowed the design of a material with the appropriate porous structure (pore size distribution of *ca.* 11.8 nm, BET surface area of 481 m<sup>2</sup> g<sup>-1</sup> and pore volume of 0.55 cm<sup>3</sup> g<sup>-1</sup>) and superhydrophobic character that provided a suitable mass transfer of reagents and product to and from the catalytic sites. Due to the wettability properties of the material, acetophenone was absorbed preferentially and the catalytic sites within the porous polymer were enriched with the reactants, leading to a pseudo-concentration effect. The superhydrophobicity also favoured an efficient transfer of the more polar product from the polymer network to the water phase. Noteworthily, when an analogous polymer without nanoporosity was used instead of **137**, low levels of conversion were observed (<5% yield). This is in good agreement with the above mentioned results reported by Itsuno using gel-type resins (Fig. 6).<sup>115–120</sup>

Thus the immobilisation strategy determines again the activity of the resulting immobilised catalyst. This can be further highlighted by the immobilisation of BINOL-derived phosphoric acids (Fig. 30). This chiral organocatalyst has been supported by polymerisation of the corresponding monomeric derivatives with styryl substituents in either the 3,3'- or 6,6'-positions of the BINOL skeleton with styrene and DVB.<sup>206</sup>

Alternatively, a microporous material with a BET surface area of 386 m<sup>2</sup> g<sup>-1</sup> was obtained by self-condensation of chiral

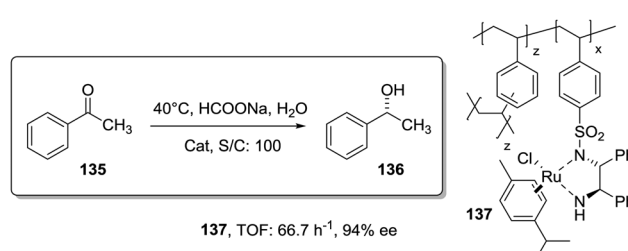
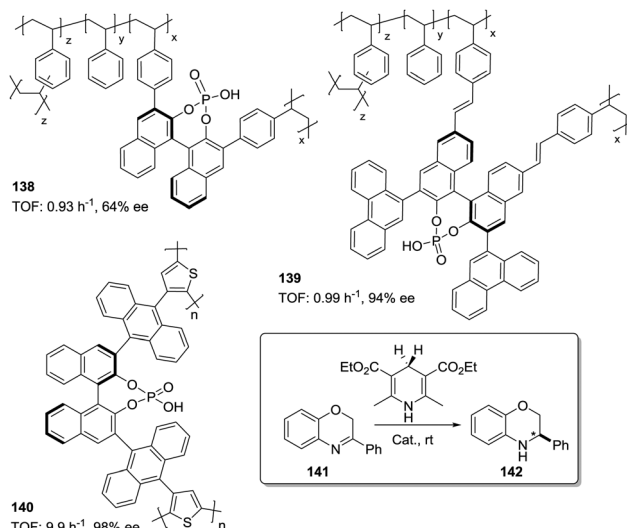


Fig. 29 Superhydrophobic mesoporous polymer prepared under solvothermal conditions containing Ru–TsDPEN for the asymmetric transfer hydrogenation of ketones.



**Fig. 30** General structures of polymer immobilized BINOL-derived phosphoric acids prepared through different approaches and used for the asymmetric transfer hydrogenation.

1,1'-binaphthalene-2,2'-diyl hydrogenphosphate (BNPPA) with 9-anthracenyl groups in 3,3'-positions and a 3-thiophenyl group at the 10-position of the anthracene units. These fragments facilitate the condensation reaction by mild oxidative coupling reaction in the presence of  $\text{FeCl}_3$ .<sup>207</sup>

Using 5 mol% of these polymer-supported catalysts **138** and **139**, a 20–24 h reaction time was reported to achieve full conversion of the imine **141** into the corresponding 3-phenyl-2H-1,4-benzoxazine (**142**) with 64% ee and 94% ee, respectively. However, for the catalyst obtained by self-condensation through oxidative coupling (**140**), the same reaction was complete within 2 hours with this catalyst being as fast as the homogeneous catalyst. The surface area and pore volume of the microporous polymer networks could be further tuned by co-polymerisation of the chiral building block in the presence of 1,3,5-tris(2-thienyl)-benzene. The resulting reaction rate for the same reaction was enhanced by increasing the accessible surface area and pore volume of the microporous polymer network. These copolymers were more active than the corresponding homopolymer **140**.<sup>208</sup>

Jiang and co-workers have exploited the post-modification of the walls of an achiral COF to immobilise in the open channels chiral organocatalytic moieties while retaining the crystallinity and porosity of the framework (Fig. 31).<sup>209,210</sup> The mesoporous imine-linked COFs were prepared by condensation of different di-aldehydes with triamines or tetramines. The presence of ethynyl groups on the walls of the pores allowed their further click reaction with pyrrolidine azide to quantitatively yield the corresponding post-functionalised COF. The materials **143** and **144** have been tested for asymmetric Michael reactions in water, displaying better activities than the homogeneous analogue, while retaining enantioselectivity. The results suggest that the crystallinity and porosity of COFs play a vital role in determining their catalytic activities. Analogous amorphous and nonporous polymeric catalytic systems required significantly longer times to complete the reaction (43 and 65 h vs. 1–2 h for the COF). It is

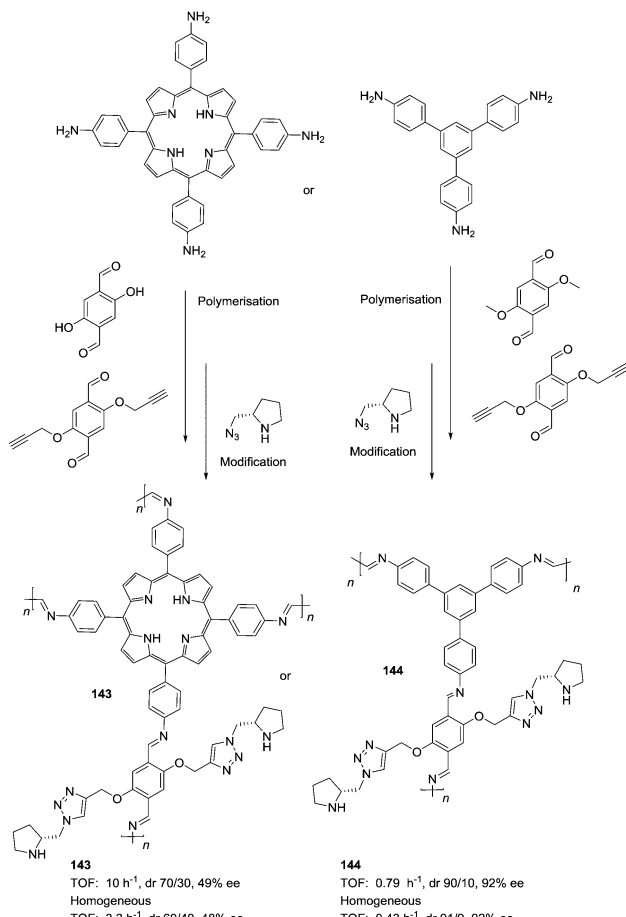


**Fig. 31** General structures of imine-linked COFs postfunctionalized with pyrrolidine units on the walls of the porous framework

worth mentioning that the catalytic activity depends upon the density of the active sites on the pore walls. A high density of pyrrolidine units in the pores induced a steric congestion impeding the mass transport through the channels.

Davies and co-workers have reported the immobilisation of dirhodium tetracarboxylate complexes derived from *N*-aryl-sulfonyl prolines (**147** and **151**) and their use as catalysts for the asymmetric cyclopropanation of alkenes using methyl aryldiazoacetates.<sup>211-214</sup> For that purpose, they developed a pyridine containing resin in order to axially coordinate the metal centers in the active complexes (Fig. 32). The resulting supported Rh species based on **149** and **153** showed a higher activity than their homogeneous analogue (derived from **148** and **152**, respectively) even considering that donor groups such as pyridine tend to deactivate dirhodium tetracarboxylates.<sup>215</sup> Some data, in particular the fact that a supported active complex could be also obtained from a resin containing no pyridine moieties (**150** and **154**), suggested that immobilisation could take place due to a microencapsulation effect.<sup>216,217</sup> The differences in activity, in this case, were attributed either to a pseudodilution effect or to the microenvironment inside the polymer.

The “microencapsulated (MC) catalysts” and “polymer incarcerated (PI) method” can be considered as a limiting case

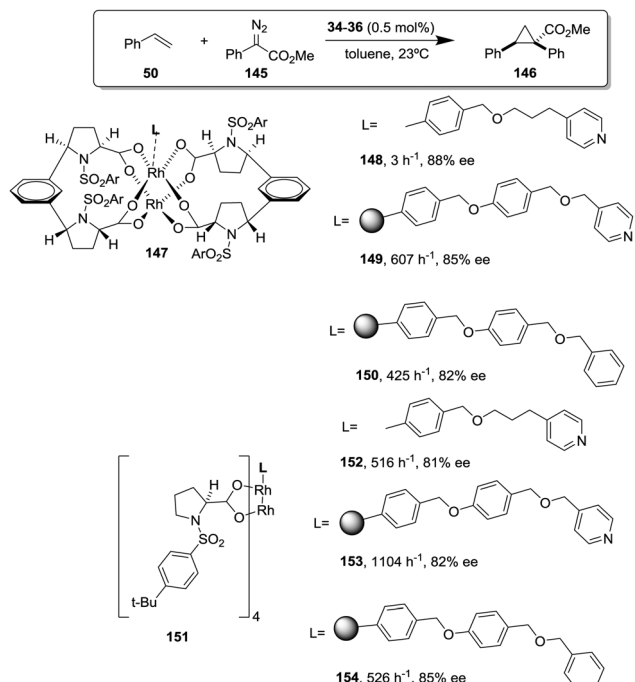


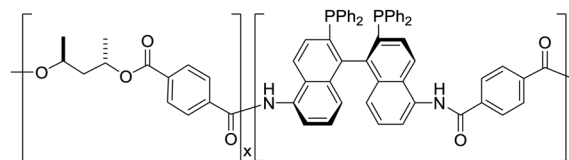
Fig. 32 Dirhodium tetracarboxylate complexes derived from *N*-arylsulfonyl prolines immobilised on resins containing pyridine.

in between soluble and insoluble supports.<sup>217</sup> In MC, catalysts are physically entrapped by a polymeric network (polystyrene derivatives in many cases) and at the same time immobilized by the interaction between the  $\pi$  electrons of the benzene rings of polystyrene and vacant orbitals of the catalysts (metal compounds). In the PI method, a catalyst is first physically microencapsulated in a dynamic system and then the microcapsules formed are crosslinked to afford the desired heterogeneous system. In these systems diffusion through the walls of the “capsule” is a key factor to determine the catalytic activity. In some particular cases, as pointed out before, the microencapsulated catalyst can be more active than the homogeneous counterpart, as is the case of micro-encapsulated  $\text{Sc}(\text{OTf})_3$ . Kinetic data revealed that its activity was higher than that of monomeric  $\text{Sc}(\text{OTf})_3$  for aldimine-selective reactions, most likely because of the higher stability of aldimine–Lewis acid complexes using polymer-supported acids.<sup>218,219</sup>

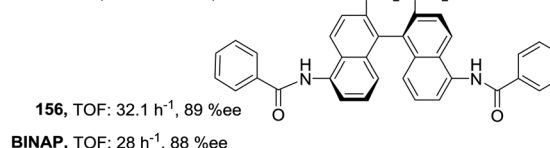
### Soluble polymers as supports

Taking into account some of the previous considerations, it seems reasonable that examples of supported species being more active than the homogeneous ones can be also found for soluble polymeric supports. For soluble polymers diffusion issues encountered in crosslinked resin can be minimised.<sup>43–45,220</sup> Soluble polymers, especially when prepared by controlled polymerisation, provide a facile control on the incorporation of catalytic sites either as pendent groups or at the main polymeric chain and an easy adjustment of the nature of the polymer matrix and the catalyst loading, just by using the suitable polymerization technique and monomeric mixture.

Thus, for instance, Fan *et al.* studied the soluble polymer **155** containing BINAP subunits for the Ru-catalyzed asymmetric



**155**, TOF:  $47.5 \text{ h}^{-1}$ , 88% ee



**156**, TOF:  $32.1 \text{ h}^{-1}$ , 89% ee

BINAP, TOF:  $28 \text{ h}^{-1}$ , 88% ee

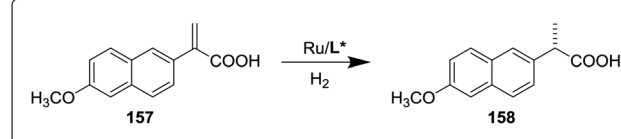


Fig. 33 General structure of soluble polymers containing BINAP fragments in the main chain studied for asymmetric Ru-catalysed hydrogenations.

hydrogenation of 2-(6'-methoxy-2'-naphthyl)acrylic acid (**157**) to form naproxen (**158**, Fig. 33).<sup>221</sup> A complete conversion was obtained with **155** after *ca.* 4 hours, while 8–9 hours were required with the use of the non-polymeric analogue **156** and 48 hours for (*S*)-BINAP itself. Similar increases in activity have been found for other related systems in which the (2*S*,4*S*)-pentanediol component was substituted by polyethyleneglycol chains.<sup>222,223</sup>

Soluble polymer-supported chiral phosphoramides (**159** and **160**) have been reported to be significantly more efficient than the corresponding homogeneous analogue (**161**) for the organocatalytic allylation of benzaldehyde with allyltrichlorosilane (Fig. 34).<sup>224</sup>

It is important to bear in mind that upon immobilization of a given catalyst, significant changes in the mechanism may occur, including changes in the molecularity of the active complexes, as shown, for instance, for supported Sharpless alkene epoxidation catalysts.<sup>225</sup> For these supported chiral phosphoramides, the loading of the catalytic sites on the polymer is rather high (DF = 37–100% of the aromatic rings functionalised).

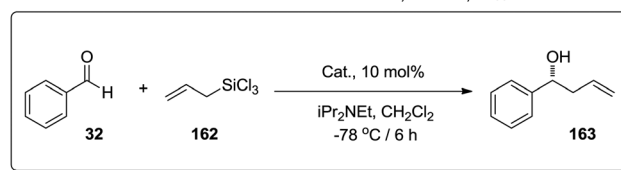
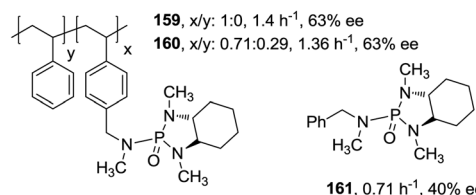


Fig. 34 General structure of soluble polymers containing chiral phosphoramides as pendant groups for asymmetric organocatalytic allylations.

Hence, the pseudo-concentration on the polymeric matrix facilitates site-site interactions.

The 2.4 times increase in activity observed for phosphoramido chiral Lewis bases **159** supported on soluble polystyrene can be assigned to an increase of the local concentration of the phosphoramido units around the polymer chain, as it has been shown that from the two possible transition states detected in solution for the allylation of aromatic and unsaturated aldehydes with allyltrichlorosilanes, the one involving two phosphoramides presents higher reactivity.<sup>226–228</sup>

The increased local concentration on the support facilitates faster catalytic processes involving bimetallic pathways with lower substrate to catalyst ratios. This has been exploited to improve the activity of metal-salen catalysts by varying the density of catalytic sites along a polymeric backbone.<sup>36,229–232</sup>

Based on this approach, Weck and coworkers developed highly active polymeric Al-salen complexes for the asymmetric addition of cyanide to  $\alpha,\beta$ -unsaturated imides with high yields and enantioselectivities (Fig. 35).<sup>233</sup> The catalyst **166** was designed by incorporating a flexible poly(norbornene) backbone and a long linker to facilitate the bimetallic pathway and four quaternary carbon atoms at the periphery of the catalytic site to improve selectivity. With this rational design, the reaction progressed significantly faster with the supported catalyst than with its small molecule analogue. The catalytic transformation using 15 mol% of **166** was complete within 6 h while the same catalyst loading for the non-supported analogue resulted in less than 50% conversions. At lower catalytic loadings (5 mol%), a similar activity was maintained while for the homogeneous analogue less than 5% of the product was found.

The incorporation of different monomeric units in the polymeric framework may lead to cooperativity. Xie *et al.* have synthesised a pH-responsive soluble polymer by copolymerization of dimethyl aminopropyl acrylamide and *N*-*p*-styrenesulfonyl-1,2-diphenylethylenediamine.<sup>234</sup> The *N*-alkyl moieties appeared to play a cooperative role accelerating the Ru-catalysed asymmetric transfer hydrogenation of ketones in water, whereas the mono-*N*-tosylated derivative moiety played a pivotal role in chiral induction (Fig. 36). The polymer 167 exhibited excellent

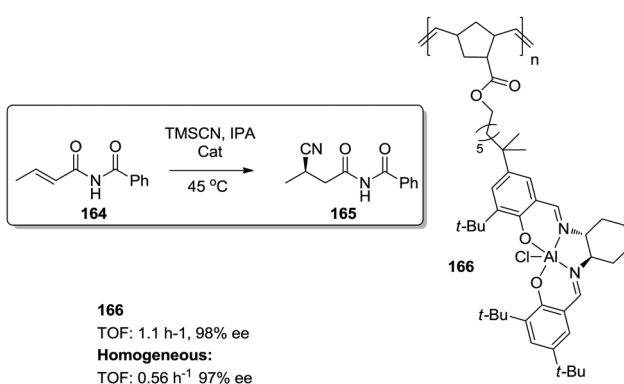


**Fig. 35** General design of polymeric Al–salen complexes for the asymmetric addition of cyanide to  $\alpha,\beta$ -unsaturated imides involving bimetallic pathways

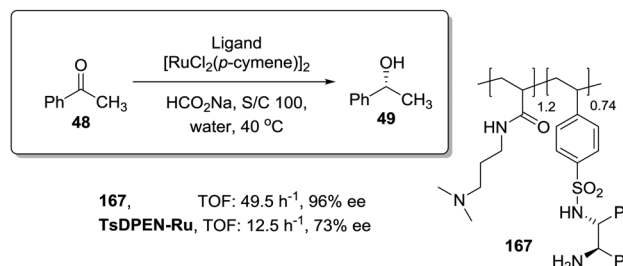


**Fig. 36** General structure of the pH-responsive soluble linear polymer containing TsDPEN units and dimethyl aminopropyl fragments providing a cooperative effect to increase the activity of the Ru-catalysed asymmetric transfer hydrogenation.

pH-induced phase-separation behaviour in water. It could be dissolved in water when the pH of the solution was lower than 6.5 and precipitated completely from water when the pH was above 8.5. Furthermore, the catalyst shows an enhanced activity in comparison with the soluble counterpart.

The polymer architecture can be designed using different controlled radical polymerisation (CRP) techniques to influence and tune the reactivity of catalysts in interesting ways. For instance, linear amphiphilic block copolymers, obtained by CRP, can self-assemble in water into nanomicelles, which may provide a hydrophobic environment to lower the interfacial energy of the reaction system and promote organic reactions in water.<sup>46</sup> In this regard, O'Reilly and co-workers have covalently attached to the hydrophobic core of a polymeric micelle 4-(dimethylamino)pyridine (DMAP) catalytic moieties for acylation reactions in water employing non-water-soluble substrates. The reactivity of the tethered organocatalyst within the nanostructure was found to be extremely high, improving in some cases the acylation rates up to 100 times compared to those for unsupported DMAP in organic solvents.<sup>235,236</sup> Based in those principles, they developed a series of efficient immobilised chiral organocatalysts. For instance, L-proline tethered to amphiphilic block copolymers (**169**), synthesized via reversible addition-fragmentation chain transfer (RAFT) polymerisation, self-assembled in water leading to highly active catalytic nanoreactors providing an effective concentration of the hydrophobic reagents, thus increasing their effective molarity, based on the difference in core-shell polarity (Fig. 37).<sup>237</sup>

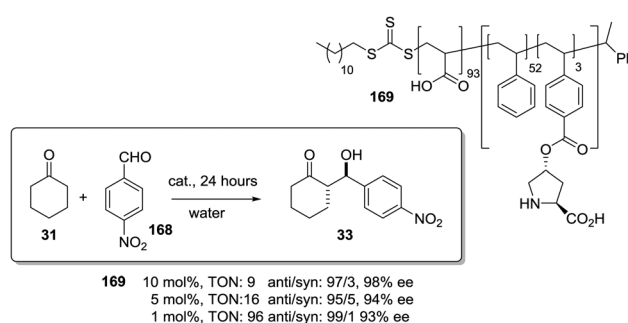


**Fig. 37** Amphiphilic linear polymer with proline organocatalytic units able to form nanomicelles in water catalysing aldol reactions

Low catalyst loadings (1 mol%) of this micellar system catalysed the aldol reaction in water more efficiently than the unsupported L-proline in organic solvents at 10% loading. The modularity of the CRP also allowed the introduction of thermoresponsive polymeric block units in the immobilised systems enabling the control of solubility and activity by temperature.<sup>238</sup> Noteworthily other stimuli such as the ion concentration could also be used to tune the catalytic activity of related block polymeric systems.<sup>239</sup>

Zhang *et al.* have reported the immobilisation of a Mn-salen complex onto soluble “smart” poly-*N*-(isopropylacrylamide) (PNIPAAm) by axially coordinating a supported amine group to the metal center. The resulting macromolecule (**170**) containing hydrophobic and hydrophilic blocks spontaneously self-assembled in water to form micelles with a hydrophobic catalytic core and a hydrophilic surface.<sup>240</sup> A significant acceleration in the reaction rate for the epoxidation of olefins was observed reaching an unprecedented TOF value ( $2.48 \times 10^3 \text{ h}^{-1}$ ) in the aqueous epoxidation of styrene, being up to 6 times more active than the homogeneous Mn-salen neat complex (Fig. 38).

Again, a “pseudo-concentration effect” at the core of the aggregate was used to explain the activity enhancement. The hydrophobic core provides a microenvironment with a high local concentration of catalytic sites along with the concentrated hydrophobic substrates, while the hydrophilic surface guarantees water solubility and the self-assembly of the polymer in the corresponding micelles. The advantages of this approach are further developed with the introduction of a thermo-responsive polymeric block in the polymeric framework.<sup>241</sup> The amphiphilic nature of the polymeric catalyst allowed self-assembly in a micellar system while the thermo-sensitive properties facilitated its recovery. Thus, a chiral Ti-salen complex tethered to a hydrophobic block of a thermo-responsive amphiphilic copolymer (poly(*N*-isopropylacrylamide-*co*-*N,N*-dimethyl acrylamide), poly-(NIPAAm-*co*-DMAAM)) displayed an outstanding catalytic activity and selectivity in the asymmetric sulfoxidation in water for a wide range of methyl aryl sulfides.

A similar catalytic enhancement in water has been reported for the cyclopropanation reaction catalysed by copper-bis(oxazoline) complexes immobilised on the hydrophobic domain of a polymersome membrane (**173**). These crosslinked polymersomes were obtained by a click reaction of a well-defined soluble block polymer poly(ethyleneglycol)-*b*-poly-(styrene-*co*-4-vinylbenzyl-azide) with a C<sub>2</sub>-BOX modified with an alkyne functionality (Fig. 39).<sup>242</sup> The conversion obtained with the catalytic

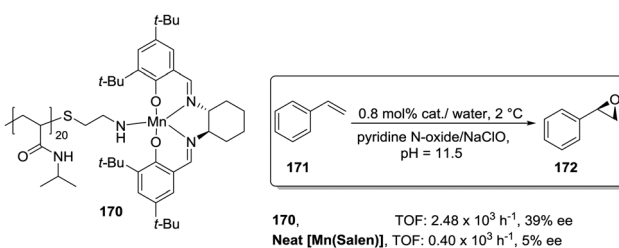


Fig. 38 Amphiphilic linear polymer containing Mn-salen fragments able to form micellar structures in water and catalyse the epoxidation of alkenes.

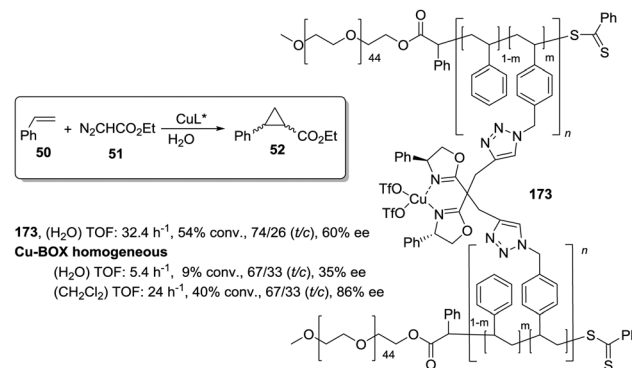


Fig. 39 General structure of polymersomes containing Cu-BOX subunits used for the enantioselective cyclopropanation of styrene.

polymersomes was comparable with the conversion of the parent catalyst in CH<sub>2</sub>Cl<sub>2</sub> and, more importantly, surpassed the activity found for the homogeneous Cu-BOX in water. The catalyst inside the polymersomes is surrounded by a hydrophobic environment from which water is excluded, favoring the desired process since water affects both conversion and enantioselectivity of the asymmetric cyclopropanation reaction. This also produced substrate selectivity. Hydrophobic substrates were readily converted into the corresponding cyclopropane products, while hydrophilic substrates did not undergo the reaction. The same strategy has been used, with similar positive effects, for the asymmetric aldol reaction in water catalysed by immobilised L-proline.<sup>243</sup>

Meijer and coworkers prepared random terpolymers, by controlled RAFT polymerization, bearing in their structure a catalytic unit, a block polymer defining the solubility and an additional block containing chiral benzene-1,3,5-tricarboxamide groups for self-assembly (Fig. 40).<sup>244,245</sup> This additional block defines the folding of the polymer in water to form a confined reaction space, mimicking the specific folding of proteins.<sup>246</sup> In the case of the polymer **174** containing L-proline as the catalytic

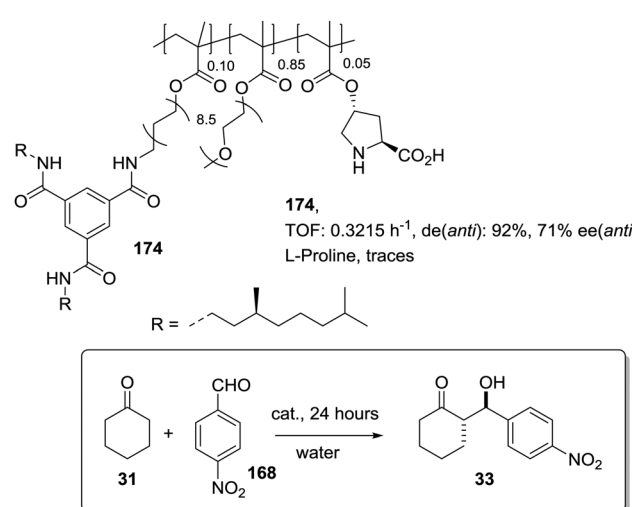


Fig. 40 General structure of a responsive terpolymer prepared by RAFT polymerization and containing proline catalytic units active for the aldol reaction.

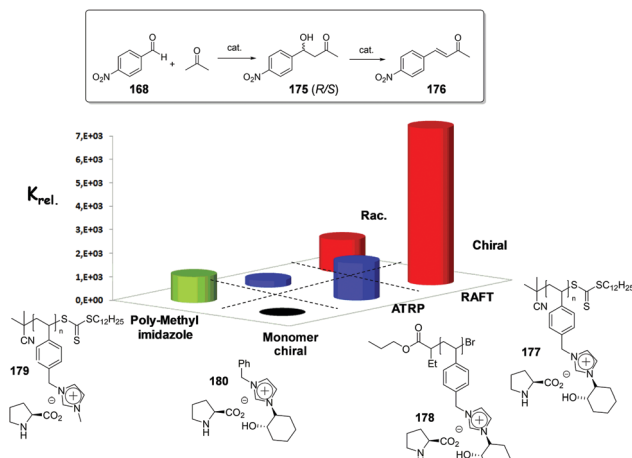


Fig. 41 Influence of the polymerization protocol on the activity of proline incorporated into polymeric ionic liquids.

unit, the polymer behaved as an enzyme mimic, as its catalytic activity was only expressed in its folded conformation. The structure of the polymer could be fine-tuned to obtain an exceedingly active catalyst.

Chiral monomeric imidazolium salts have been used to build up polymers with a well organised secondary structure (Fig. 41).<sup>247</sup> The right self-assembly of the monomeric units generated a highly ordered macromolecular structure with a complex hierarchical architecture, which can provide an adequate microenvironment for an efficient catalytic activity. A highly active and selective system for the aldol reaction was obtained for reactions both in water and in the presence of water. Thus, for instance, in acetone containing some water ( $\text{H}_2\text{O}$ -acetone 1:4) the polymeric catalysts obtained were up to *ca.*  $6.6 \times 10^3$  times more active than their corresponding monomeric counterpart, while in water the only active catalyst was the polymeric one. This enhancement in catalytic activity was related to some degree of chirality transfer to the main polymeric chain, producing a more properly organised polymeric structure and, therefore, a more efficient catalyst. A better transfer of the chirality was obtained for the polymers prepared by RAFT polymerization (177). The catalysts prepared by RAFT polymerization of the chiral monomer were more active and enantioselective than the ones prepared by ATRP (atom transfer radical polymerisation) or grafting.

Similar trends have been also observed for a range of well-defined copolymers of styrene and styryl functionalized L-proline prepared by RAFT polymerisation.<sup>248</sup> The self-assembly of these functionalized copolymers into well-defined aggregates in DMF/water provided a unique microenvironment for L-proline positively influencing the catalysis of the aldol reaction.

### Multi-catalytic systems. Wolf and Lamb approaches

Finally, the preparation of active multi-catalytic systems based on the use of mutually incompatible individual catalysts constitutes a special case of catalytic activity enhancement using polymeric immobilised catalysts.<sup>249</sup> The combination in solution of two non-compatible catalysts produces an inactive

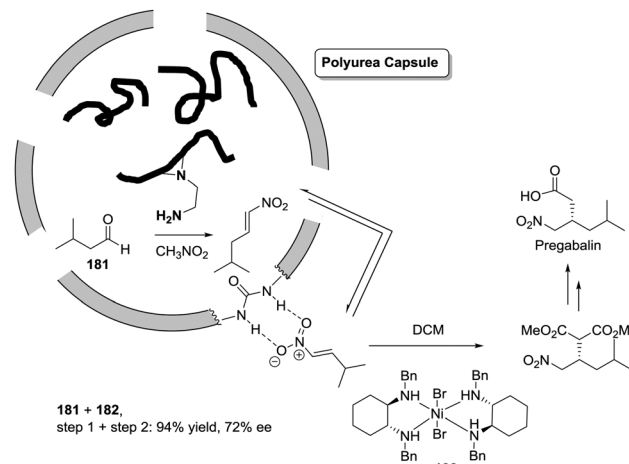


Fig. 42 Multicatalytic system based on the encapsulation of PEI in a polyurea capsule.

dual catalyst system. On the contrary, different tools have been developed for the immobilization of those catalysts on polymeric phases so that site isolation is achieved to produce an active dual catalytic system.<sup>250,251</sup> Novel approaches to exploit this possibility include the use of sol-gel and star polymers,<sup>252,253</sup> as well as polymeric microcapsules.<sup>254,255</sup>

One of such examples is shown in Fig. 42.<sup>256</sup> The reaction of nitromethane with an alkylaldehyde is catalysed by polyethylenimine (PEI) 181, which may also catalyse the addition of a second molecule of nitromethane. On the other hand, the Ni-based Lewis acid 182 catalyses the addition of dimethylmalonate to  $\beta$ -nitroalkane to give the corresponding Michaelis adduct.<sup>257</sup> When both catalysts were mixed in solution, free PEI strongly coordinated with Ni, making it inactive and only low yields of the Michaelis adduct (<5%) were obtained.

The microencapsulation of PEI, *via* interfacial polymerization using polyethylenimine (PEI) and a diisocyanate, prevents interaction between the polyamine and the nickel catalyst. By this isolation of the two catalytic sites, the Michaelis adduct was obtained in good yield and enantioselectivity. It should be noted that not only did the polymeric shell allowed a right isolation but the ureas present in the shell of the PEI-microcapsules also contributed to accelerate the nickel-catalysed Michaelis addition.<sup>258</sup>

The anchoring of two incompatible catalytic functionalities (acidic and basic) to two different solid matrices also allows achievement of one-pot multistep reactions. It has been shown, for instance, how a sulfonic acid resin could be used as the acidic catalyst, while a superparamagnetic spinel ferrite nanoparticle functionalized at the surface with amino groups was the basic catalyst.<sup>259</sup> The very different nature of the solid supports provided the development of simple separation protocols for the individual catalysts.

Shell cross-linked micelles (SCMs) can also be used to compartmentalise two incompatible catalysts (*e.g.* an acid catalyst in the shell and a base in the core). The immobilisation of a dual-catalyst was achieved by using an amphiphilic triblock



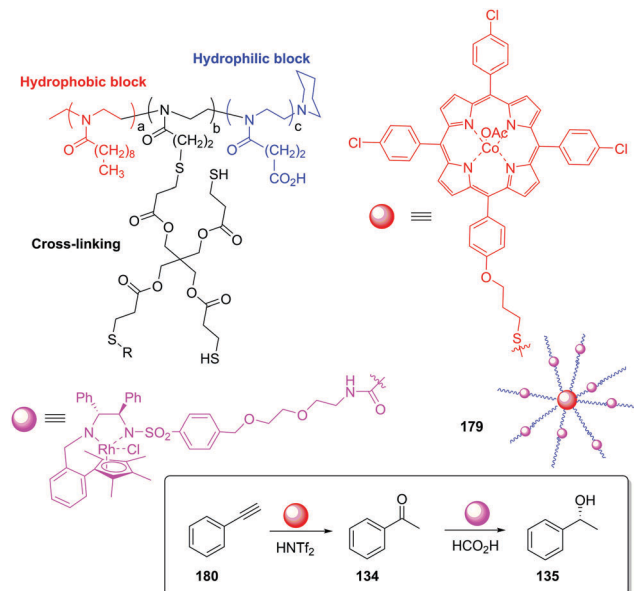


Fig. 43 Compartmentalisation of stereoincompatible catalysts at the core and shell of SCMs for one-pot asymmetric cascade processes.

copolymer of poly(2-oxazoline) with orthogonal functional groups on the side-chain that could covalently cross-link the micelle and separate two incompatible catalysts in two isolated domains of a single micelle (**183**). This bifunctional SCM was used in the acid–base catalysed one-pot tandem deacetalization–nitroaldol reaction showing excellent catalytic activity,<sup>260</sup> and also for the compartmentalisation of stereoincompatible catalysts for one-pot asymmetric cascade reactions.<sup>261</sup> The Co-catalysed hydration of an alkyne proceeded in the hydrophobic core, while the Rh-catalysed asymmetric transfer hydrogenation of the intermediate ketone into a chiral alcohol took place in the hydrophilic shell (Fig. 43). While the tandem reaction also worked when the two catalysts were immobilized on different micelles, the multi-compartmentalized micelle containing both catalysts gave significantly better results.

The site isolation properties of non-interpenetrating star polymers have been exploited for encapsulation of multiple, otherwise incompatible, catalysts for asymmetric cascade reactions that involve iminium, enamine, and H-bonding catalysis (Fig. 44). In the case of the encapsulation in the core of soluble star polymers, an efficient one-pot multi-component asymmetric cascade reaction could be carried out with the participation of three different substrates and a catalytic combination involving four species, two of them polymer-bound (**185** and **186**) and two small molecules (**187** and **188**). For this system, the multistep reaction took place with good yield and enantioselectivity, while the use of a combination of the corresponding small molecules and/or linear polymer analogues led to little or no cascade reaction.<sup>262</sup>

## Stability

As mentioned, facilitation of the reuse and recycling of supported chiral catalysts represents one of the most important advantages

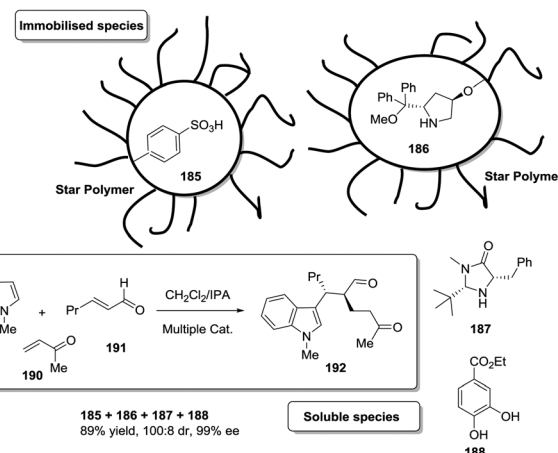


Fig. 44 Encapsulation of incompatible catalytic species at the core of star polymers.

associated with them. This, along with some of the intrinsic properties of the corresponding support, can contribute significantly to enhance their stability and increase their lifetime. In this context, it is necessary to consider both the possibility of reusing the catalyst in successive runs (as many as achievable) and/or for long periods of time and the possibility of its regeneration once the system is not efficient anymore, which is particularly relevant for chiral catalysts where the chiral component and the functional support itself can be the most costly components of the system.

## Number of runs

The general idea that immobilization onto a support contributes to greatly improve the stability of reagents and catalysts is well established and has been confirmed by data from diverse laboratories. Since the initial reports by pioneering researchers in the field, the use of supported chiral catalysts needs to demonstrate their capacity to be used for several runs.<sup>263</sup>

Although many reports just describe the results for a limited number of reuses (4–5 cycles), examples can be found on systems reused, in batch experiments, for 15 or more runs.<sup>78,211,264</sup> The incorporation of cinchona-derived fragments into polymeric matrices has been exploited by different groups active in the field of organocatalysis often with excellent results.<sup>265</sup> The immobilization of mono- and bis-cinchona alkaloid derivatives on polystyrene resins using click chemistry for the attachment to the support has allowed the preparation of very stable organocatalysts.<sup>266</sup> Some polymer-supported dimeric cinchona systems (**193**, Fig. 45) were able to efficiently catalyze the asymmetric amination of 2-oxindoles for 100 runs, with more than 5300 h of active life, maintaining the activity (>99% yield) and the enantioselectivity of the final product (>90% ee).<sup>267</sup>

Textiles have been recently reported as excellent polymeric supports for the immobilization of a variety of organocatalytic systems using photochemical approaches for their functionalization.<sup>268</sup> The incorporation of a chiral cinchona derivative provided an efficient chiral organocatalyst for the alcoholytic desymmetrization of a cyclic anhydride that could

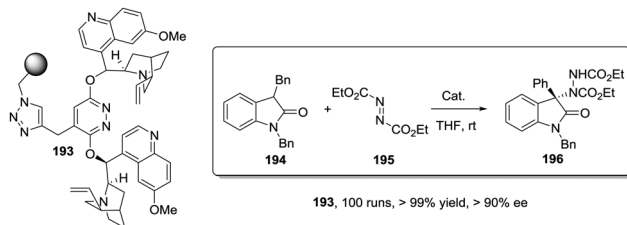


Fig. 45 Polymer supported dimeric cinchona derivatives used for the asymmetric amination of oxindoles.

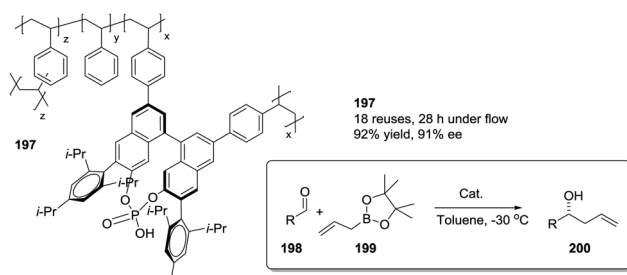


Fig. 46 Polymer supported TRIP used for the asymmetric allylboration of aldehydes.

be reused for 300 runs.<sup>269</sup> The activity and the corresponding enantioselectivity were maintained essentially constant for the first 200 cycles and the further deactivation could be compensated, at least partly, by an increase in the catalyst loading.

It is worth mentioning that in some instances the reuse of the catalyst is carried out not on the same process but for alternative processes.<sup>270</sup> An example is the use of polystyrene-supported TRIP phosphoric acid catalyst (197) for the asymmetric allylboration of aldehydes (Fig. 46).<sup>271</sup> This catalyst was used under batch conditions for 18 reuses with different substrates without detecting any deactivation and with excellent yields and enantioselectivities in most cases.

**Number of runs versus slow deactivation.** The number of runs the catalyst can be used provides only limited information on the contribution of immobilization to increase the stability of the catalyst. The reused catalyst must behave efficiently in terms of both activity and selectivity. A full assessment should require the analysis of changes in the kinetics of the processes of interest with the reuse or at least obtaining the corresponding TOF values for intermediate conversions. This has only been studied in a limited number of processes.<sup>96,97,162,265</sup> A polymer-supported Ru-BINAP catalyst was prepared by ROMP of the corresponding Ru-BINAP derivative and it could be reused for more than 30 cycles achieving excellent yields (> 99%) and enantioselectivities (95% ee) for the asymmetric hydrogenation of 1'-acetonaphthone, after a proper optimization of the corresponding protocol for the reaction and for recovery.<sup>272</sup> The turnover frequency was calculated to be  $750 \text{ h}^{-1}$  at 75% conversion for all the individual runs demonstrating that during the successive cycles the catalyst maintained the same activity as the original catalyst and the homogeneous analogue.

In different instances, some deactivation of the supported catalysts is observed for the first run(s) up to achieving a constant level of activity. In this case, it is assumed that the most accessible sites are more easily deactivated. Very often, in particular in the case of organometallic catalysts, those accessible sites correspond with metal species that are not linked to the supported ligands but just physically entrapped. Although the room temperature solventless octane hydrosilylation catalysed by supported Pt complexes reported by Drake *et al.* does not involve chiral catalysis, it illustrates very well these issues as much as an extensive analysis of leaching and recycling.<sup>273</sup> The activity of the supported-Pt catalysts decreased with the first uses up to reaching an activity plateau, but isomerization decreased for the reused systems, being much lower than that observed for the homogeneous catalyst. The long-term stability of one of the supported catalysts was evaluated after 17 months of its synthesis (stored in contact with air) and 14 months after the first extensive recycling test. The activity for the hydrosilylation process was slightly reduced initially, but fell off with further recycling. However, the level of isomerization was very low and remained so through the reuse. The authors explained this reduction in activity and the concurrent improvement in selectivity based on the oxidation of unbound or weakly bound Pt located on or near the resin surface to  $\text{PtO}_2$ . As isomerization has been associated with the presence of unbound metal in solution, the former oxidation process would lead to a reduction in both activity and isomerization.

**Long-term experiments.** A small continuous reduction in activity and sometimes in selectivity/enantioselectivity can be observed for different supported chiral catalysts in long-term experiments. Sometimes, this is counterbalanced by increasing the reaction time during the new runs. Nagashima and Davies studied a series of bridged dirhodium tetraprolinates supported on an Argopore-Wang resin functionalized with a pyridine fragment able to coordinate to the metal (Fig. 32) and which were capable of maintaining at a steady level over 15 cycles the yield (87–91%) and the enantioselectivity (85–88% ee) for the cyclopropanation of styrene with methyl phenyldiazoacetate, but at the expense of increasing the reaction time from 18 to 92 minutes (6 times increase).<sup>211–214</sup> This long-term stability is also sensitive to the nature of the reactions and/or substrates under study. The above mentioned iridium based polymer-supported chiral-at-metal Lewis acid catalyst 3 (Fig. 1) retained 95% of its catalytic activity for five runs and could be used for 15 cycles by increasing the reaction time from 48 to 112 h with the same yield (99%) and selectivity (96% ee) as in the first cycle.<sup>78</sup> In the case of the titanium catalyst derived from silica-supported BINOL (201) shown in Fig. 47, the ethylation of 4-chlorobenzaldehyde using  $\text{Et}_2\text{Zn}$  was studied for 10 runs with only a small reduction in yield (from 91 to 85%) and enantioselectivity (from 96 to 90%), while the arylation of 1-naphthaldehyde with  $\text{PhMgBr}$  was reported to occur with 85% yield (94% ee) in the first run and 99% yield (88% ee) for the tenth, although some variability of results within this range of values was obtained for this process for the whole series of experiments.<sup>274</sup> The ethylation of 1-naphthaldehyde



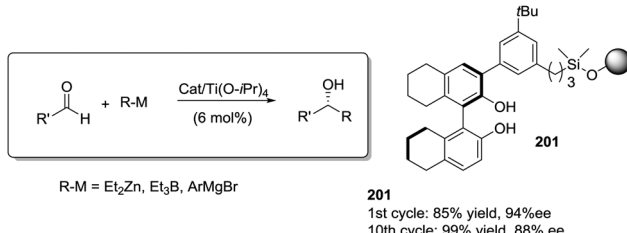


Fig. 47 Silica supported BINOL used for the Ti-catalysed alkylation and arylation of aldehydes.

with  $\text{Et}_3\text{B}$  showed excellent reproducibility in terms of yield and enantioselectivity for ten consecutive runs (85–89% yield and 96% ee).

#### Air-moisture

In general, the stabilisation effect is particularly marked when very reactive, water and air sensitive species are involved. In the case of PS-DVB and related resins, the hydrophobicity of the matrix is likely to contribute to avoid decomposition of such systems. The formation of hydrophobic cavities around the active sites can improve the stability of air/water sensitive species. The introduction of air or moisture in the polymeric matrix was associated with a very small decrease in activity observed for polymer-supported Rh-phosphine-phosphite catalysts in asymmetric hydrogenations (<3% after 11 runs, 97% ee for all runs).<sup>275</sup> The small Rh leaching detected in the first cycles did not affect the efficiency of reuse and this leaching was attributed to physically adsorbed Rh species. In the self-supported Mn-salen chiral system reported by Roy *et al.* for the epoxidation of non-functionalized olefins, the oxidative degradation of the complex was considered to be responsible of the deactivation.<sup>276</sup> After modification of the oxidant and optimization of the recycling process the system could be used up to 8 times maintaining the yield and enantioselectivity, but at the expense of an increase in the reaction time. Bissesar *et al.* have described the preparation of a self-supported Ni(II) metallocopolymer capable of acting as an efficient catalyst for the Michael reaction.<sup>277</sup> They reported that the self-supported system presented a high air and moisture stability and no change was observed after being maintained in air for two weeks, while the related mononuclear Ni(II) complex decomposed after two days' exposure to air. In some of the reactions studied, the catalyst could be reused for up to 11 runs maintaining the activity and enantioselectivity (85–83% yield, 99–97% ee). In order to design stable supported species, two factors must be kept in mind: (i) the existence of a robust and appropriate link between the ligand and the support and (ii) the chemical stability of the catalytic entities being immobilised. Even though these points seem to be quite obvious, they should be carefully considered.

#### Deactivation through the metal

In many organometallic complexes deactivation of supported catalysts is generally related to the leaching of the resin-bound catalytic metal or to the possibility of forming deactivated metal species that remain in the polymeric matrix.<sup>278</sup>

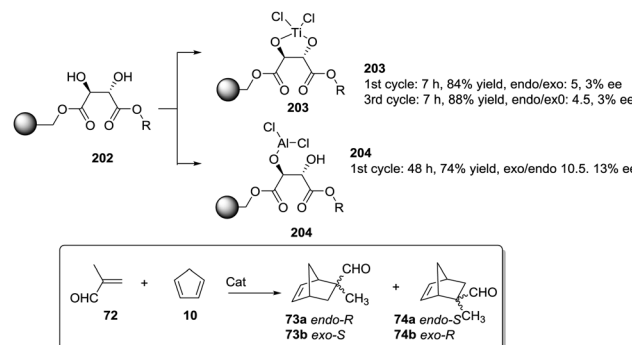


Fig. 48 Polymer supported Ti and Al complexes of immobilized tartrate esters used as Lewis acid catalysts for the Diels–Alder reaction of methacrolein and cyclopentadiene.

When supported catalysts derived from tartaric acid based ligands (Fig. 48) were assayed for the Diels–Alder reaction between methacrolein and cyclopentadiene,<sup>278</sup> a sharp contrast was observed for the Al and Ti derivatives of the polymer-supported ester of tartaric acid (202). When the corresponding catalysts were assayed for the Diels–Alder reaction, a rapid decrease in the performance (for both activity and selectivity) was detected for 204. A different situation was found, however, for the Ti catalyst 203 based on a stronger chelate complex. In this case a decrease in activity was observed for the first runs but after the fourth run the activity remained essentially constant for a long period. A significant metal leaching was not detected either for Al or for Ti species, which suggests that in these polymer-supported catalytic systems decomposition of the catalytic site can be accompanied by the formation, inside the polymeric matrix, of insoluble species (*i.e.* metal oxides). The blockage of the porous structure is a common deactivation mechanism for catalysts based on microporous or mesoporous supports, in particular those of inorganic nature.<sup>279</sup>

In the case of polymer-supported TADDOLates prepared by Seebach, the kinetic studies revealed, in general, a decrease in activity for successive runs.<sup>136,137,167–169</sup> Only the functional polymer prepared from dendrimer 99 (Fig. 20) retained the original rates. It is interesting to note that this polymer was the only one to maintain the original swelling properties. This suggests that the deactivation mechanism can follow a similar pattern with decomposition of some catalytic sites accompanied by precipitation, inside the polymer, of inorganic particles, which decreases swelling and accessibility to the remaining catalytic centers.

The enantioselective epoxidation of olefins using chiral Mn(III)-salen catalysts is a useful synthetic transformation that suffers from deactivation through the formation of inactive  $\mu$ -oxo-Mn(IV) dimeric species, and a variety of supports have been studied in order to minimize this deactivation process and facilitate recovery and reuse.<sup>280</sup> Huang *et al.* have reported on the use of a variety of hybrid organic–inorganic supports for the immobilization of Mn-salen catalytic species and found that leaching and formation of  $\mu$ -oxo-Mn(IV) species were the main deactivation mechanisms.<sup>281</sup> Although the catalysts were



reused for 9 cycles, some of the optimal systems revealed that the conversion decreased from 99% to 67% and the enantioselectivity from >99% to 62% ee, while the Mn content decreased from 0.73 to 0.45 mmol g<sup>-1</sup>.<sup>282</sup>

### Non-covalent immobilisation and leaching

Of course, leaching and the associated deactivation are often found in chiral catalysts supported through non-covalent interactions.<sup>39,283</sup> This is a common situation when inorganic supports are employed.<sup>284</sup> However, the commercially available Rh-(S,S)-EthylDuphos has been anchored efficiently *via* ionic interactions on phospho tungstic acid dispersed on the surface of aluminum oxide and the stability could be improved by combining a continuous flow process with an appropriate reactor design, allowing for the preparation of an active pharmaceutical ingredient in kilogram scale with excellent enantioselectivity.<sup>285</sup> The reactor set-up used suggests that the activation of release and catch strategies can be essential in this regard to limit the leaching and maintain the activity. Developing release and catch strategies is also important to implement the stability in systems based on MNPs (in particular PdNPs) supported on functional polymeric surfaces.<sup>270,286</sup> When cellulose was used as a support for RhNPs and the system applied for the enantioselective 1,4-addition of arylboronic acids to enones and enoates in the presence of chiral diene ligands, no Rh leaching was detected in the reaction mixture.<sup>287</sup> In the case of a Cu(II) exchanged zeolite modified by direct adsorption of cinchonidine and applied to the asymmetric Henry reaction, the authors studied in detail the deactivation mechanism and observed that after the reaction, the cinchonidine fragments were no longer attached to copper but hydrogen bonded to surface silanols.<sup>288</sup> The immobilization of the Noyori catalyst Ru-(R-BINAP) by encapsulation in silica nanocages has been used for the enantioselective hydrogenation of  $\beta$ -ketoesters showing a very good stability, with around 1% Ru leaching after the first cycle, but only *ca.* 0.3% leaching for the second run.<sup>289</sup> The reaction conditions can be very important. Chiral Rh phosphine-phosphite catalysts have been immobilized on sulfonated polystyrene resins and studied for the enantioselective hydrogenation of olefins.<sup>290</sup> When the reaction was carried out in MeOH, a significant Rh leaching was detected (9–18%) for each run, while the leaching was much lower when the solvent was changed to water (<1%). Leaching is also a problem associated with chiral organocatalysts based on amines or polyamines immobilized on acidic resins through protonation and electrostatic interactions and some strategies have been devised for its minimization.<sup>291,292</sup>

### Detachment-transformation of the ligand

The importance of the nature and chemical stability of the chiral ligand for long-term stability was clearly illustrated by Hodge and co-workers.<sup>293</sup> When the supported gel-type camphor derivative **205** (Fig. 49) was used as the catalyst in the reaction of aldehydes with Et<sub>2</sub>Zn, the first catalytic cycle afforded a chemical yield >95% with >94% ee. However, after being used for *ca.* 275 h the chemical yields and ee values

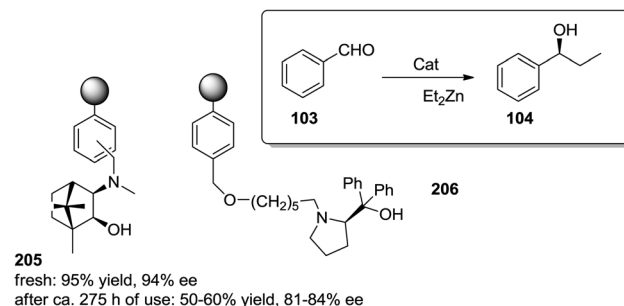


Fig. 49 Examples of polymer supported amino alcohols studied for the ethylation of aldehydes with Et<sub>2</sub>Zn.

dropped to 50–60% and to 81–84%, respectively (a decrease of *ca.* 2.5% in chemical yield and *ca.* 1.0% in ee per run).

It is worth mentioning that the study was carried out in a continuous flow system in order to avoid physical abrasion of the beads through their extensive use and for easy recycling. Data suggested that the secondary  $\beta$ -amino alcohol would be gradually transformed into a  $\beta$ -amino ketone losing its catalytic properties. In the light of this, the same authors designed a more robust and chemically inert supported chiral moiety (**206**) based on prolinol.<sup>294</sup> The corresponding polymers could be successfully used in batch at least nine times without any significant loss of activity or enantioselectivity, showing the importance of choosing the right arrangement of linker, ligand, matrix and reaction conditions in order to achieve a good long-term stability. In the case of the iridium catalysts 2–3 presented in Fig. 1, the authors reported that a good stability was only achieved when the ligand was attached to the resin through an amide bond, while the related system containing an ester bond was much less stable, which was attributed to the more robust amide linkage.<sup>78</sup> This is also illustrated in the case of L-proline derivatives supported as the corresponding zirconium phosphates (**207**) or phosphonates (**208**) (Fig. 50).<sup>295</sup> While the phosphate link was shown to be relatively unstable, the phosphonate bond was stable allowing the recovery of the catalyst by centrifugation (>92%) and its reuse for 6 successive runs.

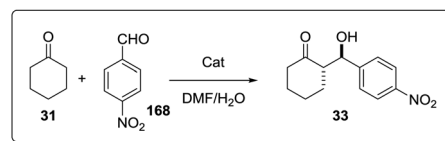
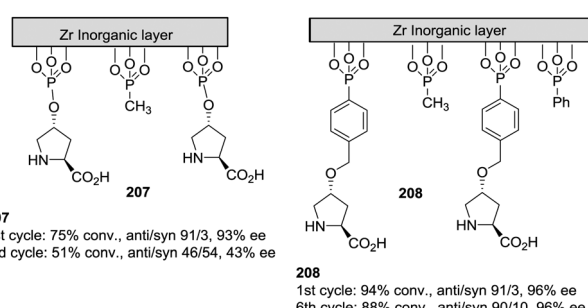


Fig. 50 Proline supported on zirconium through phosphate or phosphonate bonds and studied as an organocatalyst for aldol reactions.



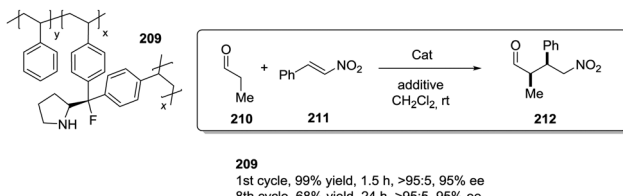


Fig. 51 Polymer supported fluorinated organocatalyst derived from proline and studied for the enantioselective Michael addition.

Another factor to be considered is the limited mechanical stability of lightly crosslinked polymers, which may affect negatively their long-term use in particular under mechanical stress (*i.e.* magnetic stirring). The polymer **209** (Fig. 51) containing a fluorinated organocatalytic fragment has been prepared by suspension polymerization and assayed for the enantioselective Michael addition of propanal and (*E*)- $\beta$ -nitrostyrene.<sup>296</sup>

Recycling experiments showed that a full conversion maintaining a high enantioselectivity (>95% ee) could be obtained for 7–8 runs, but at the expense of increasing the reaction time from 1.5 to 24 h. This loss of activity was partly attributed to the mechanical degradation of the polymer. The use of continuous flow systems, as will be discussed below, has been reported to improve the stability of supported systems by reducing this mechanical degradation,<sup>263,293</sup> and this was also exploited in the case of the supported organocatalyst **209**, allowing its continuous use for 13 h with a single substrate to obtain multigram amounts of the desired product or to sequentially use this flow setup with 13 different substrates for a total of 18.5 h of use.

Mechanical stability can also be achieved by the use of more rigid polymeric matrices. On the other hand, the higher mobility of the functional groups in resins with a low degree of crosslinking can also affect negatively the stability of the resulting species, in particular when the catalytic centers can be deactivated, or lead to diminished selectivity, through site–site interactions.<sup>36,297,298</sup>

The use of macroporous polymers with a high and adjustable crosslinking degree and the desired porosity would limit those deactivation processes and increase the turnover and the lifetime of the polymer.<sup>54,55,181,206,299</sup> As a matter of fact, monolithic macroporous materials can be some of the most suitable materials for the preparation of flow systems due to their porosity properties.<sup>170,171,300,301</sup> The morphology of these macroporous materials, when appropriately tailored, avoids diffusional problems and allows them to act as stable and easily recoverable microreactors. However, the properties of the corresponding polymeric support need to be properly optimized for each specific application.

In a recent report on the use of polymer-supported diarylprolinols as organocatalysts for the continuous flow cyclopropanation reaction, it has been shown that the best performance was obtained with catalysts **213** based on a microporous resin and **214** of monolithic nature (Fig. 52).<sup>302</sup> Under flow conditions the activity of the monolith remained constant for 24 h and then became rapidly deactivated, which was assigned to the collapse of the macroporous structure. The catalyst based on the microporous

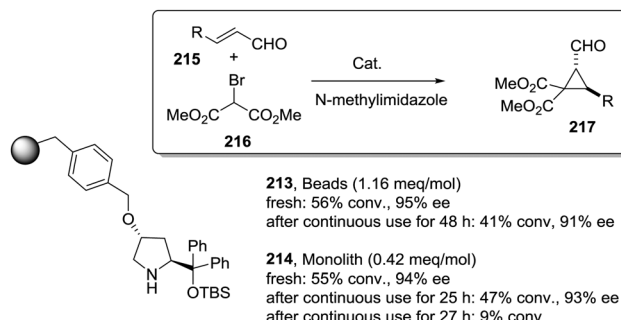


Fig. 52 General structure of supported diarylprolinol derivatives studied as organocatalysts for the cyclopropanation reaction.

resin could be used for the same transformation for 48 h without a significant reduction in the performance. Besides, this catalyst could be used then for several other transformations up to a total of 76 h working in flow.

### Recycling protocol

The protocol for recycling is also an essential factor to be considered. This usually involves, for an insoluble polymer, filtering and washing. All these steps need to be carried out under conditions that do not affect the reactive species. The use of monolithic polymeric sticks has been shown to facilitate these recycling protocols. For a variety of polymer supported BINOL phosphates acting as chiral Bronsted acids in asymmetric organocatalytic transfer hydrogenation more than 10 runs could be applied without appreciable loss in activity and enantioselectivity.<sup>206</sup> Even small losses of material in the work-up or due to the mechanical breakdown of the resin preclude a long-term use of the supported species. We have to bear in mind that just a loss of about 10% of the material used for each recycle would reduce our catalyst to about 30% of the initial amount after 10 cycles. For insoluble resins, minimisation of losses is better achieved with an experimental design in which the solvent is filtered out of the resin, keeping this in the reaction vessel. Thus, Takeda *et al.* have used a commercial parallel synthesizer for easy catalyst separation and recycling and were able to carry out the rhodium(II)-catalysed enantioselective intramolecular C–H insertion of a diazo- $\beta$ -ketoester for 100 cycles with the observation of the same yield (88%) and enantioselectivity (92% ee) as in the first run and without the need to increase the reaction time (20 min for all cycles).<sup>303</sup>

**Soluble supports.** Full recovery is particularly critical for the use of soluble supports requiring an additional precipitation step (or other separation procedures). The preparation of polytopic bis(oxazoline)-based ligands allowed obtaining self-supported catalytic systems in the presence of copper.<sup>304</sup> These coordination polymers re-dissolved in the reaction medium when applied to the enantioselective cyclopropanation of styrene with diazoacetate and then precipitated spontaneously at the end of the reaction. They were reused for up to 20 cycles but a decrease in the activity was observed along with smaller changes in selectivity and enantioselectivity. The recovery of ferrocenylmethyl aziridino alcohol ligands supported on a



dendrimer structure and used for the catalytic addition of  $\text{Et}_2\text{Zn}$  to aldehydes was achieved by precipitation with *n*-hexane and centrifugation, and the recovered material could be used for 9 consecutive runs with non-significant decreases in yield and enantioselectivity.<sup>305</sup> The protocol for full precipitation of a polymer-supported chiral gold catalyst partially soluble in the reaction solvent was shown to be critical.<sup>306</sup> When using methanol or diethyl ether for precipitation, the recycling was inefficient, but when using *n*-hexanes for the recovery the catalyst could be used for five runs maintaining the high enantioselectivity but requiring longer times to achieve appropriate conversions. The recovery and reuse of a bisprolinamide supported on polyhedral oligomeric silsesquioxanes (POSS) for five cycles has been described through precipitation with a cosolvent and filtration.<sup>307</sup> The recovery efficiency was 85–92% for each individual cycle and although the enantioselectivity remained essentially constant at 93% ee, the yield decreased from 82% (1st run) to 70% (5th run). Temperature-responsive hairy polymers containing proline have been used for the direct asymmetric aldol reaction in water and a recovery >97% was obtained by centrifugation. However, the performance of the recovered supported catalysts differed significantly depending on the working temperature of the previous catalytic cycle, with some reduction in activity being always observed.<sup>308</sup> In this kind of hairy microparticles, the polymer morphology has been demonstrated to be very important to understand not only the catalytic performance but also the potential for efficient reuse.<sup>309</sup>

**Magnetic supports.** In recent years, magnetic nanoparticles (MNPs) have been used extensively as supports for the immobilization of a variety of catalysts including enantioselective catalysts.<sup>310</sup> The grafting of a polymeric shell onto their surface often facilitates the attachment of the catalytic fragments.<sup>311</sup> It has been reported that the use of imidazolidinone supported on MNPs showed a better recycling efficiency than a related organocatalyst attached to a polystyrene support for the Friedel–Crafts alkylation of indoles.<sup>312</sup> A drastic decrease in yields and a significant decrease in enantioselectivity was observed in the last case upon reusing. However, a parallel study comparing related systems for this reaction concluded that the polystyrene-supported catalyst provided not only better enantioselectivities but also a higher stability.<sup>313</sup> Although both supported catalysts could be easily recovered from the reaction media, after 5 runs both showed a decrease in activity, this being more relevant for the MNP-based system (from 68 to 27% yield) than for the polymer-based system (from 71 to 50% yield). A similar trend was found for enantioselectivity, decreasing from 65 to 48% ee for the modified MNPs and from 84 to 79% ee for the polystyrene based system. Up to 20 reuses have been described for a chiral oxo-vanadium pseudoephedrine complex immobilized on MNPs, with some decrease in activity being observed for the 20th run in the oxidation of sulfides to sulfoxides.<sup>314</sup>

### Continuous flow

Clearly the work under flow conditions represents an optimal setup achieving long-term stability as it minimizes the operations that could lead to deactivation of the catalytic sites. This has

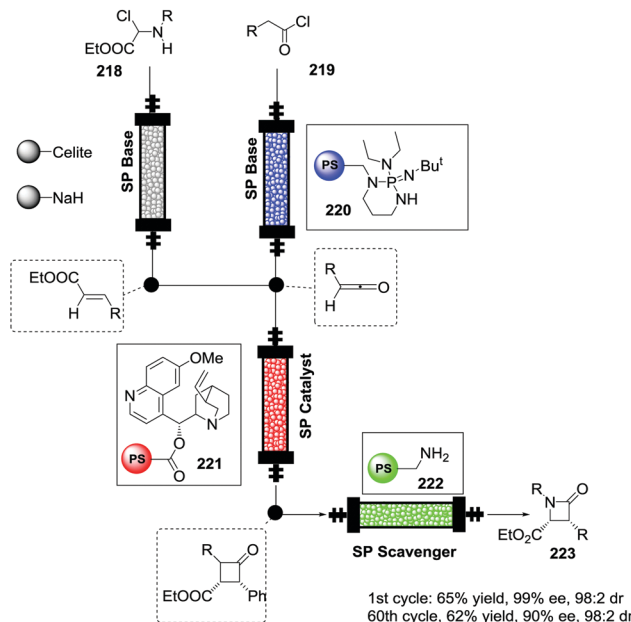


Fig. 53 Multistep flow process for the preparation of  $\beta$ -lactams.

been highlighted by the recent achievements in the field of flow chemistry, including flow chemistry processes for the preparation of enantiopure compounds through chiral catalysis.<sup>315–318</sup> A pioneering and clear exemplification of the advantages of the long-term stability of the supported species for flow processes was reported by Lectka and coworkers in the continuous asymmetric synthesis of different  $\beta$ -lactams (223) (Fig. 53).<sup>319</sup> They assembled several columns packed with suitable supported reagents, catalysts and scavengers (220–222) required for the different synthetic and purification steps. The system could be reused sixty times with no significant loss in selectivity or yield (90% ee and 62% yield for the 60th run, in comparison with 99% ee and 65% yield for the first cycle) after following the proper protocols of washing and regeneration.

This concept has been proved by the design of a continuous flow system based on monolithic catalytic columns containing a bicyclic chiral amino alcohol fragment (224) and its application to the addition reaction of  $\text{Et}_2\text{Zn}$  to aldehydes (Fig. 54).<sup>320</sup> The monolithic column 224 allowed the design of an efficient flow-system with an excellent activity and selectivity. Besides, this catalytic system could be reused several times with no loss of its catalytic efficiency, in terms of conversion, chemoselectivity and enantioselectivity.

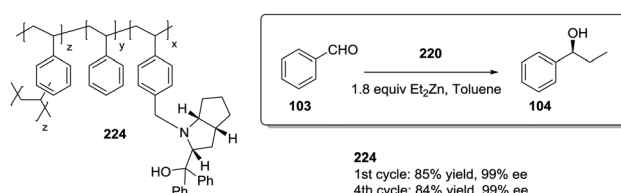


Fig. 54 General structure of the monolithic polymer containing chiral bicyclic amino alcohol units studied for the ethylation of aldehydes.



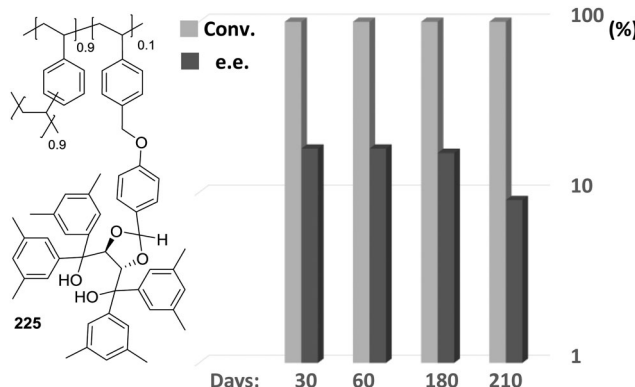


Fig. 55 General structure of monolithic TADDOLs assayed under flow conditions for long-term stability.

In the case of polymer-supported Ti-TADDOLates prepared as monolithic columns (225), an extraordinary long-term stability has been observed.<sup>132,321</sup> Ti species derived from resins such as 225 were assayed as catalysts for the Diels–Alder reaction between cyclopentadiene and *N*-acryloyl-3-oxazolidinone. In general those supported Ti-TADDOLates maintained their integral performance for several months without the need of any special care except those mentioned for the work-up protocols. In the case of the derivative containing 3,5-dimethylphenyl groups at the  $\alpha$ -position the activity remained even when, after the sixth month of use, it was left open in air for an additional month. In this case, however, some loss in selectivity was found (Fig. 55). Similar results were obtained for other monolithic columns containing polymer-supported Ti-TADDOLates related to 225 but with different substitution patterns on the aromatic rings; the corresponding catalytic systems were active, in some cases, for more than one year (Fig. 55).<sup>322</sup>

After screening a series of resin-bound di- and tri-peptides directly prepared on the resin by solid phase peptide synthesis (SPPS) techniques, Ötvös *et al.* found that a simple supported dipeptide containing an N-terminal proline and acid side chain at the C-terminus provided the best results as an organocatalyst for the asymmetric  $\alpha$ -amination of aldehydes with dibenzyl azodicarboxylate (DBAD).<sup>323</sup> This supported peptide was used to prepare a packed-bed flow system that was operating for 20 h of continuous use with constant yields in the range of 84–91% and enantioselectivities in the 88–92% ee range to provide the product in gram scale. Stable flow processes with more than 24 h on stream are frequent currently.<sup>111</sup> A strategic control over the residence time was demonstrated to be a key parameter. As has been mentioned above, flow setups have allowed the preparation of the desired final products in multigram<sup>296</sup> or even kilogram scale.<sup>285</sup> Takeda *et al.* have shown that a polymer-supported dirhodium(II) complex could be applied under flow conditions for the enantioselective intermolecular cycloaddition of a diazodiketoester with styrene retaining the activity (78% yield) and enantioselectivity (99% ee) for 60 h on stream with only a small Rh leaching detected in the solution (2.1 ppm).<sup>324</sup> Some of the processes studied could be easily upscaled to produce 22 g of the desired product with a turnover

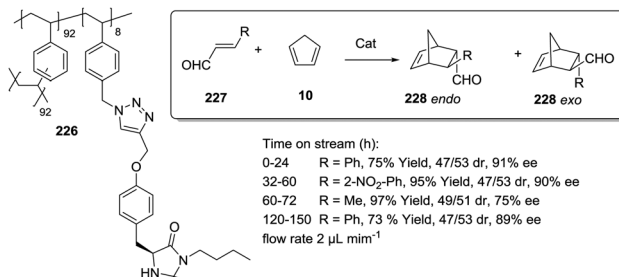


Fig. 56 Chemical structure of the organocatalytic monolith used for the Diels–Alder reactions of cyclopentadiene under flow conditions.

number of 11 700. In the case of the continuous-flow asymmetric hydrogenation of an enol ester, the use of an Rh catalyst based on a phosphine–phosphoramidite ligand immobilized on a supported ionic liquid and the use of supercritical carbon dioxide as the mobile phase allowed maintenance of the performance of the process during 233 h on stream, achieving a final turnover number of 70 400.<sup>325</sup>

The use of a monolithic reactor obtained by copolymerization of divinylbenzene and a vinylic imidazolidinone derivative (226, Fig. 56) inside a stainless steel column allowed carrying out the Diels–Alder cycloaddition of cyclopentadiene and three different  $\alpha,\beta$ -unsaturated aldehydes for around 150 h on stream achieving excellent reproducibility of the results with the same aldehyde at the beginning and at the end of this period.<sup>300</sup> Finally, a similar catalytic column was used sequentially for three different reactions continuously for a total of more than 300 h on stream. Using two coupled catalytic columns packed with a mixture of polystyrene-supported Pybox,  $\text{CaCl}_2 \cdot 2\text{H}_2\text{O}$ , and Celite, the asymmetric 1,4-addition of 1,3-dicarbonyl compounds to nitroalkenes was carried out in flow for more than 200 h, without loss of activity (95% yield for the last period) and enantioselectivity (91% ee).<sup>326</sup> The work under continuous flow was demonstrated, besides, to solve the issue of product inhibition detected in these processes.

Although biotransformations have not been considered in detail in this review, it is worth mentioning that stability issues (*i.e.* thermal and long term stability) can represent one of the bottlenecks in their practical use for some applications and this has also been approached through the immobilization of the corresponding biocatalysts on an appropriate support. Thus, in the same way that ionic liquids have been demonstrated to be able to maintain the stability of proteins, including enzymes, and are an excellent medium for biocatalysis, supported ionic liquids have also been shown to contribute to the stability of immobilized catalytic enzymes including the development of efficient flow processes.<sup>327–329</sup> Thus, the use of polystyrene monoliths modified with imidazolium groups (supported ionic liquid-like phases)<sup>330</sup> for the immobilization of CALB provided distinct advantages over other supports for esterification processes.<sup>331</sup> Optimum performance and stability was obtained with the most hydrophobic monolith that provided an excellent turnover number ( $35.8 \times 10^4$ ) working at 80 °C and 10 MP (supercritical  $\text{CO}_2$ ). This allowed developing the dynamic

kinetic resolution of *rac*-1-phenylethanol by flow processes using  $\text{scCO}_2$  and an additional acid zeolite-ionic liquid catalyst, achieving excellent results in terms of yield (92%) and enantioselectivity (> 99.9% ee).<sup>332</sup> The combination of CALB immobilized on covalently supported ionic liquids with microwave irradiation led to a 28 times activity improvement and operational stability towards reuse for 12 cycles.<sup>333</sup>

### Regeneration and reuse

When regeneration of supported species is involved, the former considerations for the work-up protocols are even more important. In this case, for supported organometallic catalysts, those protocols involve one or several additional steps to ensure the complete removal of metallic species from the polymers. This is not always easy and can require treatment under relatively strong conditions (acids, bases, *etc.*), followed by a complete washing and then treatment with the corresponding metallic species to regenerate the active sites. Although the protocols for reusing a given immobilized catalyst sometimes include adding some extra amounts of the catalytic metal in the reaction mixture, the regeneration process has been studied only in a limited number of cases.

Thus, for instance, even for the case of the supported TADDOLs, which contain a very reactive ketal functionality, Seebach has shown that a complete regeneration of the activity of the Ti catalysts for the addition reaction of dialkyl zinc to aldehydes can be achieved after washing the used functional polymer **101** (Fig. 20) with 3 M HCl followed by thorough washing and reloading with  $\text{Ti}(\text{OPr})_2\text{Cl}_2$ .<sup>137</sup> When Ti catalysts are used for the addition of dialkylzincs to benzaldehyde one equivalent of titanium is consumed at the end of the reaction, and, accordingly, it is essential to reload the resin with  $\text{TiX}_4$  species after each run. In this regard, when the polymeric Ti-TADDOLate catalyst derived from dendrimer **99** was used for the addition of  $\text{Et}_2\text{Zn}$  to PhCHO, a constant performance with respect to enantioselectivity as well as the reaction rate was found during 20 consecutive runs. However, all polymers prepared with non-dendritic TADDOL crosslinkers showed a continuous decrease in reaction kinetics and enantioselectivities, reflecting again how the long-term stability of supported catalysts and reagents is greatly influenced by the linkage used between the chiral ligand and the polymeric matrix.

In the case of Ti-TADDOLates related to **225** used as catalysts for the Diels–Alder reaction between cyclopentadiene and *N*-acryloyl-3-oxazolidinone, initial attempts for regeneration were discouraging.<sup>322</sup> Regeneration of the catalyst afforded species with a reasonable activity but with a lower selectivity. Additionally, loss of performance in successive runs was much sharper than for the original systems. However, the regenerated monolith catalysed the addition of  $\text{Et}_2\text{Zn}$  to benzaldehyde with the same performance as a fresh column. Any attempt to rationalise those discrepancies requires an analysis of the differences between the two reactions under study. An important feature of the  $\text{Et}_2\text{Zn}$  addition is that it is a ligand-accelerated reaction. This feature is absent in the Diels–Alder reaction. Thus, the presence of metallic particles/species physically entrapped on the polymeric matrix,

in a non-chiral microenvironment, could be partially responsible for the activity in the catalysis of the Diels–Alder reaction, giving rise to a decrease in the selectivity. Those particles could also catalyse the polymerisation of cyclopentadiene, a factor that has been considered to contribute to deactivate the polymeric catalysts by decreasing the porosity of the resin *via* physical entrapping or copolymerisation with residual vinylic groups. In highly crosslinked PS-DVB a significant percentage of vinylic groups can remain unreacted according to FT-Raman and NMR studies.<sup>334–336</sup> In the case of the  $\text{Et}_2\text{Zn}$  addition only the recovered chiral active sites catalyse the process. Polymer supported  $\alpha$ -amino amides assayed also for the enantioselective addition of  $\text{Et}_2\text{Zn}$  to aldehydes presented some deactivation after some cycles, but the activity and selectivity could be fully recovered after an appropriate washing protocol that included a washing with 1 M HCl.<sup>146</sup>

In the case of the silica-supported BINOL derivative (**201**) considered in Fig. 47, the regeneration of the Ti-catalyst used for 10 successive runs for the ethylation of 1-naphthaldehyde with  $\text{Et}_2\text{B}$  was studied revealing that the regenerated catalyst achieved the same performance for four additional cycles.<sup>274</sup> Lunden *et al.* reported that the polymer-supported pyridine-bis(oxazoline) ligand developed for the ytterbium-catalyzed silylcyanation of benzaldehyde could be recovered from the reaction mixture and regenerated for at least 30 times.<sup>264</sup> In their study of silica-supported organocatalysts for stereoselective Diels–Alder reactions under flow conditions, Porta *et al.* analysed the regeneration of the organocatalytic column after 200 h of use and found that in this way the life of the reaction was prolonged to 300 h in total, but the performance of this regenerated catalytic column was slightly lower than that of the fresh system.<sup>337</sup>

### Selectivity

One of the main aims of the use of a catalyst is, besides the lowering of activation energies, to increase the selectivity of the process under consideration. From a theoretical and practical point of view, enantioselectivity, and in general stereoselectivity, is the most important goal to be achieved. The very small energy differences at the transition states that determine the stereochemical course of the reaction, in particular for enantiotopic transition states, make this an always difficult target. Minor changes in the reaction conditions/environment can interfere as to drastically modify those differences and, accordingly, alter the selectivity of a given reaction. This explains the key role that the polymer matrix can play in determining the selectivity in polymer-supported catalysts and reagents. The polymeric framework is a major factor in determining the actual microenvironment of the active site.

It is often considered, as a general rule, that the selectivity observed for a given chiral catalyst tends to be reduced when heterogenisation is carried out. This is not necessarily true, however, and very different trends can be found. Most of the targeted homogeneous catalysts to be immobilised are selected from those that perform, after long and costly optimisation,



with excellent (enantio)selectivities ( $>95\%$  ee). Hence, upon immobilisation, in the best scenario the levels of selectivity will be maintained, obscuring such cases in which the matrix induces a positive effect and highlighting, on the contrary, those in which a negative effect is found. Therefore, a careful examination of the different aspects of the immobilisation process should be taken into consideration to shed light on the effect of the support regarding selectivity.

In order to really assess the effect of the matrix, the first point to be considered is to ensure that proper comparisons are being made. Quite often, the structural changes made in the chiral ligand in order to provide the required features for the immobilisation are responsible for the changes observed and not the immobilisation itself. Therefore, as mentioned, it is essential to compare results obtained for homogeneous and supported ligands having the same structure.

This is clearly illustrated in the case of the immobilised Cu-BOX used as catalyst for the cyclopropanation reaction of styrene in the presence of ethylazodicarboxylate (Fig. 57). As outlined before, an efficient bisoxazoline immobilization (polymer **109**) can be carried out either by homo-polymerisation of the derivative **103** containing two vinylbenzyl groups at the methylene bridge (see Fig. 21) or by copolymerisation in the presence of styrene and DVB.<sup>172–175</sup> When the initial Cu loaded catalyst (**109d**) was used for the cyclopropanation reaction, a *trans/cis* selectivity of 60:40 and an enantioselectivity of 46% ee (*trans*) and 42% ee (*cis*) were obtained (Fig. 57). These results were far away from the ones obtained for the homogeneous derivative **230** and suggested a negative effect of the immobilisation. This is not true, however, as the decrease in the selectivity is not associated with the heterogenisation process itself, but with the change in the nature of the substitution at the methylene bridge. Thus, when the appropriate homogeneous bisoxazolines, containing two benzyl groups at the methylene bridge, **230** and **231** were synthesised, the results obtained under the same conditions for the polymeric species prepared by polymerisation (**109b–f** and **228**) were essentially identical or even slightly better than those found for the homogeneous counterpart.

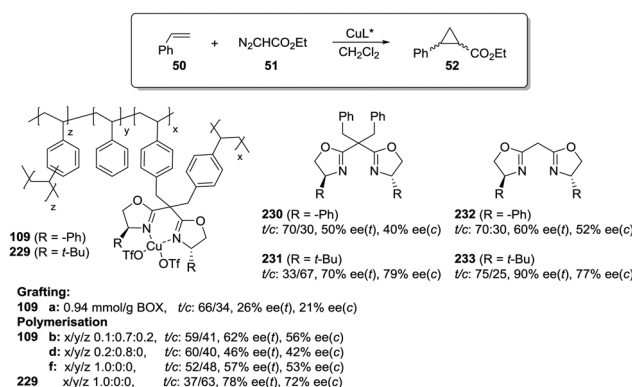


Fig. 57 Comparison of selectivity for different polymer supported Cu-BOX catalysts with that of related soluble analogues for the cyclopropanation of styrene.

It is worth mentioning here that the enantioselectivity observed for the related catalyst prepared by grafting onto a Merrifield resin (**109a**) was much lower (*t/c*: 71/29; ee 26% (*trans*), 21% (*cis*)). This represents a situation that is not uncommon: very often similar polymer-bound chiral ligands can be prepared both by grafting onto a preformed resin or by polymerisation of the corresponding functional monomer containing the chiral fragment. In many instances, selectivities found for catalysts prepared using the second strategy are higher, in particular when high degrees of crosslinking are involved. It is important to mention that the supported catalyst is prepared by polymerization of the corresponding di-vinyllic chiral monomer (**105**, Fig. 21) which provides additional crosslinking. During the polymerisation the chiral moieties are almost randomly distributed throughout the polymeric matrix and the polymer itself may become chiral, to some extent, creating many different chiral microenvironments. The exact microenvironment distribution depends on a complex series of factors, such as solvents, polarity of monomers, kinetics of polymerization of each monomer, etc.<sup>80,82</sup> Chiral moieties will be incorporated as cross linkers but can also be integrated in the linear chain (with unreacted alkene groups left). This can lead to catalytic sites with different selectivity profiles that can largely affect the enantioselectivity depending on their distribution and accessibility. These effects can be enhanced in flow processes, as illustrated by the results with the monolith **109b** when used under continuous flow conditions.<sup>338</sup> At low flow rates (2 mL min<sup>-1</sup>) the immobilised catalyst led to better enantioselectivities than the homogeneous catalyst under batch conditions (ee: 71% (*trans*), 50% (*cis*) vs. 50% (*trans*), 40% (*cis*)). The flow forces the reactants to pass-through the active sites, minimising diffusional problems, and also allows an increase in the instant S/C ratio. The former results suggest that immobilisation of the catalyst can produce positive effects on selectivity after the appropriate design of the whole set of experimental conditions. Similar effects have been also observed, for the same reaction, with the chiral Ru-PYBOX monolith **119d** (Fig. 23).<sup>339</sup> The immobilised catalyst provided, under flow conditions, better enantioselectivities (*trans/cis*: 85:15, 82% ee (*trans*), 45% ee (*cis*) in CH<sub>2</sub>Cl<sub>2</sub> or *trans/cis*: 85:15, 89% ee (*trans*), 56% ee (*cis*) in scCO<sub>2</sub>) than those found for the homogeneous catalyst in batch (*trans/cis*: 87:13, 77% ee (*trans*), 48% ee (*cis*) in CH<sub>2</sub>Cl<sub>2</sub>).

It can be expected that these effects could be minimised when attaching the catalytic sites to the polymer through a long spacer. This strategy was very successful for supporting Cu-BOX catalysts **114** and **115** from BOX ligands, prepared by grafting or polymerisation respectively, lacking the C<sub>2</sub> symmetry and tethered to the polymeric network through a long aliphatic linker (Fig. 22).<sup>182,183</sup> In this case, no polymeric effect was found, with both heterogeneous catalysts showing comparable selectivities (**114**: *trans/cis*: 67/33, 92% ee (*trans*), 90% ee (*cis*) and **115**: *trans/cis*: 67/33, 93% ee (*trans*), 90% ee (*cis*)) to those achieved for the homogeneous counterpart.

On the contrary the positive role played by the proximity of the polymeric backbone to the catalytic site was highlighted for the case of supported pyridineoxazoline (PYOX) (Fig. 58) for



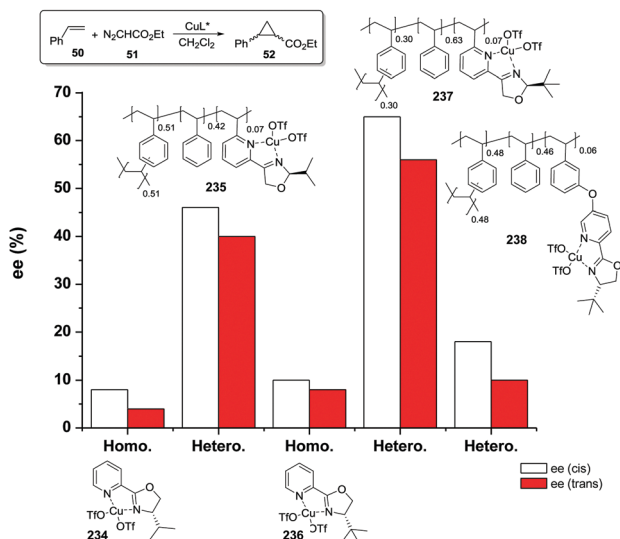


Fig. 58 General structures of the polymer-supported and homogeneous Cu-PYOX catalysts studied for the cyclopropanation of styrene.

which a remarkable enhancement in enantioselectivity was reported.<sup>340</sup> In contrast with the almost no-enantioselection obtained with both homogeneous catalysts 234 and 236 in solution, the analogous supported catalysts led to a significant asymmetric induction, 46% ee (*cis*) and 40% ee (*trans*) for 235 and 65% ee (*cis*) and 56% ee (*trans*) for 237. The steric hindrance provided by the rigid highly crosslinked polymeric backbone around the position 6 of pyridine can cooperate with the bulky substituent at the oxazoline ring to enhance the differences in energy for the different possible transition states, enhancing the chirality transfer and accordingly the enantioselectivity. To check the existence of this positive ‘polymeric effect’, a catalyst 238 with a phenoxy spacer was also synthesized. The introduction of the spacer led to a reduction of the enantioselectivity relative to 237, supporting the positive role played by the polymeric network in the sevenfold improvement in enantioselectivity observed for the supported Cu-PYOX catalyst 237.

Similar effects have been described for the immobilized Cu-PYOX catalyst 239 (Fig. 59) prepared from the linear soluble poly[(-)-*S*-4-*tert*-butyl-2-(3-vinylpyridin-2-yl)-oxazoline] in the

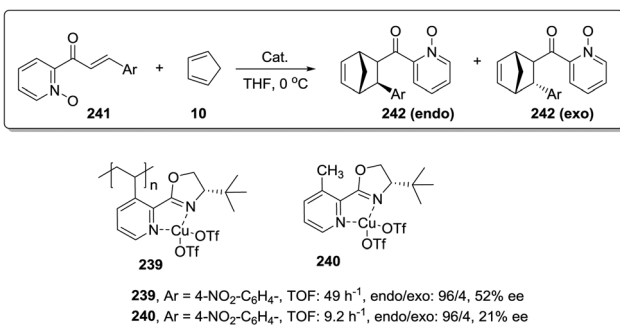


Fig. 59 Homogeneous and supported Cu-PYOX complexes as catalysts for the Diels–Alder reaction of 2-alkenyl pyridine *N*-oxide and cyclopentadiene.

Diels–Alder reaction between 2-alkenyl pyridine *N*-oxide (241) and cyclopentadiene (10).<sup>341</sup> The polymeric catalyst (239) showed an enhancement of both activity (fivefold increase) and enantioselectivity (2.5 times increase) in comparison with the unsupported homogeneous analogue (240). It was considered that the high population of Cu(II)-PYOX groups around the polymer backbone brings about a high local concentration of the catalytic sites providing a constrained environment for the Diels–Alder reaction, which favours the stereoselectivity.

In the light of these results, the proximity of the catalytic site to the polymeric framework and their relative spatial disposition, which can be tuned by the right selection of the tethering point and the use or not of spacer, seem to be key parameters in the design of polymer-supported catalysts with a positive polymeric effect. This can define, among other parameters, site-isolation and accessibility, but also the steric hindrance in the proximity of the catalytic center, which are essential to fine-tune the catalyst performance. Thus, for instance, in the case of BINOL Yang *et al.* reported a positive polymeric effect when BINOL was anchored to the polymer at 3,3'-position of the BINOL subunit. The polymeric body was designed as a bulky substituent to improve the steric control of the reaction. The *C*<sub>2</sub>-symmetric supported catalyst 244 provided much higher enantioselectivities than its homogeneous counterpart (243) for the diethylzinc addition to benzaldehyde (see Fig. 60).<sup>342</sup> Noteworthily, the BINOL supported derivative (246) lacking the *C*<sub>2</sub> symmetry showed only a slightly better performance than the homogeneous analogue (245). Both the higher hindrance and rigidity of the supported BINOL 244 may be at the origin of this positive effect. To some extent, the polymer backbone can freeze the proper conformation of the naphthyl rings making

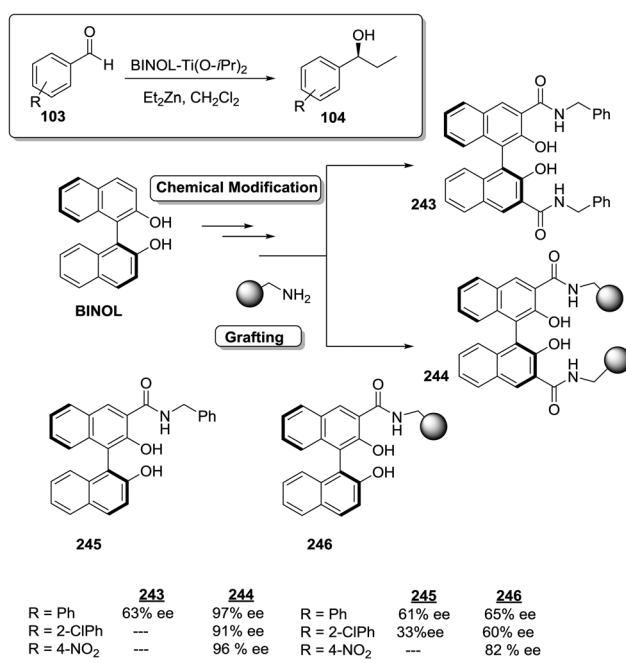


Fig. 60 Supported and homogeneous 3,3'-substituted BINOL derivatives for the Ti-catalysed Et<sub>2</sub>Zn addition to aldehydes.



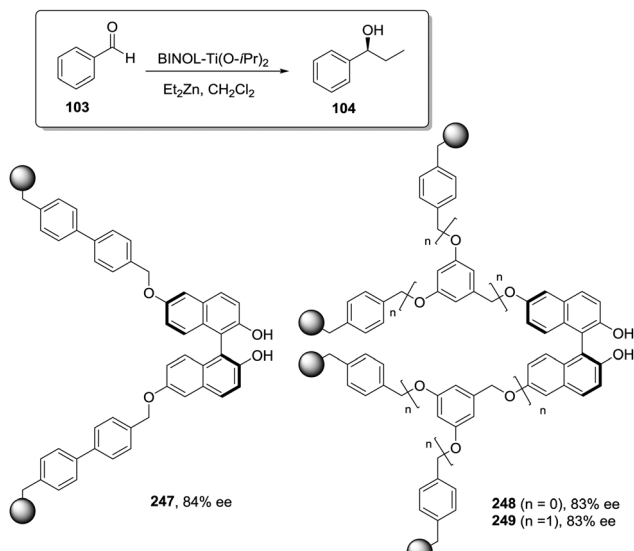


Fig. 61 Supported 6,6'-substituted BINOL derivatives incorporating long spacers for the Ti-catalysed  $\text{Et}_2\text{Zn}$  addition to aldehydes.

their twisting more difficult. This effect would be more important in the case of the 3,3'- $C_2$ -BINOL supported derivative (244) attached to two polymeric chains, greatly restricting the conformational flexibility of the two naphthyl rings, than in the case of the supported ligand 246 with only one polymeric arm.

In an alternative approach, Sellner *et al.* (Fig. 61) selected the attachment *via* the 6,6'-positions using long spacers (247) and dendrimeric spacers (248–249). The corresponding supported BINOL derivatives were prepared by copolymerisation of different 6,6'-branched  $C_2$ -BINOL crosslinking monomers with styrene.<sup>343</sup> The distance from the crosslinking points to the catalytic centre was large enough in resins 247–249 as to provide a good accessibility to the active sites and as to afford an appreciable degree of flexibility, and no polymer effect, neither positive nor negative, was detected. Selectivities achieved were comparable to those obtained in solution, even considering that the catalytic active sites were placed in the crosslinked region of the polymer.

However, when a similar approach was investigated using much more rigid 3,3' and 6,6'  $C_2$ -BINOL crosslinking agents to obtain supported BINOLs 250 and 251, a negative matrix effect was found (Fig. 62).<sup>344</sup> The enantioselectivities observed were in all cases lower than in solution, being strongly affected by the substitution pattern of the supported BINOL. In this sense, the polymers containing 6,6'-disubstituted BINOLs showed higher selectivities than those with the more hindered 3,3'-disubstituted-BINOLs (78% ee for 251 vs. 20% for 250).

The very rigid framework achieved in these polymers and the steric interference of the polymeric matrix, particularly in 250, can prevent the diol moiety from achieving a proper conformation and limit the accessibility to the active sites. This is in good agreement with the work of Hodge and coworkers using supported aminoalcohols, who demonstrated that in those cases where the aldehyde and  $\text{Et}_2\text{Zn}$  cannot diffuse freely into the polymer to reach the catalytic sites, a non-catalysed reaction

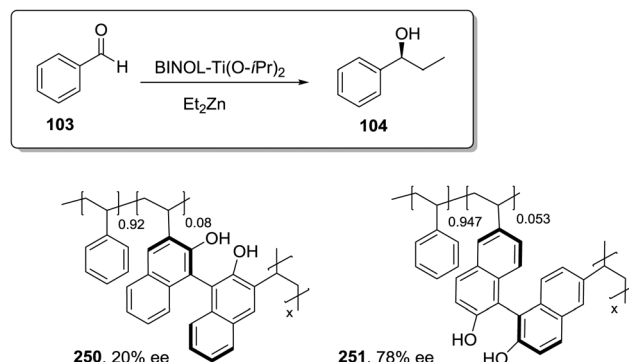


Fig. 62 Supported 3,3' and 6,6'-substituted BINOL derivatives fusing very short spacers for the Ti-catalysed  $\text{Et}_2\text{Zn}$  addition to aldehydes.

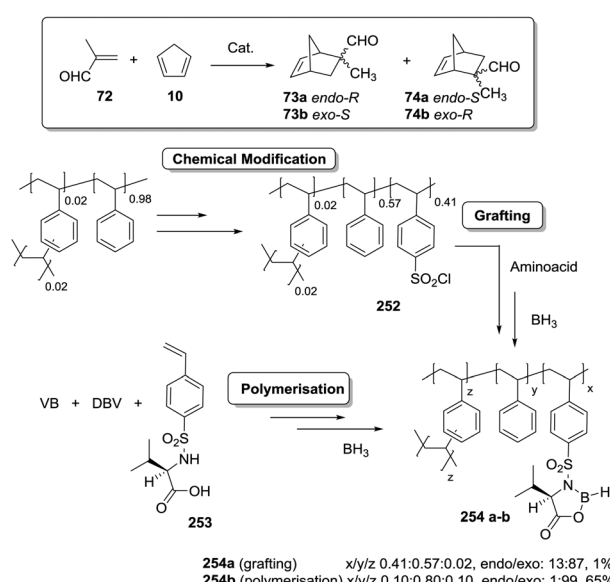


Fig. 63 Preparation of chiral boron supported catalysts for the Diels–Alder reaction between cyclopentadiene and methacrolein.

is possible giving a racemate and so reducing the stereochemical performance.<sup>293,294,345</sup>

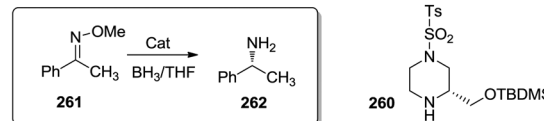
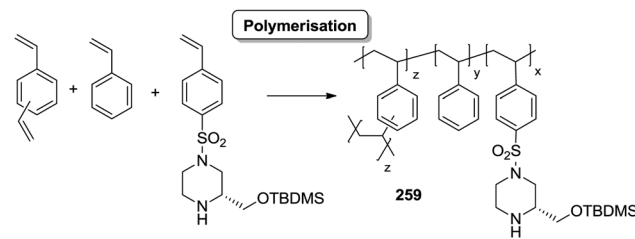
A related effect was described, for instance, by Kamahori *et al.* in their study of boron species, prepared from polymer supported chiral  $N$ -sulphonyl amino acids, for the catalysis of the Diels–Alder reaction between cyclopentadiene and methacrolein (Fig. 63).<sup>346</sup> The catalyst 254a, prepared by grafting, from resin 252, was essentially unselective, whilst a 57% ee was found for 254b prepared by polymerisation of the  $N$ -vinylbenzylsulfonyl amino acid 253. A possible explanation for this behaviour was suggested by the solvent effects observed in homogeneous solution. The selectivity observed in THF was much higher (86% ee) than that in  $\text{CH}_2\text{Cl}_2$  (20% ee), suggesting that the non-donor solvent  $\text{CH}_2\text{Cl}_2$  favours the presence of non-selective aggregates. Immobilisation through grafting does not destroy such a possibility, as functionalisation occurs in the more accessible sites of the resin in a very flexible matrix, allowing for site-to-site interactions. Those are much more difficult when the functional groups are introduced by polymerisation

in a highly crosslinked matrix. According to this, the use of a  $\text{CH}_2\text{Cl}_2/\text{THF}$  mixture with the supported catalyst **254b** had a minor effect on the selectivity. It was also observed that an increase in loading was accompanied by up to a 4 times decrease in enantioselectivity.

Similar improvements in asymmetric induction for the immobilised catalyst were also found for the asymmetric transfer hydrogenation of aromatic ketones in water. The supported catalyst **44a** (Fig. 7) provided higher enantioselectivities than the homogeneous analogue (water-soluble modified TsDPEN)<sup>347</sup> for the Ru and Ir-catalysed reduction of aromatic ketones (e.g.:  $\text{C}_6\text{H}_5\text{COCH}_3$  98% vs. 94% ee,  $\text{C}_6\text{H}_5\text{COCH}_2\text{CH}_3$  96 vs. 86% ee, *p*-Cl- $\text{C}_6\text{H}_4\text{COCH}_3$  99% vs. 91% ee, Napt $\text{COCH}_3$  87% vs. 87% ee).<sup>119,348</sup>

The effect of loading is crucial for the performance of many supported reagents and catalysts. In the case of the enantioselective reduction of acetophenone with a LAH derivative of the resin-bound ephedrine, enantioselectivity values ranged from 55% for a resin containing 2.1 mmol g<sup>-1</sup> to 79% for a loading of 0.7 mmol g<sup>-1</sup>.<sup>349</sup> The same phenomenon has been reported by Seebach for supported Ti-TADDOLate catalysts, where better enantioselectivities were observed for the polymers with lower loadings.<sup>167</sup> In other cases, however, high loadings have been found to be associated with better enantioselectivities. Thus, the enantioselectivities achieved for the asymmetric borane reduction of acetophenones (**257**) catalysed by polymer-supported chiral sulphonamides (**255**) showed a steady improvement when the functionalisation degree was slightly increased (63, 75 and 85% ee, respectively for loadings of 2.23 mmol g<sup>-1</sup>, 2.26 mmol g<sup>-1</sup> and 2.29 mmol g<sup>-1</sup>). Additionally the enantioselectivity obtained in this case by the supported catalyst was higher than that by the homogeneous analogue **256** (Fig. 64).<sup>350,351</sup>

Itsuno *et al.* have reported another remarkable example highlighting a positive matrix effect on both reactivity and selectivity (Fig. 65).<sup>352</sup> This enhancement may well be related to pseudodilution/isolation effects related to immobilization. Thus, after the adequate optimization of the polymeric catalyst, the supported oxazaborolidine derived from **259b** showed a better performance in terms of activity and selectivity than the low molecular counterpart (**260**). When used at room temperature for the borane reduction of the acetophenone *O*-methoxy



#### Homogeneous:

**260:** 50 °C, 61% Yield, 84% ee  
rt, 0% Yield,

#### Polymerisation

**259a:** x/y/z: 0.10:0.80:0.10, 50 °C, 56% Yield, 72% ee  
rt, 0% Yield,

**259b:** x/y/z: 0.10:0.88:0.02, 50 °C, 77% Yield, 60% ee  
0 °C, 0% Yield,

**259c:** x/y/z: 0.20:0.70:0.10, rt, 60% Yield, 82% ee  
0 °C, 0% Yield, 90% ee

**259d:** x/y/z: 0.20:0.78:0.02, rt, 65% Yield, 96% ee  
0 °C, 70% Yield, 99% ee

**259e:** x/y/z: 0.30:0.68:0.02, rt, 37% Yield, 90% ee

Fig. 65 Polymer supported piperazine methanol ligands for the catalytic borane reduction of *O*-methoxy oximes.

oxime (**261**), **259b** led to 65% yield and 96% ee. These results were even better at 0 °C (70% yield and 99% ee). However, the process with the homogeneous **260** did not occur under the same experimental conditions. The temperature should be increased to 50 °C to achieve 61% yield and 84% ee. This may be related to the formation of inactive/nonselective aggregates in solution at room temperature. An increase in temperature may favour the breakdown of such aggregates liberating the active forms of the catalyst. In the case of the supported catalyst, the formation of aggregates will not be favoured, allowing the involvement of the active catalytic species even at lower temperatures.

A similar effect can be accounted for in the case of the supported amino-alcohol **224** (Fig. 54) obtained as a polymeric monolith and used as a catalyst for the  $\text{Et}_2\text{Zn}$  addition to benzaldehyde under flow conditions.<sup>320</sup> The polymer prepared by polymerisation showed an improved selectivity (99% ee) in comparison with those found for the related homogeneous catalyst (87% ee) or the one immobilised onto a Merrifield resin by grafting protocols (89% ee).

Sundararajan *et al.* prepared a polymeric analogue of chiral  $C_2$ -symmetric (*R,R*)-3-aza-3-benzyl-1,5-dihydroxy-1,5-diphenylpentane (**266**) by copolymerization of the corresponding vinylic derivative with styrene and DVB (Fig. 66).<sup>353</sup> The corresponding supported Al complex (**265**) catalysed the Michael additions of nitromethane and the addition of thiophenols to unsaturated cycloalkenones. In the case of the Michael addition between nitromethane and chalcone **267**, the supported catalyst **265a** led to higher asymmetric induction (51% ee) than the related homogeneous analogue (**266**, 5% ee). However, for the polymer **265b**, with lower crosslinking content and higher styrene

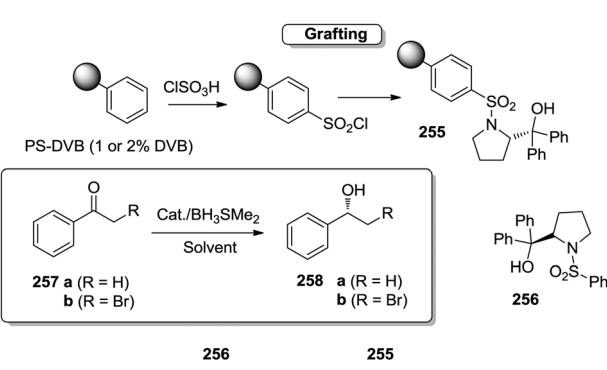


Fig. 64 Polymer supported chiral sulfonamides for the enantioselective reduction of acetophenones.



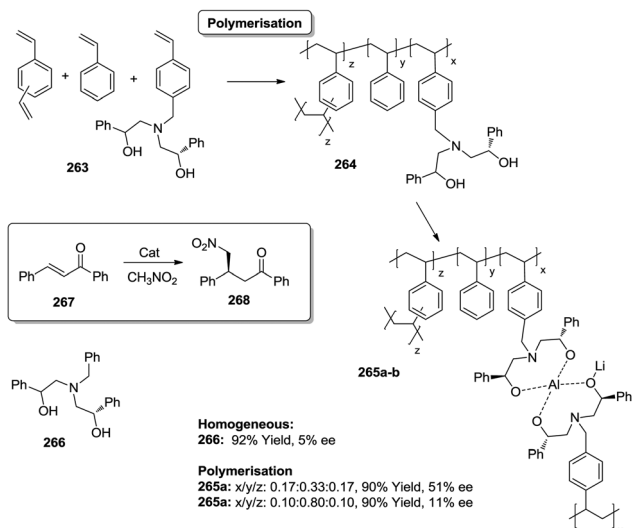


Fig. 66 Polymer supported Al complexes for the asymmetric Michael addition.

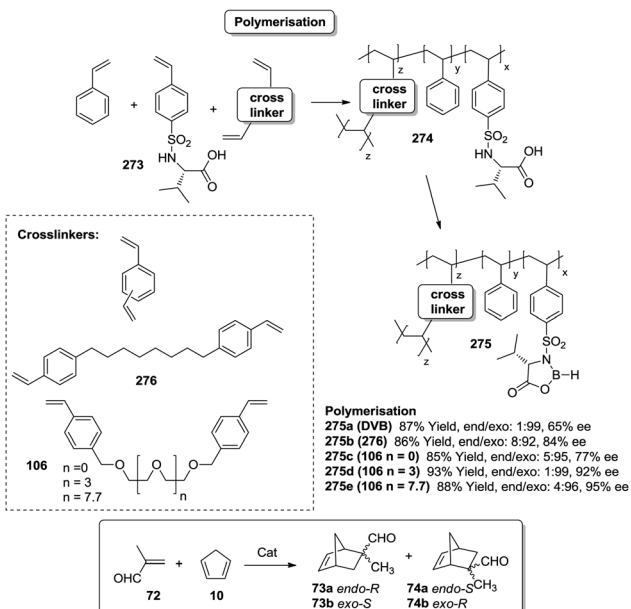


Fig. 68 Preparation of supported oxazaborolidines by polymerization involving different crosslinkers.

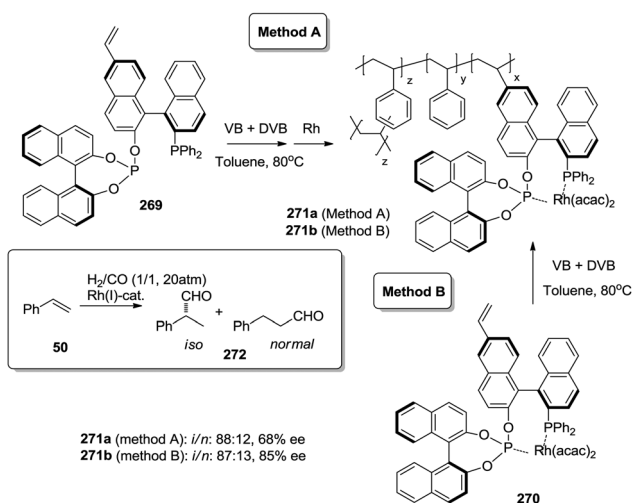


Fig. 67 Polymer supported (R,S)-BINAPHOS prepared by two alternative polymerisation approaches.

incorporation, the enantioselectivity significantly dropped (11% ee). The crosslinking degree can define the rigidity of the ligand, modifying to some extent the steric restrictions around the catalytic site and leading to more efficient heterobimetallic catalysts inducing a better chiral transfer.

The formation of different active species as a consequence of different polymerisation procedures has been proved for the Rh-catalysed asymmetric hydroformylation of styrene involving two polymer supported (R,S)-BINAPHOS ligands (271, Fig. 67).<sup>354,355</sup> When the polymerisation of 269 was performed in the absence of the metal, the ligand adopted a conformation that apparently was not suitable to coordinate the Rh. Thus the resulting polymeric catalyst 271a gave rise to a modest selectivity of 68% ee (method A). However, the conformation of the ligand could be fixed in a suitable disposition when the polymerisation was performed directly with the corresponding chiral Rh-monomeric

complex (270) (method B). Indeed, a better selectivity was obtained under the same conditions (85% ee).

Another important factor to be considered is the crosslinking. When the immobilised catalysts are prepared by a bottom-up approach by direct polymerisation of the chiral functional monomers, different crosslinking agents can lead to different microenvironments, which, in turn, can modify, even enhance, the asymmetric induction of a given reaction. This was the case of the Diels–Alder reaction between methacrolein and cyclopentadiene catalysed by polymeric chiral oxazaborolidines obtained by polymerisation in the presence of different crosslinking agents.<sup>92</sup> The selectivities found were significantly influenced by the crosslinkers (Fig. 68). The polymeric catalyst 275a derived from DVB catalysed the reaction with moderate selectivity (65% ee), while the polymeric catalyst prepared with the more flexible crosslinking agent 276 gave an enhanced enantioselectivity (275b, 84% ee). This was comparable to the selectivity obtained from using the unsupported catalyst in solution as reported by Helmchen (86% ee).<sup>356</sup> Finally, the polymeric catalyst with a longer oxyethylene crosslinker gave enantioselectivities as high as 95% ee (275e), results that are superior to those obtained with the related homogeneous catalyst in solution.

When supported Al catalysts derived from polymeric prolinols 65–66 (Fig. 10) were used for the same Diels–Alder reaction, selectivities found were low or moderate, being similar for the functional polymers prepared by grafting or by polymerisation (suspension or “bulk” polymerisation) using low crosslinking degrees (up to 20%), but a twofold increase in ee was found when the crosslinking (DVB) was increased to 90%.<sup>357</sup>

The polymer-supported Rh catalysts obtained through the copolymerization of (S)-5,5'-divinyl-BINAP (277) also exhibited better enantioselectivity than the corresponding homogeneous

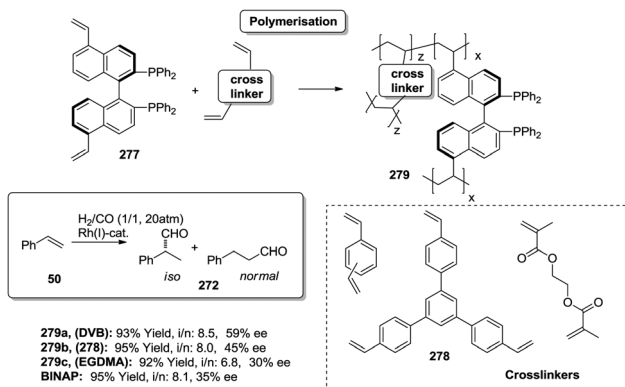


**Fig. 69** Polymerisation of a vinylic BINAP derivative in combination with different crosslinkers for the Rh-catalysed hydroformylation.

complex (Fig. 69).<sup>358</sup> The BINAP immobilisation was performed by copolymerisation of 277 with different crosslinking agents (DVB, 1,3,5-tri(4-vinylphenyl)benzene (278) and EGDMA) and the corresponding Rh-complexes were assayed in the asymmetric hydroformylation of styrene. The results showed that the pore structures had little effect on the yields, but had a clear effect on the regioselectivity and enantioselectivity. Catalysts 279a and 279b exhibited higher enantioselectivity (59% and 45% ee, respectively) than the related homogeneous system (35% ee). However, 279c containing ethylene glycol dimethacrylate as crosslinker provided only a modest enantioselectivity of 30% ee. These results highlight once again that the nature of the crosslinkers can be used to modify/improve the selectivity.

A very particular case regarding the influence of polymerization on enantioselectivity is given by the preparation of polymers displaying intrinsic main chain chiral organization, in particular through the adoption of helical structures.<sup>29,30</sup> In many cases, the reported asymmetric inductions are rather limited.<sup>247</sup> In the last few years, however, different groups have reported examples in which the helical organization of the polymeric chain provides a significant contribution towards the enantioselectivity for a variety of catalytic reactions. In some instances it has been reported that the presence of helicity can increase the enantioselectivity from 18% ee for the non-helical support to 94% ee for the helical one.<sup>359</sup> In some extreme cases, even attachment of achiral catalyst groups on the helical polymer matrix, whose helix sense is switchable, allows selective production of both enantiomers with enantioselectivities higher than 90% ee in several mechanistically different palladium-catalyzed and organocatalytic asymmetric reactions.<sup>360-362</sup>

Cinchona-alkaloid derived quaternary ammonium salts have been immobilized through ionic interactions to polymers possessing sulfonate groups and were used as supported organocatalysts in the asymmetric alkylation of *N*-diphenylmethylene glycine *tert*-butyl ester (283, Fig. 70).<sup>363</sup> Their synthesis was approached either by polymerization of a chiral quaternary ammonium sulfonate monomer or by the immobilization of a chiral quaternary ammonium salt onto a sulfonated polymer through an ion exchange reaction. In this particular case, both approaches provided similar results. The enantioselectivity

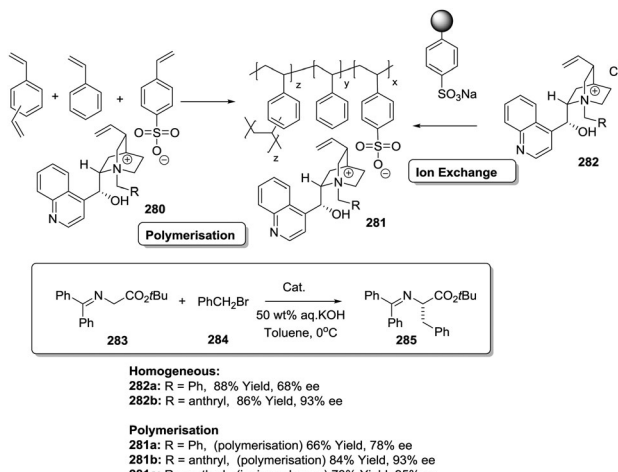


**Fig. 70** Preparation of polymer supported quaternary ammonium salts derived from cinchona alkaloids by polymerization and ion exchange as catalysts for asymmetric alkylations.

obtained by using the polymeric catalyst **281a** (78% ee) was higher than that obtained from the unsupported salt **282a** (68% ee). The 9-anthracenemethyl derivative of the cinchonidine-based quaternary ammonium salt gave better enantioselectivities both in solution (**282b**, 93% ee) and with the supported derivative (**281b**, 93% ee; **281c**, 95% ee).

Based on the immobilisation through ionic bonding and due to the exceptional stability of the quaternary ammonium sulfonate salts, the same authors have developed a very versatile strategy to immobilise different chiral salts in the main polymeric chain.<sup>364</sup> This strategy is based on bringing together different modular building blocks (monomeric or dimeric chiral salts and sulfonate salts) to create a chiral ionic polymer allowing fine-tuning of the catalytic efficacy from a bottom-up approach. In this way by tuning the structure of these building blocks, the polymer main chain can be adjusted to positively affect the conformation of the catalytic sites enhancing the catalytic efficiency.<sup>365</sup> Fig. 71 schematically represents some of the strategies developed using cinchona-alkaloid-derived quaternary ammonium salts as chiral catalysts for the asymmetric benzylation of *N*-diphenylmethylene glycine *tert*-butyl ester. Main chain supported chiral salts immobilised by completely ionic interaction, combining both ionic and covalent bonds or just solely based on covalent immobilisation have been successfully obtained.<sup>366–370</sup> A wide range of structural building blocks have been evaluated in order to optimise the supported catalyst. In most of the cases, it has been possible to adjust the polymer structure to obtain catalysts (286–289) which are often more selective than the homogeneous analogues.

The great modularity of the approach has also allowed extending this methodology to other types of organocatalysts opening avenues to a wide range of asymmetric transformations.<sup>371,372</sup> For instance, main chain polymers **290–291** derived from chiral imidazolidinone have been reported as efficient organocatalysts for the Diels–Alder reaction (Fig. 72).<sup>373–375</sup> By using the right combination of building blocks, the immobilized

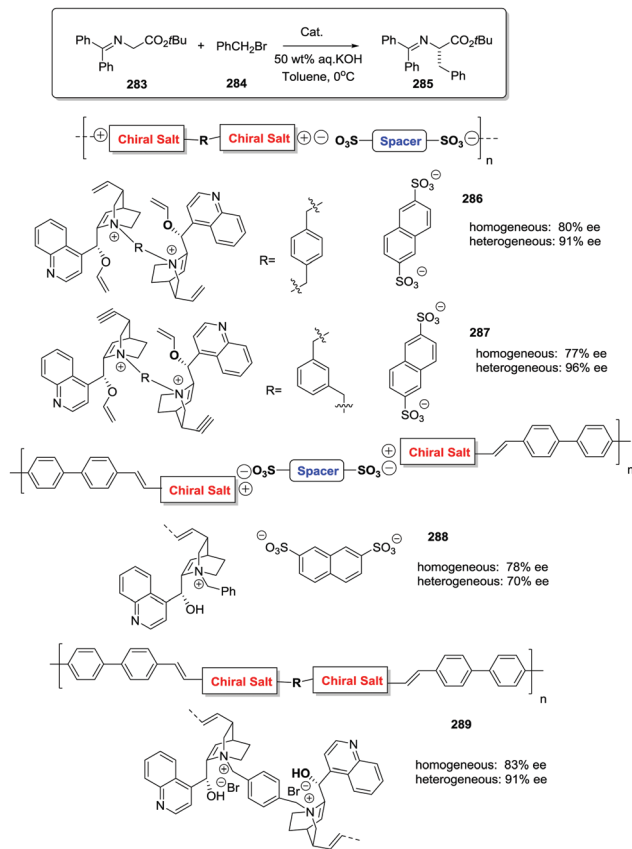


Fig. 71 Preparation of polymer-supported quaternary ammonium salts derived from cinchona alkaloids by polymerization and ion exchange as catalysts for asymmetric alkylations.

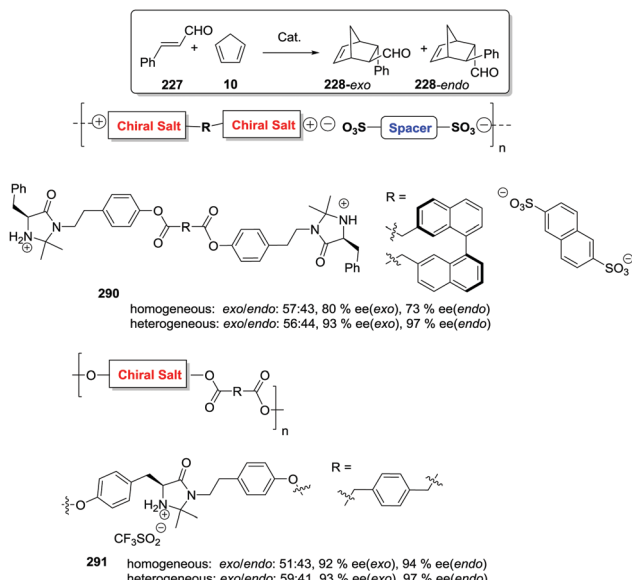


Fig. 72 Preparation of polymer-supported ammonium salts derived from MacMillan Imidazolidinone by polymerization and ion exchange as catalysts for Diels–Alder reaction.

systems displayed an equivalent or even better selectivity than the homogeneous counterpart.

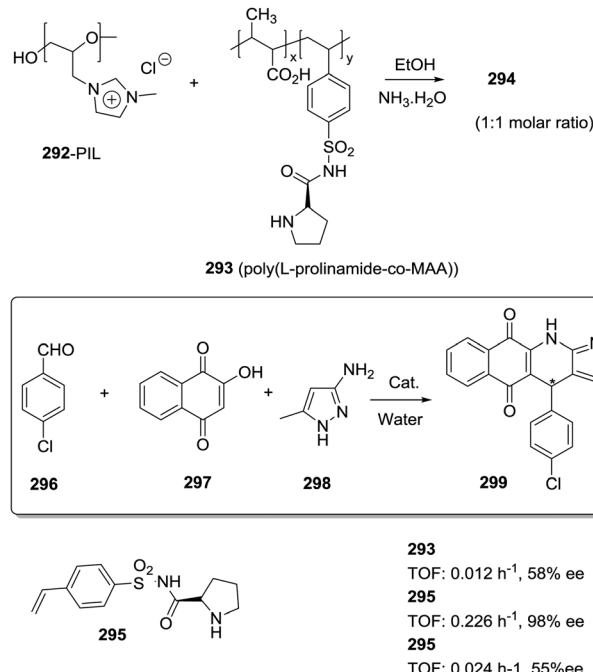


Fig. 73 Preparation of a nanoparticle-supported catalyst by *in situ* ionic complexation between an imidazolium-based polymer ionic liquid (PIL) and poly(L-prolinamide-*co*-MAA) for the three component reaction.

The ionic complexation has been also employed by Hu, Li and co-workers to obtain a nanoparticle-supported catalyst by *in situ* ionic complexation between an imidazolium-based polymer ionic liquid (PIL) and poly(L-prolinamide-*co*-MAA) (Fig. 73).<sup>376</sup> The structure and hydrophobicity–hydrophilicity balance of the nanoparticles can be fine-tuned by varying the PIL reaction ratio and by applying different anions.

The chiral solid efficiently catalysed both Aldol and multi-component reactions (MCRs) in water exhibiting much better catalytic activity and enantioselectivity than its homogeneous catalytic analogue. For instance, the poly(L-prolinamide-*co*-MAA) copolymer (293) and the corresponding monomer (295) gave modest activity and enantioselectivity for the three component reaction between 4-chlorobenzaldehyde (296), 2-hydroxy-1,4-naphthoquinone (297), and 3-amino-5-4-methylpyrazole (298) at 80 °C in water. However, the activity and enantioselectivity found for the nanoparticle-supported catalyst (294) clearly surpassed those values. The combination of both polymeric elements creates a polymeric nanoparticle with a PIL outer structure that facilitates the mass transfer of reaction substrates into the nanoparticle and creates the required micro-environment for the induction of chirality.

Similar selectivity enhancement can be also found when soluble polymers are carefully designed. For instance, the immobilization of [Mn(salen)] complexes on smart polymers can render catalytic systems which are not only more active but also more selective than the homogeneous counterpart (Fig. 74). The introduction of adequate building blocks in the polymer structure contributes to tune and enhance the asymmetric induction by favoring the polymer self-assembly in a micellar

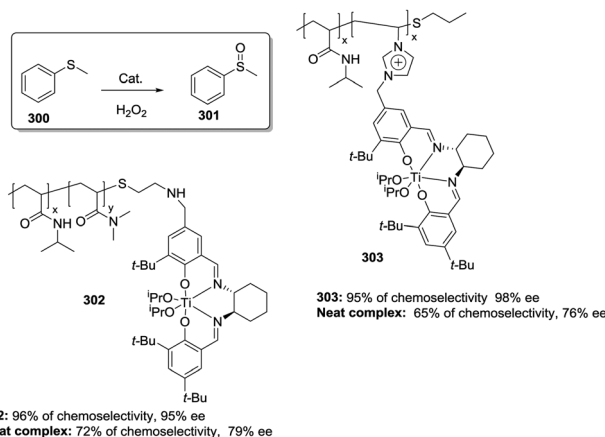


Fig. 74 Soluble chiral Ti-Salen complexes as catalysts for highly enantioselective sulfoxidation in water.

well-organized structure. Thus, the polymeric catalyst **302** led to quantitative conversion ( $>99\%$ ) of methyl phenyl sulfide (**301**) with up to 96% chemoselectivity and 95% enantioselectivity, whereas the neat complex was far less efficient (9% conversion with 72% chemoselectivity and 79% enantioselectivity).<sup>241</sup> In a similar way, amphiphilic block copolymer **301** based on the *N*-isopropylacrylamide and vinylimidazolium ionic liquid modified chiral salen  $Ti^{IV}$  complex (poly[NIPAAm-*co*-PIL-[Ti(salen)]]) efficiently catalyzed the enantioselective oxidation of aryl sulfide in water. The optimized supported catalyst showed, for the oxidation of methyl phenyl sulfide in water, better activity and selectivity (almost quantitative yield (95%), 95% of chemoselectivity and with up to 98% ee) than the related neat monomeric catalyst (48% of conversion, 65% of chemoselectivity and 76% of ee).<sup>377</sup> In this case, the stable structure of the self-folded single-chain polymeric nanoparticles (SCPNs) and the presence of the ionic liquid moiety in the confined SCPNs provide a suitable micro-environment to favor the concentration of the reactants and to induce a better enantioselection.

## Dendrimers

In the same way that catalytic activity can be enhanced by the “positive dendrimer effect”, under certain circumstances an enhancement in the selectivity, especially the chiral induction, can be achieved upon catalyst immobilization on a dendritic support. In this regard, Ribourdouille *et al.* have demonstrated that Pd-PYRPHOS catalytic units immobilized onto polyamidoamine dendrimers (PAMAM) can surpass the selectivity found for the monomeric reference.<sup>378</sup> The higher generation dendrimers decorated with a chiral Pd-complex (PAMAM(PYRPHOS-PdCl<sub>2</sub>)<sub>64</sub>, **304**) rendered a better chiral induction (69% ee) in the allylic amination than the monomeric model (**305**, 9% ee). The improvement was related to the changes in the conformational flexibility and preferential orientation of the aryl substituents of the diphosphine by increased crowdedness at the periphery of the dendrimer upon increasing the dendrimer wedges (Fig. 75).

Similar positive effects have been reported by Zhang *et al.* for the asymmetric hydrogenation of  $\alpha$ -dehydroamino acid esters and enamides catalyzed by Rh-chiral dendritic monodentate

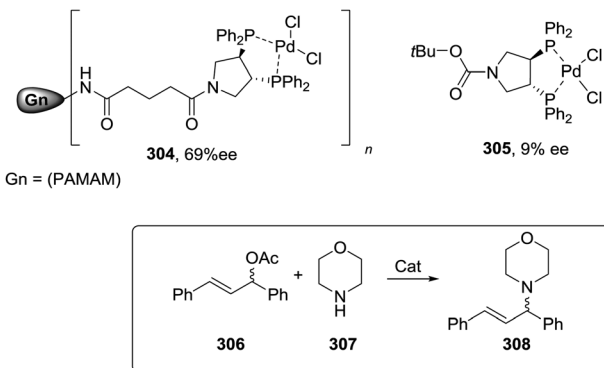


Fig. 75 Dendrimer supported Pd-PYRPHOS catalysts for the allylic amination displaying an enhanced chirality transfer than the unsupported catalyst.

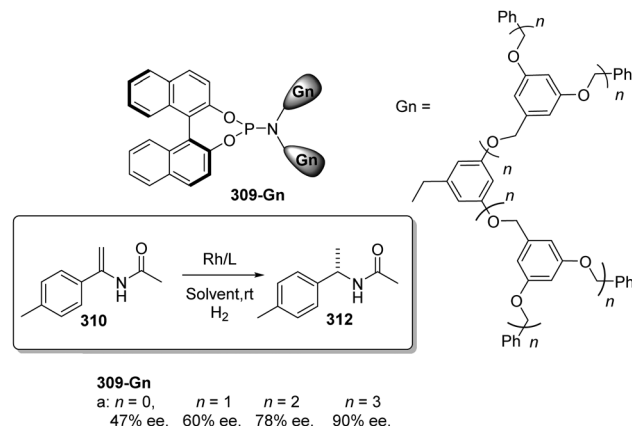


Fig. 76 Dendritic chiral monodentate phosphoramidite ligands developed for enantioselective Rh-catalysed hydrogenations.

phosphoramidite complexes (Fig. 76).<sup>379</sup> The corresponding chiral dendritic ligands (**309**) were obtained through substitution of the dimethylamino moiety in the original monodentate phosphoramidite by Fréchet-type polyaryl ether dendritic wedges. In this case, the catalytic unit is located at the core and not at the periphery. As an illustrative example, the enantioselectivity for the hydrogenation of *N*-(1-(*p*-tolyl)vinyl)acetamide (**310**) increased from 47% ee for the monomeric catalyst to 92% ee for the third dendrimer generation. However, a negative dendrimer effect on the catalytic activity was observed. This suggests an effective encapsulation of the catalytic unit within the dendritic wedges. The increasing steric repulsion between dendritic wedges might influence the chiral pocket of the catalyst where the hydrogenation reaction occurs enhancing the selectivity in comparison with the monomeric catalyst, but at the expense of reducing the rate of the reaction.

Different approaches for the preparation of BINAP systems immobilized on dendrimers have been reported. The existence of a “dendrimer effect” seems to depend on the immobilization strategy applied. The BINAP containing dendritic wedges at the 5,5'-position of the binaphthyl backbone linked by amide groups (Fig. 13) induced a positive dendrimer effect regarding the catalytic activity for the hydrogenation of  $\beta$ -keto esters;



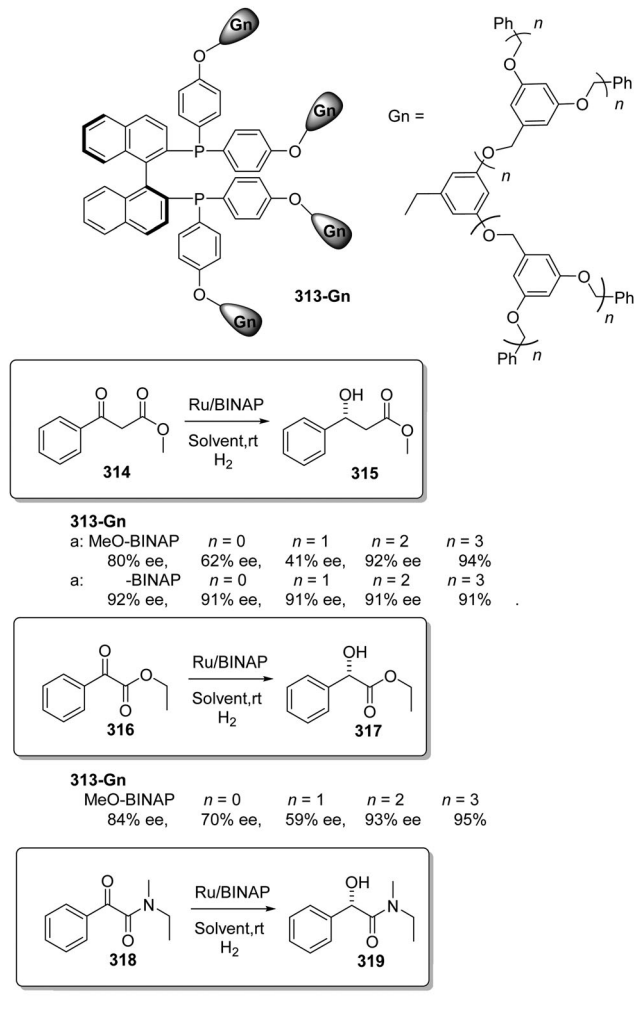


Fig. 77 BINAP systems with dendritic wedges attached to the four phenyl rings on the P atoms, used for the Ru-catalysed asymmetric hydrogenation.

however no improvement in selectivity was observed. In this case, the dendritic units are far away from the chiral center.<sup>150</sup> However, when the dendritic units are directly attached to the diphenylphosphine chelating units of the BINAP (313-Gn) significant dendrimer effects can be found for the ruthenium-catalysed asymmetric hydrogenation of  $\beta$ -keto esters (314) or  $\alpha$ -ketoesters (316), as well as  $\alpha$ -ketoamides (318) (Fig. 77).<sup>380,381</sup> Indeed, the high-generation catalysts exhibited excellent enantioselectivities, which were superior to those obtained from the related small molecular catalysts. The attachment of bulky dendritic wedges on the four phenyl rings at the P atoms was able to fine-tune the steric environment around the metal center. The increasing steric repulsion between the dendritic wedges might be responsible for the different arrangement of the four phenyl rings, and consequently modulate the catalytic behaviour of the [Ru(Gn-BINAP)] complexes.

Chen *et al.* have designed chiral Ti-salen complexes on the periphery of a polyamidoamine (PAMAM) dendrimer capable of providing enhanced activity, chemoselectivity and enantioselectivity in comparison with the unsupported catalyst. The peripheral

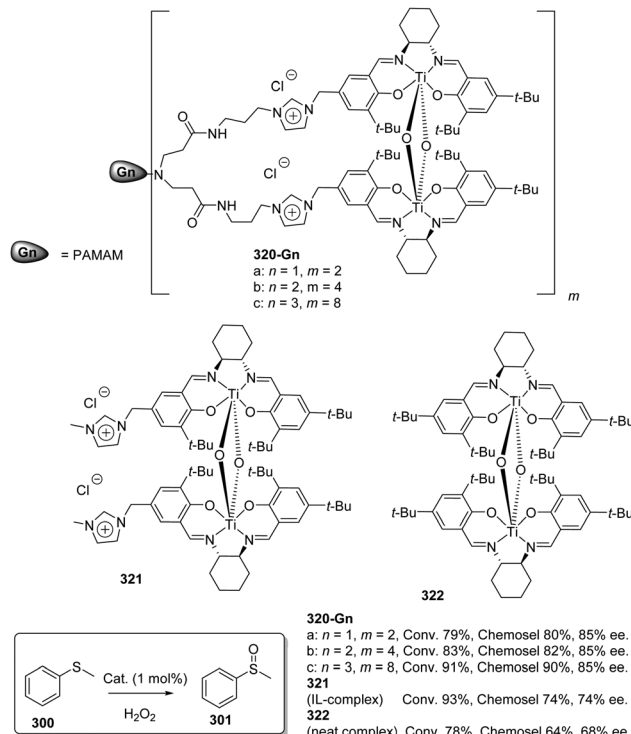


Fig. 78 Ti-salen complexes attached to PAMAM dendrimers through an imidazolium linker used for the asymmetric oxidation of sulfides.

free amine groups of PAMAM provide a suitable grafting point for the Ti-salen complex (Fig. 78).<sup>382</sup> However, in the initial design, the dense packing of active sites at the periphery of PAMAM increased the difficulty for all complexes to adopt their preferred conformation, which is detrimental to catalysis. This was overcome by the introduction of IL-like units as spacers (320-Gn). The role of this spacer was multiple. It located the chiral complexes away from the dendrimer backbone, ensured a high local concentration of the catalyst and allowed achieving the preferred conformation of the active sites, favouring the intramolecular cooperation between the catalytic sites and therefore enhancing the selectivity. Furthermore, the IL-like units modified the hydrophilic/hydrophobic balance of the support making it more compatible with organic sulfides and aqueous  $\text{H}_2\text{O}_2$ , facilitating the mass transfer of the reagents and therefore enhancing the activity. The performance of the catalyst 320-Gn (conv. 91%, chemoselectivity 90% and 85% ee) was enhanced relative to that of the analogue 321 (conv. 93%, chemoselectivity 74% and 74% ee) and was even better than that of the homogeneous analogue 322 (conv. 78%, chemoselectivity 64% and 68% ee).

Gissibl *et al.* have immobilized azabis(oxazoline) ligands onto the terminal groups of phosphorus-containing dendrimers (polyphosphorhydrazone, PPH) (327-Gn). The corresponding copper(II) complexes were used as immobilised catalysts for the asymmetric benzoylation of diols (Fig. 79).<sup>383</sup> Interestingly, an excellent enantioselectivity was observed for the first and the second generation, but there was a large detrimental effect with the third generation. The dendritic catalysts afforded compound

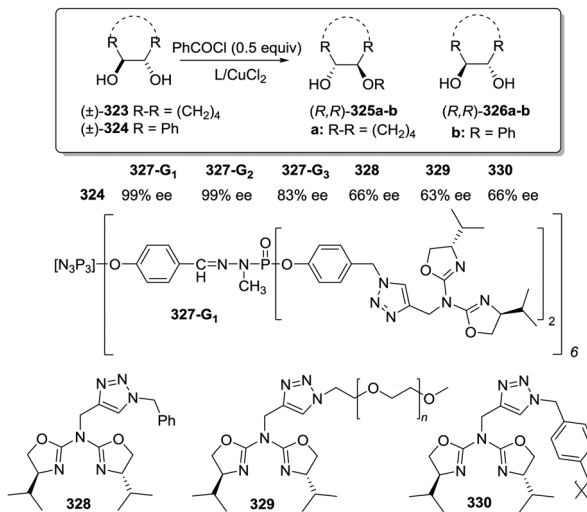


Fig. 79 General structure of azabis(oxazoline) ligands attached to PPH dendrimers and their homogeneous, PEG and PS supported analogues assayed for the asymmetric benzoylation of diols.

**324b** with better selectivities than the monomeric counterpart (**328**) or those found for the azabis(oxazolines) supported onto soluble polymers such as MEOPEG (**329**) or polystyrene (**330**).<sup>384</sup> The lack of selectivity found for these non-dendritic systems was associated with the ability of the achiral triazole moiety, used as a linker for the attachment, to coordinate with copper.<sup>385</sup> In the case of the dendrimers the triazole moieties were suggested to be soaked in the globular structure of the dendrimer and only the chiral azabis(oxazoline) fragments were located at the periphery of the dendrimer and exposed enough to coordinate to copper, avoiding non- or less selective reaction pathways.

A very impressive enhancement in selectivity related to a positive dendrimer effect has been reported by García *et al.* for the Rh-catalysed [2+2+2] cycloaddition reactions between *N*-tosyl-1,6-diyne and 2-methoxynaphthalene alkynyl derivatives (Fig. 80).<sup>386</sup> The phosphoramidite ligands for Rh complexation were also immobilized onto the peripheral groups of PPH dendrimers (**331-G<sub>n</sub>**). An enhancement in both yield and enantioselectivity through a positive dendrimer effect was observed. The monomer (**332**) almost induced no enantiomeric excess, whereas all the generations of the dendrimers, from **331-G<sub>1</sub>** to **331-G<sub>3</sub>**, afforded a very high enantioselection. It should be noted that the dimeric homogeneous system (**333**) was not more efficient than the monomer **332**, excluding simple cooperative site-site effects. These data pointed out to an effect associated with a large number of chiral entities in close proximity.

### Topicity inversion

The effect of the polymer can be so important that the morphology of the polymeric backbone can even alter the topicality of the resulting products. The literature contains a limited number of examples of polymer-bound enantioselective catalysts for which the topicality of the resulting products can be controlled through the morphology of the support with the potential for achieving a dual stereocontrol.<sup>387</sup>

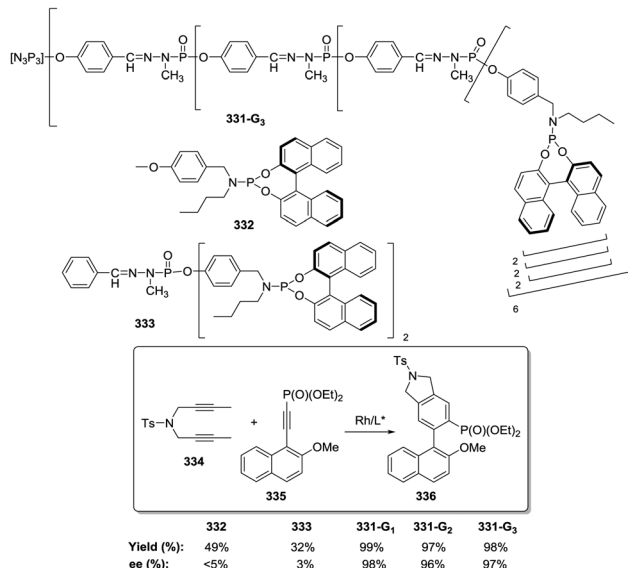


Fig. 80 General structures of dendritic and non-dendritic phosphoramidite ligands studied for Rh-catalysed [2+2+2] cycloaddition reactions.

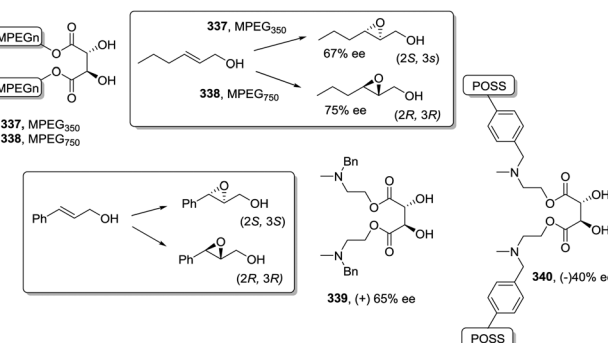


Fig. 81 Examples of supported tartrate ligands providing topicality reversal of the major enantiomer associated with the nature of the achiral polymeric support.

Two of such examples have been reported for catalysts derived from immobilized tartaric acid esters and used for the enantioselective Sharpless asymmetric epoxidation reaction (Fig. 81). Reed *et al.* found that in the epoxidation of 2-hexen-1-ol when using poly(ethylene glycol) *trans*-esterified chiral tartrates (**337**–**338**), the enantioselection observed could be reversed depending on the PEG chain length.<sup>388</sup> A clear change in topicality was found to occur when the molecular weight of the PEG chain acting as the support was around 800 or higher. Similarly, García *et al.* have also reported that when using for this chiral epoxidation a supported tartrate derivative **340**, immobilised onto polyhedral oligomeric silsesquioxanes (POSS), a reversed enantioselectivity was observed with regard to the use of the related non-supported ligand **339**.<sup>389</sup> In both cases, the change in enantioselectivity was proposed to occur as a result of the coexistence of two Ti-ligand complexes which differ in the molecularity of the ligand, one with a monomeric ligand and the other with a dimeric ligand. The POSS support and the



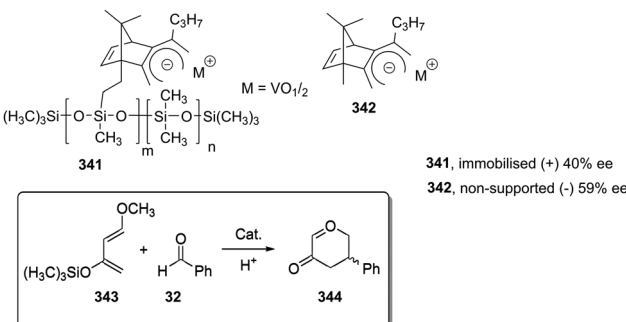


Fig. 82 Reversal of enantioselectivity upon immobilization of an oxovanadium complex in a Diels–Alder reaction.

longer PEG chains seem to favor 2 : 1 instead of 2 : 2 Ti : ligand complexes.

The possibility of site isolation or preconcentration of the catalytic sites as a function of polymer structure and morphology has also been exploited to achieve a dual stereocontrol in the case of supported amino amides that are able to provide the two enantiomers for the Ni(II) catalysed  $\text{Et}_2\text{Zn}$  addition to aldehydes depending on the ligand : metal ratio.<sup>390,391</sup>

Schurig and coworkers had also reported a reversal in enantioselectivity upon immobilization for the hetero-Diels–Alder reaction between *trans*-1-methoxy-3-trimethylsiloxy-1,3-butadiene (343) and benzaldehyde catalysed by an oxovanadium complex (Fig. 82). The (1*R*)-(+)-oxovanadium(IV) bis[3-heptafluorobutanoyl-camphorate] attached onto a soluble polymeric dimethylsiloxane support (341) provided the corresponding adduct with a similar enantioselectivity but with an opposite configuration than the one found for the unsupported catalyst 342.<sup>392</sup>

Another example clearly illustrating the importance of the immobilization strategy is given by immobilised Ti-TADDOLates as catalysts for the Diels–Alder reaction between cyclopentadiene and 3-crotonyl-1,3-oxazolidin-2-one (Fig. 83).<sup>132,321,322</sup> The systems prepared by polymerization providing a highly cross-linked matrix showed, in some cases, a better selectivity than the analogues prepared by grafting and even better than the homogeneous counterpart. For instance, the enantioselectivity obtained at 0 °C for the monolithic Ti-TADDOLate from 349b (43% ee) was significantly higher than that observed for the homogeneous (from 345, 20% ee) and grafted (from 349a, 13% ee) analogues, under the same conditions. A very remarkable result, supporting the effect of the polymer, was obtained with the monolithic derivative 225 (Ar =  $-3,5-(\text{CH}_3)_2\text{C}_6\text{H}_3-$ ). In this case, the major *endo* enantiomer obtained with the monolithic ligand 225b was the 2*S*,3*R* isomer instead of the 2*R*,3*S* isomer obtained with the homogeneous analogue 346 or with the supported catalyst 225a prepared by grafting. The steric interactions between the structural components of the TADDOL structure can be modified during the polymerization to form part of a very rigid crosslinked matrix. This effect can be so dramatic that it leads to a different kind of asymmetric induction.

The aromatic subunits at the groups bound to the C-2 position of the dioxolane ring are important, as it has been shown that  $\pi$ – $\pi$  interactions with the  $\alpha$ -substituent play a key

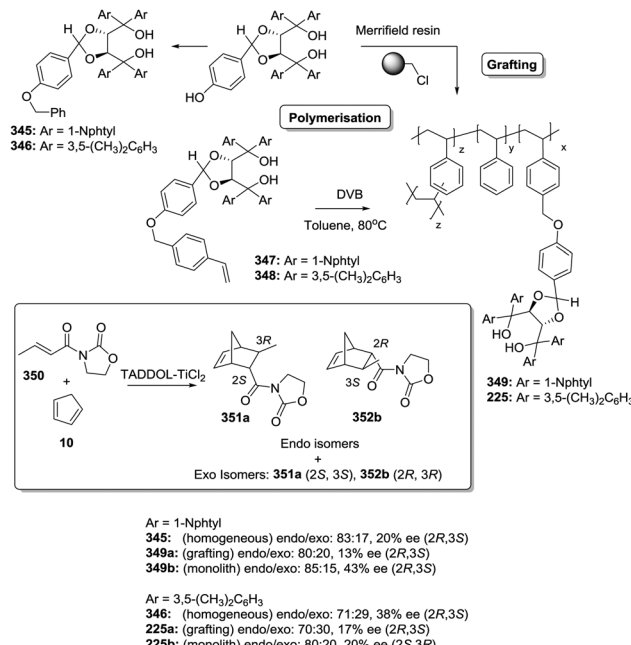


Fig. 83 Effect of the immobilisation strategy of TADDOLs on the use of Ti-TADDOLates as catalysts in Diels–Alder reactions.

role in determining both the nature of the most stable conformer and the relative stability of the possible transition states.<sup>393,394</sup> In this regard, polymerization of the corresponding vinylic TADDOL in a very rigid, highly crosslinked matrix might modify or even preclude some of those  $\pi$ – $\pi$  interactions between the aromatic group at C-2 and one of the 3,5-dimethylphenyl substituents at the  $\alpha$ -positions, modifying the relative energies of the participating transition states, and favouring in this way the formation of the *endo*-2*S*,3*R* adduct. The generation of main-chain chirality/chiral cavities derived from the polymerization of a chiral vinylic monomer should not be excluded.

As mentioned above (Fig. 30) BINOL phosphoric acids (BNPPA) modified at the 3- and 3'-positions with fragments containing thiophenyl groups can be immobilized by direct oxidative coupling of the thiophenes to build up a polymeric network with intrinsic beneficial properties, such as high surface area and distinctive microporosity.<sup>207,208,395</sup> Remarkably, the corresponding immobilized organocatalyst (354) was not only able to surpass the enantioselectivity of the related monomer (353) in solution but was also able to invert the absolute configuration of the product obtained (56% ee (*S*) for 354 vs. 34% ee (*R*) for 353) (Fig. 84). In this case, the crosslinking close to the reactive center resulted in a significantly bigger steric hindrance, which seems to benefit the conformation more favourably for the formation of the *S*-enantiomer in opposition to the more flexible system (353). In good agreement with this, the introduction of more bulky anthracen-9-yl substituents at the 3,3'-positions of the BINOL led to higher enantioselectivities for the monomeric and the polymeric organocatalysts (99% ee (*S*) for 140).<sup>207</sup> In this case, both the monomeric and the polymeric systems provided the *S*-enantiomer confirming the importance of the steric hindrance.



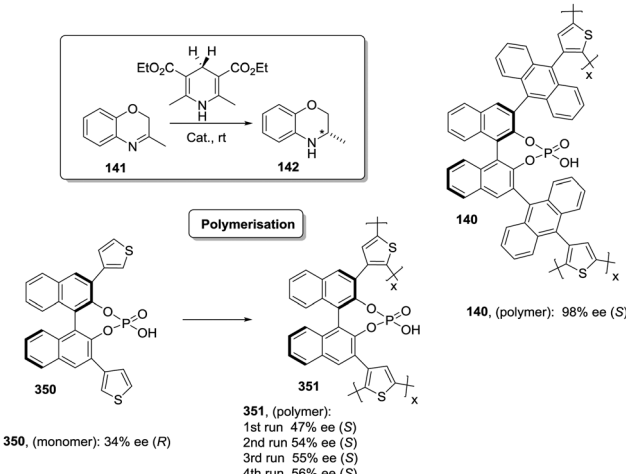


Fig. 84 Microporous polymeric BINOL phosphoric acids displaying reversed enantioselection compared to the monomeric unit.

## Conclusions

Although many additional examples of polymer supported chiral catalytic systems can be found in the literature, the examples presented here illustrate with clarity how the support is not an innocent partner and plays an essential role in defining the performance of these systems. The support needs to be considered as an essential design factor for the preparation of chiral immobilized catalysts. Through an appropriate design and selection of the physico-chemical properties of the polymeric support, it is possible to contribute to enhance the desired properties of the corresponding catalytic system in terms of its activity, stability and selectivity, including the enantioselectivity in the case of chiral systems considered here. Still, however, there is a need for further studies aiming to properly understand the molecular basis of many of the positive support effects discussed here. This will allow in the future a rational approach to the development of new and improved polymer supported chiral catalysts.

## Conflicts of interest

There are no conflicts to declare.

## Acknowledgements

Financial support from MINECO (CTQ2015-68429-R) and GV (PROMETEO/2016/071) is acknowledged.

## Notes and references

- 1 H.-J. Federsel, *Nat. Rev. Drug Discovery*, 2005, **4**, 685–697.
- 2 C. Challener, *Pharm. Technol.*, 2016, **40**, 28–29.
- 3 S. Wendeborn, E. Godineau, R. Mondière, T. Smejkal and H. Smits, Chirality in Agrochemicals, in *Comprehensive Chirality*, ed. E. M. Carreira and H. Yamamoto, Elsevier, Amsterdam, 2012, vol. I, pp. 120–166.
- 4 C. Lamberth, S. Jeanmart, T. Luksch and A. Plant, *Science*, 2013, **341**, 742–746.
- 5 G. M. R. Tombo and D. Belluš, *Angew. Chem., Int. Ed. Engl.*, 1991, **30**, 1193–1215.
- 6 C. Wang, D. Lu, J. Yang, Y. Xu, C. Gong and Z. Li, *Curr. Protein Pept. Sci.*, 2017, **18**, 15–21.
- 7 E. N. Jacobsen, A. Pfaltz and H. Yamamoto, *Comprehensive Asymmetric Catalysis*, Springer-Verlag, Berlin, 1999.
- 8 H. U. Blaser and E. Schmidt, *Asymmetric Catalysis on Industrial Scale: Challenges, Approaches and Solutions*, John Wiley & Sons Inc., New York, 2003.
- 9 Q.-L. Zhou, *Privileged Chiral Ligands and Catalysts*, Wiley-VCH, Weinheim, 2011, ISBN: 978-352732704-1.
- 10 W. S. Knowles, *Angew. Chem., Int. Ed.*, 2002, **41**, 1998–2007.
- 11 R. Noyori, *Angew. Chem., Int. Ed.*, 2002, **41**, 2008–2022.
- 12 K. B. Sharpless, *Angew. Chem., Int. Ed.*, 2002, **41**, 2024–2032.
- 13 B. List, *Chem. Rev.*, 2007, **107**, 5413–5415.
- 14 D. W. C. MacMillan, *Nature*, 2008, **455**, 304–308.
- 15 R. Noyori, *Asymmetric Catalysis in Organic Synthesis*, Wiley, New York, 1994.
- 16 Q.-H. Fan, Y.-M. Li and A. S. C. Chan, *Chem. Rev.*, 2002, **102**, 3385–3466.
- 17 A. M. P. Salvo, F. Giacalone and M. Gruttaduria, *Molecules*, 2016, **21**, 1288.
- 18 T. Frenzel, W. Solodenko and A. Kirschning, in *Polymeric Materials in Organic Synthesis and Catalysis*, ed. M. R. Buchmeiser, Wiley-VCH, Weinheim, 2003, ch. 4.
- 19 T. J. Dickerson, N. N. Reed and K. D. Janda, in *Polymeric Materials in Organic Synthesis and Catalysis*, ed. M. R. Buchmeiser, Wiley-VCH, Weinheim, 2003, ch. 5.
- 20 A. Kirschning, H. Monenschein and R. Wittenberg, *Angew. Chem., Int. Ed.*, 2001, **40**, 650–679.
- 21 S. V. Ley, I. R. Baxendale, R. N. Bream, P. S. Jackson, A. G. Leach, D. A. Longbottom, M. Nesi, J. S. Scott, R. I. Storer and S. J. Taylor, *J. Chem. Soc., Perkin Trans. 1*, 2000, 3815–4195.
- 22 M. Heitbaum, F. Glorius and I. Escher, *Angew. Chem., Int. Ed.*, 2006, **45**, 4732–4762.
- 23 S. Itsuno and M. Hassan, *RSC Adv.*, 2014, **4**, 52023–52043.
- 24 S. Hibner, J. G. de Vries and V. Farina, *Adv. Synth. Catal.*, 2016, **358**, 3–25.
- 25 C. Yu and J. He, *Chem. Commun.*, 2012, **48**, 4933–4940.
- 26 J. M. Notestein and A. Katz, *Chem. – Eur. J.*, 2006, **12**, 3954–3956.
- 27 C. E. Song, D. H. Kim and D. S. Choi, *Eur. J. Inorg. Chem.*, 2006, 2927–2935.
- 28 J. M. Thomas and R. Raja, *Acc. Chem. Res.*, 2008, **41**, 708–720.
- 29 E. Yashima, N. Ousaka, D. Taura, K. Shimomura, T. Ikai and K. Maeda, *Chem. Rev.*, 2016, **116**, 13752–13990.
- 30 R. P. Megens and G. Roelfes, *Chem. – Eur. J.*, 2011, **17**, 8514–8523.
- 31 (a) A. Ikeda, K. Terada, M. Shiotsuki and F. Sanda, *J. Polym. Sci., Part A: Polym. Chem.*, 2011, **49**, 3783–3796; (b) K. Maeda, K. Tanaka, K. Morino and E. Yashima, *Macromolecules*, 2007, **40**, 6783–6785; (c) H. Zhang, W. Yang and J. Deng, *J. Polym. Sci., Part A: Polym. Chem.*, 2015, **53**, 1816–1823.



32 (a) M. Reggelin, M. Schultz and M. Holbach, *Angew. Chem., Int. Ed.*, 2002, **41**, 1614–1617; (b) M. Reggelin, S. Doerr, M. Klussmann, M. Schultz and M. Holbach, *Proc. Natl. Acad. Sci. U. S. A.*, 2004, **101**, 5461–5466.

33 (a) T. Yamamoto, Y. Akai, Y. Nagata and M. Suginome, *Angew. Chem., Int. Ed.*, 2011, **50**, 8844–8847; (b) Y. Akai, T. Yamamoto, Y. Nagata, T. Ohmura and M. Suginome, *J. Am. Chem. Soc.*, 2012, **134**, 11092–11095; (c) T. Yamamoto, R. Murakami and M. Suginome, *J. Am. Chem. Soc.*, 2017, **139**, 2557–2560.

34 A. Warshawsky, *Isr. J. Chem.*, 1979, **18**, 318–324.

35 B. Altava, M. I. Burguete, E. Garcia-Verdugo, S. V. Luis, M. J. Vicent and J. A. Mayoral, *React. Funct. Polym.*, 2001, **48**, 25–35.

36 N. Madhavan, C. W. Jones and M. Weck, *Acc. Chem. Res.*, 2008, **41**, 1153–1165.

37 E. S. Choong, *Annu. Rep. Prog. Chem., Sect. C: Phys. Chem.*, 2005, **101**, 143–173.

38 *Chiral Catalyst Immobilization and Recycling*, ed. D. E. de Vos, I. F. J. Vankelecom and P. A. Jacobs, Wiley-VCH, New York, 2000.

39 J. M. Fraile, J. I. García and J. A. Mayoral, *Chem. Rev.*, 2009, **109**, 360–417.

40 P. Barbaro and F. Liguori, *Chem. Rev.*, 2009, **109**, 515–529.

41 E. Bayer and W. Schumann, *J. Chem. Soc., Chem. Commun.*, 1986, 949–952.

42 P. Wentworth and K. D. Janda, *Chem. Commun.*, 1999, 1917–1924.

43 D. E. Bergbreiter, Polymeric reagents and catalysts, *ACS Symp. Ser.*, 1986, **308**, 17–41.

44 D. E. Bergbreiter, J. Tian and C. Hongfa, *Chem. Rev.*, 2009, **109**, 530–582.

45 D. E. Bergbreiter, *ACS Macro Lett.*, 2014, **3**, 260–265.

46 A. Lu and R. K. O'Reilly, *Curr. Opin. Biotechnol.*, 2013, **24**, 639–645.

47 R. van Heerbeek, P. C. J. Kamer, P. W. N. M. van Leeuwen and J. N. H. Reek, *Chem. Rev.*, 2002, **102**, 3717–3756.

48 D. Wang and D. Astruc, *Coord. Chem. Rev.*, 2013, **257**, 2317–2334.

49 E. de Jesús and Juan C. Flores, *Ind. Eng. Chem. Res.*, 2008, **47**, 7968–7981.

50 A. Akelah and D. C. Sherrington, *Chem. Rev.*, 1981, **81**, 557–587.

51 J. Lu and P. H. Toy, *Chem. Rev.*, 2009, **109**, 815–838.

52 R. B. Merrifield, *J. Am. Chem. Soc.*, 1963, **85**, 2149–2154.

53 M. Benaglia, A. Puglisi and F. Cozzi, *Chem. Rev.*, 2003, **103**, 3401–3430.

54 H. P. Hentze and M. Antonietti, *Rev. Mol. Biotechnol.*, 2002, **90**, 27–53.

55 T. Gokmen and F. E. Du Prez, *Prog. Polym. Sci.*, 2012, **37**, 365–405.

56 M. Gericke, J. Trygg and P. Fardim, *Chem. Rev.*, 2013, **113**, 4812–4836.

57 D. Hudson, *J. Comb. Chem.*, 1999, **1**, 403–457.

58 P. H. Toy and K. D. Janda, *Tetrahedron Lett.*, 1999, **40**, 6329–6332.

59 D. Lumpi, C. Braunshier, E. Horkel, C. Hametner and J. Fröhlich, *ACS Comb. Sci.*, 2014, **16**, 367–374.

60 P. H. Toy, T. S. Reger and K. D. Janda, *Aldrichimica Acta*, 2000, **33**, 87–93.

61 S. Das, P. Heasman, T. Ben and S. Qiu, *Chem. Rev.*, 2017, **117**, 1515–1563.

62 R. Dawson, A. I. Cooper and D. J. Adams, *Prog. Polym. Sci.*, 2012, **37**, 530–563.

63 M. Rose, *ChemCatChem*, 2014, **6**, 1166–1182.

64 Q. Sun, Z. Dai, X. Meng and F.-S. Xiao, *Chem. Soc. Rev.*, 2015, **44**, 6018–6034.

65 X. Zou, H. Rena and G. Zhu, *Chem. Commun.*, 2013, **49**, 3925–3936.

66 J. Huang and S. R. Turner, *Polym. Rev.*, 2017, **6**, 1–41.

67 L. Tan and B. Tan, *Chem. Soc. Rev.*, 2017, **46**, 3322–3356.

68 Y. Zhang and J. Y. Ying, *ACS Catal.*, 2015, **5**, 2681–2691.

69 U. Díaz and A. Corma, *Coord. Chem. Rev.*, 2016, **311**, 85–124.

70 Q. Sun, Z. Dai, X. Meng, L. Wang and F.-S. Xiao, *ACS Catal.*, 2015, **5**, 4556–4567.

71 P. Kaur, J. T. Hupp and S. T. Nguyen, *ACS Catal.*, 2011, **1**, 819–835.

72 A. I. Cooper, *Adv. Mater.*, 2009, **21**, 1291–1295.

73 Y. Xu, S. Jin, H. Xu, A. Nagai and D. Jiang, *Chem. Soc. Rev.*, 2013, **42**, 8012–8031.

74 N. B. McKeown and P. M. Budd, *Chem. Soc. Rev.*, 2006, **35**, 675–683.

75 T. Ben and S. Qiu, *CrystEngComm*, 2013, **15**, 17–26.

76 *Catalytic Asymmetric Synthesis*, ed. I. Ojima, Wiley-VCH, Weinheim, 2nd edn, 2005.

77 *Asymmetric Catalysis on Industrial Scale: Challenges, Approaches and Solutions*, ed. H. U. Blaser and H.-J. Federsel, Wiley-VCH, Weinheim, 2nd edn, 2010.

78 V. A. Larionov, T. Cruchter, T. Mietke and E. Meggers, *Organometallics*, 2017, **36**, 1457–1460.

79 B. Corain, M. Zecca and K. Jerabek, *J. Mol. Catal. A: Chem.*, 2001, **177**, 3–20.

80 P. Hodge, *Chem. Soc. Rev.*, 1997, **26**, 417–424.

81 D. Walsh, D. Wu and Y.-T. Chang, *Curr. Opin. Chem. Biol.*, 2003, **7**, 353–361.

82 D. C. Sherrington, *Chem. Commun.*, 1998, 2275–2286.

83 A. Deratani, G. D. Darling, D. Horak and J. M. J. Fréchet, *Macromolecules*, 1987, **20**, 767–772.

84 R. Santini, M. C. Griffith and M. Qi, *Tetrahedron Lett.*, 1998, **39**, 8951–8954.

85 B. P. Santora, M. R. Gagné, K. G. Moloy and N. S. Radu, *Macromolecules*, 2001, **34**, 658–661.

86 A. R. Vaino and K. D. Janda, *J. Comb. Chem.*, 2000, **2**, 579–596.

87 S. W. Gerritz, *Curr. Opin. Chem. Biol.*, 2001, **5**, 264–268.

88 B. S. Lee, S. Mahajan and K. D. Janda, *Tetrahedron Lett.*, 2005, **46**, 807–810.

89 A. Guyot, P. Hodge, D. C. Sherrington and H. Widdecke, *React. Polym.*, 1992, **16**, 233–259.

90 M. Watanabe and K. Soai, *J. Chem. Soc., Perkin Trans. 1*, 1994, 837–842.



91 K. Soai and M. Watanabe, *Tetrahedron: Asymmetry*, 1991, **2**, 97–100.

92 K. Kamahori, K. Ito and S. Itsuno, *J. Org. Chem.*, 1996, **61**, 8321–8324.

93 A. Marrocchi, P. Adriaensens, E. Bartollini, B. Barkakaty, R. Carleer, J. Chen, D. K. Hensley, C. Petrucci, M. Tassi and L. Vaccaro, *Eur. Polym. J.*, 2015, **73**, 391–401.

94 F. Montanari and P. Tundo, *J. Org. Chem.*, 1981, **46**, 2125–2130.

95 P. L. Anelli, F. Montanari and S. Quici, *J. Chem. Soc., Perkin Trans. 2*, 1983, 1827–1830.

96 P. L. Anelli, B. Czech, F. Montanari and S. Quici, *J. Am. Chem. Soc.*, 1984, **106**, 861–869.

97 P. W. Dyer, S. Handa, T. B. Reeve and S. Suhard, *Tetrahedron Lett.*, 2005, **46**, 4753–4756.

98 A. Seki, F. Ishiwata, Y. Takizawa and M. Asami, *Tetrahedron*, 2004, **60**, 5001–5011.

99 L.-J. Zhao, H. S. He, M. Shi and P. H. Toy, *J. Comb. Chem.*, 2004, **6**, 680–683.

100 L.-J. Zhao, C. K.-W. Kwong, M. Shi and P. H. Toy, *Tetrahedron*, 2005, **61**, 12026–12032.

101 R. Pedrosa, J. M. Andrés, D. P. Ávila, M. Ceballos and R. Pindado, *Green Chem.*, 2015, **17**, 2217–2225.

102 J. M. Andres, N. de La Cruz, M. Valle and R. Pedrosa, *ChemPlusChem*, 2016, **81**, 86–92.

103 L. Wang and F.-S. Xiao, *ChemCatChem*, 2014, **6**, 3048–3052.

104 S. Cañellas, C. Ayats, A. H. Henseler and M. A. Pericàs, *ACS Catal.*, 2017, **7**, 1383–1391.

105 B. Thierry, J.-C. Plaquevent and D. Cahard, *Tetrahedron: Asymmetry*, 2001, **12**, 983–986.

106 K. Hallman and C. Moberg, *Tetrahedron: Asymmetry*, 2001, **12**, 1475–1478.

107 L. Canali, J. K. Karjalainen, D. C. Sherrington and O. Hormi, *Chem. Commun.*, 1997, 123–124.

108 S. D. Alexandratos and D. H. J. Miller, *Macromolecules*, 1996, **29**, 8025–8029.

109 D. Font, S. Sayalero, A. Bastero, C. Jimeno and M. A. Pericas, *Org. Lett.*, 2008, **10**, 337–340.

110 D. Font, C. Jimeno and M. A. Pericas, *Org. Lett.*, 2006, **8**, 4653–4655.

111 C. Ayats, A. H. Henseler and M. A. Pericàs, *ChemSusChem*, 2012, **5**, 320–325.

112 E. Alza, X. C. Cambeiro, C. Jimeno and M. A. Pericàs, *Org. Lett.*, 2007, **9**, 3717–3720.

113 S. D. Alexandratos and D. H. J. Miller, *Macromolecules*, 2000, **33**, 2011–2015.

114 C.-W. Kwong, R. Huang, M. Zhang, M. Shi and P. H. Toy, *Chem. – Eur. J.*, 2007, **13**, 2369–2376.

115 S. Itsuno, *J. Synth. Org. Chem., Jpn.*, 2009, **67**, 1025–1031.

116 S. Hashiguchi, A. Fujita, J. Takehara, T. Ikariya and R. Noyori, *J. Am. Chem. Soc.*, 1995, **117**, 7562–7563.

117 H. Sugie, Y. Hashimoto, N. Haraguchi and S. Itsuno, *J. Organomet. Chem.*, 2014, **751**, 711–716.

118 N. Haraguchi, K. Tsuru, Y. Arakawa and S. Itsuno, *Org. Biomol. Chem.*, 2009, **7**, 69–75.

119 Y. Arakawa, N. Haraguchi and S. Itsuno, *Tetrahedron Lett.*, 2006, **47**, 3239–3243.

120 Y. Arakawa, A. Chiba, N. Haraguchi and S. Itsuno, *Adv. Synth. Catal.*, 2008, **350**, 2295–2304.

121 F. Guendouz, R. Jacquier and J. Verducci, *Tetrahedron*, 1988, **44**, 7095–7108.

122 S. V. Luis and I. Alfonso, *Acc. Chem. Res.*, 2014, **47**, 112–124.

123 M. I. Burguete, J. M. J. Frechet, E. Garcia-Verdugo, M. Jancó, S. V. Luis, F. Svec, M. J. Vicent and M. Xu, *Polym. Bull.*, 2002, **48**, 9–15.

124 F. M. Adrian, B. Altava, M. I. Burguete, S. V. Luis, R. V. Salvador and E. Garcia-España, *Tetrahedron*, 1998, **54**, 3581–3588.

125 B. Altava, M. I. Burguete, J. C. Frias, E. Garcia-España, S. V. Luis and J. F. Miravet, *Ind. Eng. Chem. Res.*, 2000, **39**, 3589–3595.

126 F. Adrian, M. I. Burguete, J. M. Fraile, J. I. Garcia, J. Garcia, E. Garcia-España, S. V. Luis, A. J. Royo and M. C. Sanchez, *Eur. J. Inorg. Chem.*, 1999, 2347–2354.

127 G. Nováková, P. Drabina, B. Frumarová and M. Sedláček, *Adv. Synth. Catal.*, 2016, **358**, 2541–2552.

128 M. Sedláček, P. Drabina, R. Keder, J. Hanusek, I. Císařová and A. Růžička, *J. Organomet. Chem.*, 2006, **691**, 2623–2630.

129 J. Irurre, A. Fernandez-Serrat, M. Altayo and M. Riera, *Enantiomer*, 1998, **3**, 103–120.

130 J. Irurre, A. Fernández-Serrat and F. Rosanas, *Chirality*, 1997, **9**, 191–197.

131 D. Seebach, A. K. Beck and A. Heckel, *Angew. Chem., Int. Ed.*, 2001, **40**, 92–138.

132 B. Altava, M. I. Burguete, B. Escuder, S. V. Luis, R. V. Salvador, J. M. Fraile, J. A. Mayoral and A. J. Royo, *J. Org. Chem.*, 1997, **62**, 3126–3134.

133 S. Degni, C.-E. Wilén and R. Leino, *Org. Lett.*, 2001, **3**, 2551–2554.

134 W.-K. An, M.-Y. Han, C.-A. Wang, S.-M. Yu, Y. Zhang, S. Bai and W. Wang, *Chem. – Eur. J.*, 2014, **20**, 11019–11028.

135 S. Degni, S. Strandman, P. Laari, M. Nuopponen, C.-E. Wilén, H. Tenhu and A. Rosling, *React. Funct. Polym.*, 2005, **62**, 231–240.

136 A. Heckel and D. Seebach, *Chem. – Eur. J.*, 2002, **8**, 560–572.

137 A. Heckel and D. Seebach, *Angew. Chem., Int. Ed.*, 2000, **39**, 163–165.

138 X. Wang, J. Zhang, Y. Liu and Y. Cui, *Bull. Chem. Soc. Jpn.*, 2014, **87**, 435–440.

139 S. Legrand, H. Heikkilä, I. A. Nicholls, A. Root, J. Svensson and C. R. Unelius, *Tetrahedron Lett.*, 2010, **51**, 2258–2261.

140 B. Altava, M. I. Burguete, J. I. Garcia, S. V. Luis, J. A. Mayoral and M. J. Vicent, *Tetrahedron: Asymmetry*, 2001, **12**, 1829–1835.

141 J. M. Fraile, J. A. Mayoral, A. J. Royo, R. V. Salvador, B. Altava, S. V. Luis and M. I. Burguete, *Tetrahedron*, 1996, **52**, 9853–9862.

142 M. I. Burguete, M. Collado, E. Garcia-Verdugo, M. J. Vicent, S. V. Luis, N. G. Von Keyserling and J. Martens, *Tetrahedron*, 2003, **59**, 1797–1804.

143 B. Altava, M. I. Burguete, E. Garcia-Verdugo, S. V. Luis, O. Pozo and R. V. Salvador, *Eur. J. Org. Chem.*, 1999, 2263–2267.



144 B. Altava, M. I. Burguete, M. Collado, E. García-Verdugo, S. V. Luis, R. V. Salvador and M. J. Vicent, *Tetrahedron Lett.*, 2001, **42**, 1673–1675.

145 M. I. Burguete, M. Collado, J. Escorihuela, F. Galindo, E. García-Verdugo, S. V. Luis and M. J. Vicent, *Tetrahedron Lett.*, 2003, **44**, 6891–6894.

146 J. Escorihuela, L. González, B. Altava, M. I. Burguete and S. V. Luis, *Appl. Catal., A*, 2013, **462–463**, 23–30.

147 A.-M. Caminade, P. Servin, R. Laurent and J.-P. Majoral, *Chem. Soc. Rev.*, 2008, **37**, 56–67.

148 A.-M. Caminade, A. Ouali, R. Laurent, C.-O. Turrin and J.-P. Majoral, *Chem. Soc. Rev.*, 2015, **44**, 3890–3899.

149 A.-M. Caminade, A. Ouali, R. Laurent, C. O. Turrin and J.-P. Majoral, *Coord. Chem. Rev.*, 2016, **308**, 478–497.

150 Y.-M. He, Y. Feng and Q.-H. Fan, *Acc. Chem. Res.*, 2014, **47**, 2894–2906.

151 A. John, F. M. Nachtigall and L. S. Santos, *Curr. Org. Chem.*, 2012, **16**, 1776–1787.

152 B. Helms and J. M. J. Fréchet, *Adv. Synth. Catal.*, 2006, **348**, 1125–1148.

153 A. Ouali, R. Laurent, A.-M. Caminade, J.-P. Majoral and M. Taillefer, *J. Am. Chem. Soc.*, 2006, **128**, 15990–15991.

154 E. Delort, T. Darbre and J.-L. Reymond, *J. Am. Chem. Soc.*, 2004, **126**, 15642–15643.

155 Z.-J. Wang, G.-J. Deng, Y. Li, Y.-M. He, W.-J. Tang and Q.-H. Fan, *Org. Lett.*, 2007, **9**, 1243–1246.

156 Q.-H. Fan, Y.-M. Chen, X.-M. Chen, D.-Z. Jiang, F. Xi and A. S. C. Chan, *Chem. Commun.*, 2000, 789–790.

157 G.-J. Deng, Q.-H. Fan and X.-M. Chen, *Chin. J. Chem.*, 2002, **20**, 1139–1141.

158 B. Ma, G. Deng, J. Liu, Y. He and Q.-H. Fan, *Acta Chim. Sin.*, 2013, **71**, 528–534.

159 B. Ma, Z. Ding, J. Liu, Y. He and Q.-H. Fan, *Chem. – Asian J.*, 2013, **8**, 1101–1104.

160 S. P. Smidt, A. Pfaltz, E. Martinez-Viviente, P. S. Pregosin and A. Albinati, *Organometallics*, 2003, **22**, 1000–1009.

161 B. Helms, C. O. Liang, C. J. Hawker and J. M. J. Fréchet, *Macromolecules*, 2005, **38**, 5411–5415.

162 J. Liu, Y. Feng, B. D. Ma, Y. M. He and Q. H. Fan, *Eur. J. Org. Chem.*, 2012, 6737–6744.

163 R. Breinbauer and E. N. Jacobsen, *Angew. Chem., Int. Ed.*, 2000, **39**, 3604–3607.

164 K. B. Hansen, J. L. Leighton and E. N. Jacobsen, *J. Am. Chem. Soc.*, 1996, **118**, 10924–10925.

165 A.-M. Abu-Elfotoh, K. Phomkeona, K. Shibatomi and S. Iwasa, *Angew. Chem., Int. Ed.*, 2010, **49**, 8439–8443.

166 A. Petri, D. Pini, S. Rapaccini and P. Salvadori, *Chirality*, 1999, **11**, 745–751.

167 H. Sellner, P. B. Rheiner and D. Seebach, *Helv. Chim. Acta*, 2002, **85**, 352–387.

168 P. B. Rheiner and D. Seebach, *Chem. – Eur. J.*, 1999, **5**, 3221–3236.

169 H. Sellner and D. Seebach, *Angew. Chem., Int. Ed.*, 1999, **38**, 1918–1920.

170 F. Svec, *J. Chromatogr. A*, 2010, **1217**, 902–924.

171 M. R. Buchmeiser, *Polymer*, 2007, **48**, 2187–2198.

172 M. I. Burguete, J. M. Fraile, J. I. García, E. García-Verdugo, S. V. Luis and J. A. Mayoral, *Org. Lett.*, 2000, **2**, 3905–3908.

173 M. J. Fernández, J. M. Fraile, J. I. García, J. A. Mayoral, M. I. Burguete, E. García-Verdugo, S. V. Luis and M. A. Harmer, *Top. Catal.*, 2000, **13**, 303–309.

174 M. I. Burguete, J. A. Fraile, J. I. García, E. García-Verdugo, C. I. Herreras, S. V. Luis and J. A. Mayoral, *J. Org. Chem.*, 2001, **66**, 8893–8901.

175 M. I. Burguete, J. M. Fraile, E. García-Verdugo, S. V. Luis, V. Martínez-Merino and J. A. Mayoral, *Ind. Eng. Chem. Res.*, 2005, **44**, 8580–8587.

176 H. Nogami, S. Matsunaga, M. Kanai and M. Shibasaki, *Tetrahedron Lett.*, 2001, **42**, 279–283.

177 W. Li and B. Yan, *J. Org. Chem.*, 1998, **63**, 4092–4097.

178 M. I. Burguete, E. Diez-Barra, J. M. Fraile, J. I. García, E. García-Verdugo, R. Gonzalez, C. I. Herreras, S. V. Luis and J. I. Mayoral, *Bioorg. Med. Chem. Lett.*, 2002, **12**, 1821–1824.

179 E. Diez-Barra, J. M. Fraile, J. I. García, E. García-Verdugo, C. I. Herreras, S. V. Luis, J. A. Mayoral, P. Sánchez-Verdú and J. Tolosa, *Tetrahedron: Asymmetry*, 2003, **14**, 773–778.

180 S. Xie, R. W. Allington, J. M. J. Frechet and F. Svec, *Adv. Biochem. Eng./Biotechnol.*, 2002, **76**, 87–125.

181 F. Svec and J. M. J. Frechet, Rigid Macroporous Organic Polymer Monoliths Prepared by Free Radical Polymerization, in *Monolithic materials*, ed. F. Svec, T. B. Tennikova and Z. Deyl, Elsevier, Amsterdam, 2003, ch. 2, pp. 19–50.

182 A. Mandoli, S. Orlandi, D. Pini and P. Salvadori, *Chem. Commun.*, 2003, 2466–2467.

183 A. Mandoli, R. Garzelli, S. Orlandi, D. Pini, M. Lessi and P. Salvadori, *Catal. Today*, 2009, **140**, 51–57.

184 A. Cornejo, J. M. Fraile, J. I. García, M. J. Gil, G. Legarreta, S. V. Luis, V. Martínez-Merino and J. A. Mayoral, *Org. Lett.*, 2002, **4**, 3927–3930.

185 A. Cornejo, J. M. Fraile, J. I. García, M. J. Gil, S. V. Luis, V. Martínez-Merino and J. A. Mayoral, *J. Org. Chem.*, 2005, **70**, 5536–5544.

186 O. Nestler and K. Severin, *Org. Lett.*, 2001, **3**, 3907–3909.

187 E. Burri, M. Öhm, C. Daguenet and K. Severin, *Chem. – Eur. J.*, 2005, **11**, 5055–5061.

188 E. Burri, S. M. Leeder, K. Severin and M. R. Gagné, *Adv. Synth. Catal.*, 2006, **348**, 1640–1644.

189 S. M. Leeder and M. R. Gagné, *J. Am. Chem. Soc.*, 2003, **125**, 9048–9054.

190 S. L. Vinson and M. R. Gagné, *Chem. Commun.*, 2001, 1130–1132.

191 L. Chen, Y. Yang, Z. Guo and D. Jiang, *Adv. Mater.*, 2011, **23**, 3149–3154.

192 L. Chen, Y. Yang and D. Jiang, *J. Am. Chem. Soc.*, 2010, **132**, 9138–9143.

193 Q. Sun, M. Jiang, Z. Shen, Y. Jin, S. Pan, L. Wang, X. Meng, W. Chen, Y. Ding, J. Lib and F.-S. Xiao, *Chem. Commun.*, 2014, **50**, 11844–11847.

194 Q. Sun, Z. Dai, X. Liu, N. Sheng, F. Deng, X. Meng and F.-S. Xiao, *J. Am. Chem. Soc.*, 2015, **137**, 5204–5209.

195 Q. Sun, Z. Dai, X. Meng and F.-S. Xiao, *Chem. Mater.*, 2017, **29**, 5720–5726.

196 T. Wang, Y. Lyu, K. Xiong, W. Wang, H. Zhang, Z. Zhan, Z. Jiang and Y. Ding, *Chin. J. Catal.*, 2017, **38**, 890–897.

197 Q. Sun, X. Meng, X. Liu, X. Zhang, Y. Yang, Q. Yang and F.-S. Xia, *Chem. Commun.*, 2012, **48**, 10505–10507.

198 B. Li, R. Gong, W. Wang, X. Huang, W. Zhang, H. Li, C. Hu and B. Tan, *Macromolecules*, 2011, **44**, 2410–2414.

199 T. Wang, Y. Lyu, X. Chen, C. Li, M. Jiang, X. Song and Y. Ding, *RSC Adv.*, 2016, **6**, 28447–28450.

200 X. Wang, S.-M. Lu, J. Li, Y. Liu and C. Li, *Catal. Sci. Technol.*, 2015, **5**, 2585–2589.

201 X. Wang, J. Li, S. Lu, Y. Liu and C. Li, *Chin. J. Catal.*, 2015, **36**, 1170–1174.

202 R. Marchetto, E. M. Cilli, G. N. Jubilut, S. Schreier and C. R. Nakai, *J. Org. Chem.*, 2005, **70**, 4561–4568.

203 D. A. Annis and E. N. Jacobsen, *J. Am. Chem. Soc.*, 1999, **121**, 4147–4154.

204 M. M. Zhong, H. Li, J. Chen, L. Tao, C. Li and Q. H. Yang, *Chem. – Eur. J.*, 2017, **23**, 11504–11508.

205 Q. Sun, Y. Jin, L. Zhu, L. Wang, X. Meng and F.-S. Xiao, *Nano Today*, 2013, **8**, 342–350.

206 M. Rueping, E. Sugiono, A. Steck and T. Theissmann, *Adv. Synth. Catal.*, 2010, **352**, 281–287.

207 D. S. Kundu, J. Schmidt, C. Bleschke, A. Thomas and S. Blechert, *Angew. Chem. Int. Ed.*, 2012, **51**, 5456–5459.

208 J. Schmidt, D. S. Kundu, S. Blechert and A. Thomas, *Chem. Commun.*, 2014, **50**, 3347–3349.

209 H. Xu, J. Gao and D. Jiang, *Nat. Chem.*, 2015, **7**, 905–912.

210 H. Xu, X. Chen, J. Gao, J. Lin, M. Addicoat, S. Irle and D. Jiang, *Chem. Commun.*, 2014, **50**, 1292–1294.

211 T. Nagashima and H. M. L. Davies, *Org. Lett.*, 2002, **4**, 1989–1992.

212 H. M. L. Davies and A. M. Walji, *Org. Lett.*, 2003, **5**, 479–482.

213 H. M. L. Davies, A. M. Walji and T. Nagashima, *J. Am. Chem. Soc.*, 2004, **126**, 4271–4280.

214 H. M. L. Davies and A. M. Walji, *Org. Lett.*, 2005, **7**, 2941–2944.

215 F. A. Cotton and R. A. Walton, *Multiple Bonds between Metal Atoms*, Clarendon Press, Oxford, UK, 2nd edn, 1993.

216 S. Kobayashi and R. Akiyama, *Chem. Commun.*, 2003, 449–460.

217 R. Akiyama and S. Kobayashi, *Chem. Rev.*, 2009, **109**, 594–642.

218 S. Kobayashi and S. Nagayama, *J. Am. Chem. Soc.*, 1998, **120**, 2985–2986.

219 S. Kobayashi and S. Nagayama, *Synlett*, 1997, 653–654.

220 P. H. Toy and K. D. Janda, *Acc. Chem. Res.*, 2000, **33**, 546–554.

221 Q.-H. Fan, C.-Y. Ren, C.-H. Yeung, W.-H. Hu and A. S. C. Chan, *J. Am. Chem. Soc.*, 1999, **121**, 7407–7408.

222 Q.-H. Fan, G.-J. Deng, C.-C. Lin and A. S. C. Chan, *Tetrahedron: Asymmetry*, 2001, **12**, 1241–1247.

223 Q.-H. Fan, G.-J. Deng, X.-M. Chen, W.-C. Xie, D.-Z. Jiang, D.-S. Liu and A. S. C. Chan, *J. Mol. Catal. A: Chem.*, 2000, **159**, 37–43.

224 T. Oyama, H. Yoshioka and M. Tomoi, *Chem. Commun.*, 2005, 1857–1859.

225 J. K. Karjalainen, O. E. O. Hormi and D. C. Sherrington, *Tetrahedron: Asymmetry*, 1998, **9**, 1563–1575.

226 S. E. Denmark and T. Wynn, *J. Am. Chem. Soc.*, 2001, **123**, 6199–6200.

227 S. E. Denmark and J. Fu, *J. Am. Chem. Soc.*, 2001, **123**, 9488–9489.

228 S. E. Denmark, D. M. Coe, N. E. Pratt and B. D. Griedel, *J. Org. Chem.*, 1994, **59**, 6161–6163.

229 X. Zheng, C. W. Jones and M. Weck, *J. Am. Chem. Soc.*, 2007, **129**, 1105–1112.

230 M. Holbach and M. Weck, *J. Org. Chem.*, 2006, **71**, 1825–1836.

231 P. Goyal, X. Zheng and M. Weck, *Adv. Synth. Catal.*, 2008, **350**, 1816–1822.

232 X. Zheng, C. W. Jones and M. Weck, *Chem. – Eur. J.*, 2006, **12**, 576–583.

233 N. Madhavan and M. Weck, *Adv. Synth. Catal.*, 2008, **350**, 419–425.

234 Y. Xie, M. Wang, X. Wu, C. Chen, W. Ma, Q. Dong, M. Yuan and Z. Hou, *ChemPlusChem*, 2016, **81**, 541–549.

235 P. Cotanda, A. Lu, J. P. Patterson, N. Petzetakis and R. K. O'Reilly, *Macromolecules*, 2012, **45**, 2377–2384.

236 P. Cotanda and R. K. O'Reilly, *Chem. Commun.*, 2012, **48**, 10280–10282.

237 A. Lu, P. Cotanda, J. P. Patterson, D. A. Longbottom and R. K. O'Reilly, *Chem. Commun.*, 2012, **48**, 9699–9701.

238 H. A. Zayas, A. Lu, D. Valade, F. Amir, Z. Jia, R. K. O'Reilly and M. J. Monteiro, *ACS Macro Lett.*, 2013, **2**, 327–331.

239 Y. Xu, Z. Hua, J. Zhang, J. Yang, Z. Cao, D. Zhang, L. He, V. S. J. Craig, G. Zhang and G. Liu, *Chem. Commun.*, 2016, **52**, 3392–3395.

240 Y. Zhang, R. Tan, G. Zhao, X. Luo and D. Yin, *Catal. Sci. Technol.*, 2016, **6**, 488–496.

241 Y. Zhang, R. Tan, G. Zhao, X. Luo, C. Xing and D. Yin, *J. Catal.*, 2016, **335**, 62–71.

242 M. C. M. van Oers, L. K. E. A. Abdelmohsen, F. P. J. T. Rutjes and J. C. M. van Hest, *Chem. Commun.*, 2014, **50**, 4040–4043.

243 M. C. M. van Oers, W. S. Veldmate, J. C. M. van Hest and F. P. J. T. Rutjes, *Polym. Chem.*, 2015, **6**, 5358–5361.

244 E. Huerta, P. J. M. Stals, E. W. Meijer and A. R. A. Palmans, *Angew. Chem. Int. Ed.*, 2013, **52**, 2906–2910.

245 T. Terashima, T. Mes, T. F. A. De Greef, M. A. J. Gillissen, P. Besenius, A. R. A. Palmans and E. W. Meijer, *J. Am. Chem. Soc.*, 2011, **133**, 4742–4745.

246 P. J. M. Stals, C.-Y. Cheng, L. van Beek, A. C. Wauters, A. R. A. Palmans, S. Han and E. W. Meijer, *Chem. Sci.*, 2016, **7**, 2011–2015.

247 E. Karjalainen, D. F. Izquierdo, V. Martí-Centelles, S. V. Luis, H. Tenhu and E. García-Verdugo, *Polym. Chem.*, 2014, **5**, 1437–1446.

248 A. Lu, T. P. Smart, T. H. Epps, D. A. Longbottom and R. K. O'Reilly, *Macromolecules*, 2011, **44**, 7233–7241.

249 M. C. M. van Oers, F. P. J. T. Rutjes and J. C. M. Van Hest, *Curr. Opin. Biotechnol.*, 2014, **28**, 10–16.

250 B. J. Cohen, M. A. Kraus and A. Patchornik, *J. Am. Chem. Soc.*, 1981, **103**, 7620–7629.



251 B. Voit, *Angew. Chem., Int. Ed.*, 2006, **45**, 4238–4240.

252 F. Gelman, J. Blum and D. Avnir, *Angew. Chem., Int. Ed.*, 2001, **40**, 3647–3649.

253 B. Helms, S. J. Guillaudeu, Y. Xie, M. McMurdo, C. J. Hawker and J. M. J. Fréchet, *Angew. Chem., Int. Ed.*, 2005, **44**, 6384–6387.

254 K. E. Price, B. P. Mason, A. R. Bogdan, S. J. Broadwater, J. L. Steinbacher and D. T. McQuade, *J. Am. Chem. Soc.*, 2006, **128**, 10376–10377.

255 B. P. Mason, A. R. Bogdan, A. Goswami and D. T. McQuade, *Org. Lett.*, 2007, **9**, 3449–3451.

256 S. L. Poe, M. Kobašlija and D. T. McQuade, *J. Am. Chem. Soc.*, 2006, **128**, 15586–15587.

257 D. A. Evans and D. Seidel, *J. Am. Chem. Soc.*, 2005, **127**, 9958–9959.

258 S. L. Poe, M. Kobašlija and D. T. McQuade, *J. Am. Chem. Soc.*, 2007, **129**, 9216–9221.

259 N. T. S. Phan, C. S. Gill, J. V. Nguyen, Z. J. Zhang and C. W. Jones, *Angew. Chem., Int. Ed.*, 2006, **45**, 2209–2212.

260 L.-C. Lee, J. Lu, M. Weck and C. W. Jones, *ACS Catal.*, 2016, **6**, 784–787.

261 J. Lu, J. Dimroth and M. Weck, *J. Am. Chem. Soc.*, 2015, **137**, 12984–12989.

262 Y. Chi, S. T. Scroggins and J. M. J. Fréchet, *J. Am. Chem. Soc.*, 2008, **130**, 6322–6323.

263 S. Itsuno, Y. Sakurai, K. Ito, T. Maruyama, S. Nakahama and J. M. J. Frechet, *J. Org. Chem.*, 1990, **55**, 304–310.

264 S. Lundgren, S. Lutsenko, C. Johnsson and C. Moberg, *Org. Lett.*, 2003, **5**, 3663–3665.

265 S. V. Luis, M. I. Burguete and B. Altava, Polymer Supported Organocatalysts, in *The Power of Functional Resins in Organic Synthesis*, ed. F. Albericio and J. Tulla-Puche, Wiley-WCH, Weinheim, 2008.

266 R. P. Jumde, A. Di Pietro, A. Manariti and A. Mandoli, *Chem. – Asian J.*, 2015, **10**, 397–404.

267 R. P. Jumde and A. Mandoli, *ACS Catal.*, 2016, **6**, 4281–4285.

268 T. Mayer-Gall, J.-W. Lee, K. Opwis, B. List and J. S. Gutmann, *ChemCatChem*, 2016, **8**, 1428–1436.

269 J.-W. Lee, T. Mayer-Gall, K. Opwis, C. E. Song, J. S. Gutmann and B. List, *Science*, 2013, **341**, 1225–1229.

270 V. Sans, F. Gelat, N. Karbass, M. I. Burguete, E. García-Verdugo and S. V. Luis, *Adv. Synth. Catal.*, 2010, **352**, 3013–3021.

271 L. Clot-Almenara, C. Rodríguez-Escrich, L. Osorio-Planes and M. A. Pericàs, *ACS Catal.*, 2016, **6**, 7647–7651.

272 K. R. Corbin and S. H. Bergens, *Organometallics*, 2007, **26**, 1571–1574.

273 R. Drake, D. C. Sherrington and S. J. Thomson, *J. Chem. Soc., Perkin Trans. 1*, 2002, 1523–1534.

274 J. Akai, S. Watanabe, K. Michikawa and T. Harada, *Org. Lett.*, 2017, **19**, 3632–3635.

275 F. J. L. Heutz and P. C. J. Kamer, *Dalton Trans.*, 2016, **45**, 2116–2123.

276 T. Roy, R. I. Dureshy, N. H. Khan, S. H. R. Abdi and H. C. Bajaj, *ChemPlusChem*, 2015, **80**, 1038–1044.

277 D. Bissessar, T. Achard and S. Bellemin-Laponnaz, *Adv. Synth. Catal.*, 2016, **358**, 1982–1988.

278 B. Altava, M. I. Burguete, S. V. Luis and J. A. Mayoral, *Tetrahedron*, 1994, **50**, 7535–7542.

279 T. B. Zid, M. Fadhl, I. Khedher and J. M. Fraile, *Microporous Mesoporous Mater.*, 2017, **332**, 38–47.

280 Z.-H. Shi, N.-G. Li, Q.-P. Shi, Y.-P. Tang, H. Tang, M. Z. Shen and J.-A. Duan, *Curr. Org. Synth.*, 2014, **11**, 204–243.

281 J. Huang, J. Cai, C. M. Li and X. Fu, *Inorg. Chem. Commun.*, 2014, **44**, 20–24.

282 J. Huang, L. Yuan, J. Cai, X. Chen and D. Qi, *Inorg. Chem. Commun.*, 2016, **65**, 4–8.

283 L. Zhang, S. Z. Luo and J. P. Cheng, *Catal. Sci. Technol.*, 2011, **1**, 507–515.

284 T. Cheng, Q. Zhao, D. Zhang and G. Liu, *Green Chem.*, 2015, **17**, 2100–2122.

285 Z. Amara, M. Poliakoff, R. Duque, D. Geier, G. Francio, C. M. Gordon, R. E. Meadows, R. Woodward and W. Leitner, *Org. Process Res. Dev.*, 2016, **20**, 1321–1327.

286 M. I. Burguete, E. García-Verdugo, I. García-Villar, F. Gelat, P. Licence, S. V. Luis and V. Sans, *J. Catal.*, 2010, **269**, 150–160.

287 T. Yasukawa, H. Miyamura and S. Kobayashi, *Chem. Sci.*, 2015, **6**, 6224–6229.

288 J. Deka, L. Satyanarayana, G. V. Karunakar, P. K. Bhattacharyya and K. K. Bania, *Dalton Trans.*, 2015, **44**, 20949–20963.

289 J. Peng, X. Wang, X. Zhang, S. Bai, Y. Zhao, C. Li and Q. Yang, *Catal. Sci. Technol.*, 2015, **5**, 666–672.

290 P. Kleman, P. Barbaro and A. Pizzano, *Green Chem.*, 2015, **17**, 3826–3836.

291 S. Z. Luo, J. Y. Li, L. Zhang, H. Xu and J. P. Cheng, *Chem. – Eur. J.*, 2008, **14**, 1273–1281.

292 R. Zhang, G. Yin, Y. Li, X. Yan and L. Chen, *RSC Adv.*, 2015, **5**, 3461–3464.

293 P. Hodge, D. W. L. Sung and P. W. Stratford, *J. Chem. Soc., Perkin Trans. 1*, 1999, 2335–2342.

294 P. Hodge, R. J. Kell, J. B. Ma and H. Morris, *Aust. J. Chem.*, 1999, **52**, 1041–1046.

295 M. Angeloni, O. Piermatti, F. Pizzo and L. Vaccaro, *Eur. J. Org. Chem.*, 2014, 1716–1726.

296 I. Sagamanova, C. Rodríguez-Escrich, I. G. Molnár, S. Sayalero, R. Gilmour and M. A. Pericàs, *ACS Catal.*, 2015, **5**, 6241–6248.

297 L. T. Scott, J. Rebek, L. Ovsyanko and C. L. Sims, *J. Am. Chem. Soc.*, 1977, **99**, 625–626.

298 F. Gaviña, S. V. Luis, A. M. Costero, M. I. Burguete and J. Rebek, *J. Am. Chem. Soc.*, 1988, **110**, 7140–7143.

299 F. Svec and J. M. J. Fréchet, *Science*, 1996, **273**, 205–211.

300 V. Chirolí, M. Benaglia, A. Puglisi, R. Porta, R. P. Jumde and A. Mandoli, *Green Chem.*, 2014, **16**, 2798–2806.

301 N. Karbass, V. Sans, E. García-Verdugo, M. I. Burguete and S. V. Luis, *Chem. Commun.*, 2006, 3095–3097.

302 P. Llanes, C. Rodríguez-Escrich, S. Sayalero and M. A. Pericàs, *Org. Lett.*, 2016, **18**, 6292–6295.

303 K. Takeda, T. Oohara, M. Anada, H. Nambu and S. Hashimoto, *Angew. Chem., Int. Ed.*, 2010, **49**, 6979–6983.

304 J. I. García, J. Gracia, C. I. Herrerías, J. A. Mayoral, A. C. Miñana and C. Sáenz, *Eur. J. Org. Chem.*, 2014, 1531–1540.

305 W.-X. Zhao, N. Liu, G.-W. Li, D.-L. Chen, A.-A. Zhang, M.-C. Wang and L. Liu, *Green Chem.*, 2015, **17**, 2924–2930.



306 M. Chen, Z.-M. Zhang, Z. Yu, H. Qiu, B. Ma, H.-H. Wu and J. Zhang, *ACS Catal.*, 2015, **5**, 7488–7492.

307 Y. Zhou, G. Yang, C. Lu, J. Nie, Z. Chen and J. Ren, *Catal. Commun.*, 2016, **75**, 23–27.

308 X. Li, B. Yang, X. Jia, M. Chen and Z. Hu, *RSC Adv.*, 2015, **5**, 89149–89156.

309 X. Li, M. Chen, B. Yang, S. Zhang, X. Jia and Z. Hu, *RSC Adv.*, 2014, **4**, 43278–43285.

310 R. B. N. Baig, M. N. Nadagouda and R. S. Varma, *Coord. Chem. Rev.*, 2015, **287**, 137–156.

311 X. Li, S. Zhang, B. Yang, C. Lv, X. Jia and Z. Hu, *RSC Adv.*, 2016, **6**, 86531–86539.

312 S. Pagoti, T. Ghosh and J. Dash, *ChemistrySelect*, 2016, **1**, 4386–4391.

313 S. Ranjbar, P. Riente, C. Rodríguez-Esrich, J. Yadav, K. Ramineni and M. A. Pericás, *Org. Lett.*, 2016, **18**, 1602–1605.

314 A. Rostami and B. Atashkar, *J. Mol. Catal. A: Chem.*, 2015, **398**, 170–176.

315 D. Zhao and K. Ding, *ACS Catal.*, 2013, **3**, 928–944.

316 S. Kobayashi, *Chem. – Asian J.*, 2016, **11**, 425–436.

317 R. Porta, M. Benaglia and A. Puglisi, *Org. Process Res. Dev.*, 2016, **20**, 2–25.

318 H. Ishitani, Y. Saito and S. Kobayashi, *Top. Organomet. Chem.*, 2016, **57**, 213–248.

319 A. M. Hafez, A. E. Taggi and T. Lectka, *Chem. – Eur. J.*, 2002, **8**, 4115–4119.

320 M. I. Burguete, E. García-Verdugo, M. J. Vicent, S. V. Luis, H. N. Pennemann, N. G. Keyserling and J. Martens, *Org. Lett.*, 2002, **4**, 3947–3950.

321 B. Altava, M. I. Burguete, J. M. Fraile, J. I. García, S. V. Luis, J. A. Mayoral and M. J. Vicent, *Angew. Chem., Int. Ed.*, 2000, **39**, 1503–1506.

322 B. Altava, M. I. Burguete, E. García-Verdugo, S. V. Luis and M. J. Vicent, *Green Chem.*, 2006, **8**, 717–726.

323 S. B. Ötvös, A. Szloszár, I. M. Mándity and F. Fülöp, *Adv. Synth. Catal.*, 2015, **357**, 3671–3680.

324 K. Takeda, T. Oohara, N. Shimada, H. Nambu and S. Hashimoto, *Chem. – Eur. J.*, 2011, **17**, 13992–13998.

325 Z. Zhang, G. Francio and W. Leitner, *ChemCatChem*, 2015, **7**, 1961–1965.

326 T. Tsubogo, Y. Yamashita and S. Kobayashi, *Chem. – Eur. J.*, 2012, **18**, 13624–13628.

327 P. Lozano, J. M. Bernal, S. Nieto, C. Gomez, E. Garcia-Verdugo and S. V. Luis, *Chem. Commun.*, 2015, **51**, 17361–17374.

328 E. Garcia-Verdugo, B. Altava, M. I. Burguete, P. Lozano and S. V. Luis, *Green Chem.*, 2015, **17**, 2693–2713.

329 P. Lozano, S. Nieto, J. L. Serrano, J. Perez, G. Sanchez-Gomez, E. Garcia-Verdugo and S. V. Luis, *Mini-Rev. Org. Chem.*, 2017, **14**, 65–74.

330 V. Sans, N. Karbass, M. I. Burguete, V. Compañ, E. García-Verdugo, S. V. Luis and M. Pawlak, *Chem. – Eur. J.*, 2011, **17**, 1894–1906.

331 P. Lozano, E. García-Verdugo, R. Piamtongkama, N. Karbass, T. De Diego, M. I. Burguete, S. V. Luis and J. L. Iborra, *Adv. Synth. Catal.*, 2007, **349**, 1077–1084.

332 P. Lozano, M. I. Burguete, N. Karbass, K. Montague, T. de Diego and S. V. Luis, *Green Chem.*, 2010, **12**, 1803–1810.

333 D. F. Izquierdo, J. M. Bernal, M. I. Burguete, E. Garcia-Verdugo, P. Lozano and S. V. Luis, *RSC Adv.*, 2013, **3**, 13123–13126.

334 R. V. Law, D. C. Sherrington and C. E. Snape, *Macromolecules*, 1996, **29**, 6284–6293.

335 R. V. Law, D. C. Sherrington and C. E. Snape, *Macromolecules*, 1997, **30**, 2868–2875.

336 B. Altava, M. I. Burguete, E. García-Verdugo, S. V. Luis and M. J. Vicent, *Tetrahedron*, 2001, **57**, 8675–8683.

337 R. Porta, M. Benaglia, V. Chirolí, F. Coccia and A. Puglisi, *Isr. J. Chem.*, 2014, **54**, 381–394.

338 M. I. Burguete, A. Cornejo, E. García-Verdugo, J. García, M. J. Gil, S. V. Luis, V. Martínez-Merino, J. A. Mayoral and M. Sokolova, *Green Chem.*, 2007, **9**, 1091–1096.

339 M. I. Burguete, A. Cornejo, E. García-Verdugo, M. J. Gil, S. V. Luis, J. A. Mayoral, V. Martínez-Merino and M. Sokolova, *J. Org. Chem.*, 2007, **72**, 4344–4350.

340 C. Aranda, A. Cornejo, J. M. Fraile, E. García-Verdugo, M. J. Gil, S. V. Luis, J. A. Mayoral, V. Martínez-Merino and Z. Ochoa, *Green Chem.*, 2011, **13**, 983–990.

341 H. Wang, N. Li, Z. Yan, J. Zhang and X. Wan, *RSC Adv.*, 2015, **5**, 2882–2890.

342 X. Yang, W. Su, D. Liu, H. Wang, J. Shen, C. Da, R. Wang and A. S. C. Chan, *Tetrahedron*, 2000, **56**, 3511–3516.

343 H. Sellner, C. Faber, P. B. Rheiner and D. Seebach, *Chem. – Eur. J.*, 2006, **20**, 3692–3705.

344 S. Herres, P. Hesemann and J. J. E. Moreau, *Eur. J. Org. Chem.*, 2003, 99–105.

345 D. W. L. Sung, P. Hodge and P. W. Stratford, *J. Chem. Soc., Perkin Trans. 1*, 1999, 1463–1472.

346 K. Kamahori, S. Tada, K. Lto and S. Itsuno, *Tetrahedron: Asymmetry*, 1995, **6**, 2547–2555.

347 J. Wu, F. Wang, Y. Ma, X. Cui, L. Cun, J. Zhu, J. Deng and B. Yu, *Chem. Commun.*, 2006, 1766–1768.

348 S. Itsuno, Y. Hashimoto and N. Haraguchi, *J. Polym. Sci., Part A: Polym. Chem.*, 2014, **52**, 3037–3044.

349 J. M. Fréchet, E. Bald and P. Lecavalier, *J. Org. Chem.*, 1986, **51**, 3462–3467.

350 J.-B. Hu, G. Zhao, G.-S. Yang and Z.-D. Ding, *J. Org. Chem.*, 2001, **66**, 303–304.

351 J.-B. Hu, G. Zhao and Z.-D. Ding, *Angew. Chem., Int. Ed.*, 2001, **40**, 1109–1111.

352 S. Itsuno, T. Matsumoto, D. Sato and T. Inoue, *J. Org. Chem.*, 2000, **65**, 5879–5881.

353 G. Sundararajan and N. Prabagaran, *Org. Lett.*, 2001, **3**, 389–392.

354 K. Nozaki, Y. Itoi, F. Shibahara, E. Shirakawa, T. Ohta, H. Takaya and T. Hiyama, *J. Am. Chem. Soc.*, 1998, **120**, 4051–4052.

355 S. Kinoshita, F. Shibahara and K. Nozaki, *Green Chem.*, 2005, **7**, 256–258.

356 D. Sartor, J. Saffrich and G. Helmchen, *Synlett*, 1990, 197–198.

357 B. Altava, M. I. Burguete, E. García-Verdugo, S. V. Luis, R. V. Salvador and M. J. Vicent, *Tetrahedron*, 1999, **55**, 12897–12906.



358 T. Wang, W. Wang, Y. Lyu, K. Xiong, C. Li, H. Zhang, Z. Zhan, Z. Jiang and Y. Ding, *Chin. J. Catal.*, 2017, **38**, 691–698.

359 Z. Tang, H. Iida, H.-Y. Hu and E. Yashima, *ACS Macro Lett.*, 2012, **1**, 261–265.

360 T. Yamamoto and M. Suginome, *Angew. Chem., Int. Ed.*, 2009, **48**, 539–542.

361 T. Yamamoto, T. Yamada, Y. Nagata and M. Suginome, *J. Am. Chem. Soc.*, 2010, **132**, 7899–7901.

362 Y. Yoshinaga, T. Yamamoto and M. Suginome, *ACS Macro Lett.*, 2017, **6**, 705–710.

363 Y. Arakawa, N. Haraguchi and S. Itsuno, *Angew. Chem., Int. Ed.*, 2008, **47**, 8232–8235.

364 S. Itsuno, D. K. Paul, M. A. Salam and N. Haraguchi, *J. Am. Chem. Soc.*, 2010, **132**, 2864–2865.

365 M. M. Parvez, N. Haraguchi and S. Itsuno, *Org. Biomol. Chem.*, 2012, **10**, 2870–2877.

366 N. Haraguchi, P. Ahamed, M. Parvez and S. Itsuno, *Molecules*, 2012, **17**, 7569–7583.

367 P. Ahamed, M. A. Haque, M. Ishimoto, M. M. Parvez, N. Haraguchi and S. Itsuno, *Tetrahedron*, 2013, **69**, 3978–3983.

368 M. M. Parvez, N. Haraguchi and S. Itsuno, *Macromolecules*, 2014, **47**, 1922–1928.

369 M. R. Islam, P. Ahamed, N. Haraguchi and S. Itsuno, *Tetrahedron: Asymmetry*, 2014, **25**, 1309–1315.

370 M. M. Hassan, N. Haraguchi and S. Itsuno, *J. Polym. Sci., Part A: Polym. Chem.*, 2016, **54**, 621–627.

371 S. Takata, Y. Endo, M. Shahid Ullah and S. Itsuno, *RSC Adv.*, 2016, **6**, 72300–72305.

372 M. S. Ullah and S. Itsuno, *Mol. Catal.*, 2017, **438**, 239–244.

373 N. Haraguchi, H. Kiyono, Y. Takemura and S. Itsuno, *Chem. Commun.*, 2012, **48**, 4011–4013.

374 S. Itsuno, T. Oonami, N. Takenaka and N. Haraguchi, *Adv. Synth. Catal.*, 2015, **357**, 3995–4002.

375 N. Haraguchi, T. L. Nguyen and S. Itsuno, *ChemCatChem*, 2017, **9**, 3786–3794.

376 X. Li, C. Lv, X. Jia, M. Cheng, K. Wang and Z. Hu, *ACS Appl. Mater. Interfaces*, 2017, **9**, 827–835.

377 Y. Zhang, R. Tan, M. Gao, P. Hao and D. Yin, *Green Chem.*, 2017, **19**, 1182–1193.

378 Y. Ribourdouille, G. D. Engel, M. Richard-Plouetbc and L. H. Gade, *Chem. Commun.*, 2003, 1228–1229.

379 F. Zhang, Y. Li, Z.-W. Li, Y.-M. He, S.-F. Zhu, Q.-H. Fan and Q.-L. Zhou, *Chem. Commun.*, 2008, 6048–6050.

380 W.-J. Tang, Y.-Y. Huang, Y.-M. He and Q.-H. Fan, *Tetrahedron: Asymmetry*, 2006, **17**, 536–543.

381 B. Ma, T. Miao, Y. Sun, Y. He, J. Liu, Y. Feng, H. Chenn and Q.-H. Fan, *Chem. – Eur. J.*, 2014, **20**, 9969–9978.

382 Y. Chen, R. Tan, Y. Zhang, G. Zhao and D. Yin, *ChemCatChem*, 2015, **7**, 4066–4075.

383 A. Gissibl, C. Padie, M. Hager, F. Jaroschik, R. Rasappan, E. Cuevas-Yañez, C.-O. Turrin, A.-M. Caminade, J.-P. Majoral and O. Reiser, *Org. Lett.*, 2007, **9**, 2895–2898.

384 A. Gissibl, M. G. Finn and O. Reiser, *Org. Lett.*, 2005, **7**, 2325–2328.

385 R. Rasappan, M. Hager, A. Gissibl and O. Reiser, *Org. Lett.*, 2006, **8**, 6099–6102.

386 L. Garcia, A. Roglans, R. Laurent, J. P. Majoral, A. Pla-Quintana and A. M. Caminade, *Chem. Commun.*, 2012, **48**, 9248–9250.

387 J. Escorihuela, M. I. Burguete and S. V. Luis, *Chem. Soc. Rev.*, 2013, **42**, 5595–5617.

388 N. N. Reed, T. J. Dickerson, G. E. Boldt and K. D. Janda, *J. Org. Chem.*, 2005, **70**, 1728–1731.

389 R. A. García, R. Van Grieken, J. Iglesias, D. C. Sherrington and C. L. Gibson, *Chirality*, 2010, **22**, 675–683.

390 M. I. Burguete, M. Collado, J. Escorihuela and S. V. Luis, *Angew. Chem., Int. Ed.*, 2007, **46**, 9002–9005.

391 J. Escorihuela, B. Altava, M. I. Burguete and S. V. Luis, *RSC Adv.*, 2015, **5**, 14653–14662.

392 F. Keller, H. Weinmann and V. Schurig, *Chem. Ber.*, 1997, **130**, 879–885.

393 B. Altava, M. I. Burguete, J. M. Fraile, J. I. Garcia, S. V. Luis, J. A. Mayoral, A. J. Royo and M. J. Vicent, *Tetrahedron: Asymmetry*, 1997, **8**, 2561–2570.

394 B. Altava, M. I. Burguete, E. Garcia-Verdugo, S. V. Luis, J. F. Miravet and M. J. Vicent, *Tetrahedron: Asymmetry*, 2000, **11**, 4885–4893.

395 C. Bleschke, J. Schmidt, D. S. Kundu, S. Blechert and A. Thomas, *Adv. Synth. Catal.*, 2011, **353**, 3101–3106.